FINAL REPORT

Membrane Bioreactor/Ultra Low Energy Reverse Osmosis Membrane Process for Forward Operating Base Wastewater Reuse

SERDP Project ER-2238

August 2014

Hua Wang
GE Global Research

Distribution Statement A
This document has been cleared for public release

SERDP
DOD ▪ EPA ▪ DOE

This report was prepared under contract to the Department of Defense Strategic Environmental Research and Development Program (SERDP). The publication of this report does not indicate endorsement by the Department of Defense, nor should the contents be construed as reflecting the official policy or position of the Department of Defense. Reference herein to any specific commercial product, process, or service by trade name, trademark, manufacturer, or otherwise, does not necessarily constitute or imply its endorsement, recommendation, or favoring by the Department of Defense.

REPORT DOCUMENTATION PAGE

Form Approved
OMB No. 0704-0188

The public reporting burden for this collection of information is estimated to average 1 hour per response, including the time for reviewing instructions, searching existing data sources, gathering and maintaining the data needed, and completing and reviewing the collection of information. Send comments regarding this burden estimate or any other aspect of this collection of information, including suggestions for reducing the burden, to the Department of Defense, Executive Services and Communications Directorate (0704-0188). Respondents should be aware that notwithstanding any other provision of law, no person shall be subject to any penalty for failing to comply with a collection of information if it does not display a currently valid OMB control number.

PLEASE DO NOT RETURN YOUR FORM TO THE ABOVE ORGANIZATION.

1. REPORT DATE *(DD-MM-YYYY)*	2. REPORT TYPE	3. DATES COVERED *(From - To)*
08-2014	Final Report	01-2012-08-2014

4. TITLE AND SUBTITLE
Membrane Bioreactor/Ultra Low Energy Reverse Osmosis Membrane Process for Forward Operating Base Wastewater Reuse

5a. CONTRACT NUMBER

5b. GRANT NUMBER

5c. PROGRAM ELEMENT NUMBER

6. AUTHOR(S)
Hua Wang

5d. PROJECT NUMBER
ER-2238

5e. TASK NUMBER

5f. WORK UNIT NUMBER

7. PERFORMING ORGANIZATION NAME(S) AND ADDRESS(ES)
GE Global Resesarch
1 Research Circle
Niskayuna, NY 12309-1027

8. PERFORMING ORGANIZATION REPORT NUMBER
ER-2238

9. SPONSORING/MONITORING AGENCY NAME(S) AND ADDRESS(ES)
SERDP/ESTCP
4800 Mark Center Drive, Suite 17D08
Alexandria, VA 22350-3605

10. SPONSOR/MONITOR'S ACRONYM(S)
SERDP/ESTCP

11. SPONSOR/MONITOR'S REPORT NUMBER(S)

12. DISTRIBUTION/AVAILABILITY STATEMENT
Unlimited

13. SUPPLEMENTARY NOTES

14. ABSTRACT

Forward Operating Bases (FOBs) require 25-60 gallons of potable water per soldier per day for essentials including drinking, hygiene, and food preparation, and they produce 35-50 gallons of wastewater daily per soldier. Wastewater treatment methods in FOBs include burn-out latrines, chemical latrines, sewerage lagoons, removal to off-site facilities by contractors, and rarely, a conventional wastewater treatment plant. Currently, a 600 soldier FOB requires 22 trucks per day to supply the base with fuel and water and to remove wastewater and solid waste, creating significant security risk to convoy personnel and negative environmental impact. The overall objective of this project has been to develop an innovative, easily deployable membrane bioreactor (MBR) and ultra-low energy (ULE) reverse osmosis (RO) system for on-site wastewater treatment to produces high-quality water for potable and non-potable reuse, thereby minimizing the need to transport water and wastewater to and from the FOBs.

15. SUBJECT TERMS

16. SECURITY CLASSIFICATION OF:			17. LIMITATION OF ABSTRACT	18. NUMBER OF PAGES	19a. NAME OF RESPONSIBLE PERSON
a. REPORT	b. ABSTRACT	c. THIS PAGE		112	Stuart Strand
					19b. TELEPHONE NUMBER *(Include area code)* 518-387-4147

Reset

Standard Form 298 (Rev. 8/98)
Prescribed by ANSI Std. Z39.18

Table of Contents

List of Tables 4

List of Figures 5

List of Acronyms 9

Keywords 11

Acknowledgments 12

Abstract 13

I. Introduction 15

II. Project Objectives and Approach 16

III. Project Plan and Management 17

VI. Results and Discussion 18

4.1 Task 1-Optimize Ultra-Low Energy (ULE) Nanocomposite RO Membranes 18

4.1.1 Objectives 18

4.1.2 Mesoporous Silica Nanoparticles Synthesis and Characterization 18

4.1.3 Optimize Nanocomposite RO Membrane Pilot-Scale Fabrication 27

4.1.4 Prototype RO Element Fabrication 39

4.1.5 Nanocomposite membrane characterization 41

4.1.6 Conclusions from Task 1 43

4.2 Task 2- Design and Validate Lab-Scale MBR/Ultra-Low Energy RO Wastewater Treatment System 48

4.2.1 Objectives and Approaches 48

4.2.2. Characteristics of gray water 49

4.2.3 Synthetic gray water characterization 52

4.2.4 Evaluate MBR pre-treatment of synthetic gray water using lab-scale ZW-1 MBR units 53

4.2.5 Synthetic Gray Water Treatment Using ZW-10 Pilot Scale Membrane Bioreactor and E-2 RO Wastewater Treatment System 62

4.2.6. Integration of RO system with MBR unit 76

4.2.7 Laundry and Kitchen Gray Water Treatment Using an Integrated ZW-10 Pilot Scale Membrane Bioreactor and E-2 RO Wastewater Treatment System 78

4.2.8 Development of deployable wastewater treatment system performance and cost models 88

4.2.9 Conclusions from Task 2 95

V. Conclusions and Implications for Future Research 96

5.1 Overview and Summary of Project Results 96
5.2 Conclusions 98
5.3. Implications for Future Research 99
VI. Bibliography 101
Appendix: Additional Tables 103

List of Tables

Table 1: Program schedule, tasks, and final deliverables. 17
Table 2: Performance of standard brackish water RO membrane (AG) 40
Table 3: Performance of GE's standard and ULE RO membranes. 41
Table 4: RO feed water quality specifications. 48
Table 5: Water quality specifications for MBR/RO purified water. 49
Table 6: Characteristics of gray water from containerized self-service laundry at Base Camp Integration Lab at Fort Devens, MA[22]. 50
Table 7: Characteristics of black waters from on-base toilets at Base Camp Integration Lab at Fort Devens, MA[22]. 50
Table 8: Characteristics of various gray water streams from three US Navy vessels: USS O'Hare (DD 889), USS Seattle (AE 3), and USS Sierra (AD 18)[23-27]. 51
Table 9: Characteristics various domestic gray water streams [28]. 51
Table 10: Synthetic gray water compositions. 52
Table 11: Characteristics of synthetic gray water. 52
Table 12: Characteristics of the feed water and ZW-1 MBR effluent, including turbidity, COD, BOD, TOC, and pH. 56
Table 13: Characteristics of the ZW-1 MBR influent and effluent, including TDS, TSS, ammonia, total nitrogen, and total phosphorous. 56
Table 14: Average removal efficiency for COD, BOD, TOC, TDS, TSS, and turbidity by ZW-1 MBR (excluding day 3 data). 61
Table 15: RO feed and permeate conductivity and percent rejection data. 77
Table 16: Integrated system treatment of key wastewater parameters: COD, BOD, TOC, Ammonia, Total Phosphate, TDS, and Turbidity on days 154 and 198. 77
Table 17: Typical sample analyses for drinking water testing[21]. 78
Table 18: MBR effluent quality during rapid startup. 79
Table 19: Representative wastewater generation for a 600 soldier FOB [1,2] 89
Table 20: Wastewater influent flow rate. 90
Table 21: Wastewater quality 90
Table 22: MBR effluent quality data. 90
Table 23: RO effluent quality. 91
Table 24: MBR and RO process design information. 91
Table 25: Details of MBR and RO system configuration. 92
Table 26: MBR and RO system power consumption estimate 92
Table 27: Annual MBR and RO system chemical consumption estimate 93
Table 28: Pricing for the integrated MBR/RO system. 93
Table 29: Payback calculation of the designed MBR/RO system. 94

List of Figures

Figure 1: Program summary. 15
Figure 2: a) Silica nanoparticles synthesized in aqueous phase. b) Freeze-dried silica nanoparticles. c) and d) Template- extracted silica nanoparticles following calcination at 400°C (c) and 600°C (d). 20
Figure 3: TEM images. a) Silica nanoparticles in aqueous phase at low magnification (71000x). b) Silica nanoparticles in aqueous phase at high magnification (145000x). c) EDS-analyzed region circled in white on accompanying TEM image. 21
Figure 4: SEM images. a) and b) Silica nanoparticles in aqueous phase. c) and d) Repeat syntheses of particles in aqueous phase. e) EDS-analyzed region circled in white on accompanying SEM image. 22
Figure 5: TEM images of silica nanoparticles calcined at 400°C. 23
Figure 6: SEM images. a) and b) 400°C calcined silica nanoparticles re-suspended in ethanol. c) and d) 600°C calcined silica nanoparticles re-suspended in ethanol. 24
Figure 7: SEM images. a) and b) 400°C calcined silica nanoparticles re-suspended in Isopar G. c) and d) 600°C calcined silica nanoparticles re-suspended in Isopar G. 24
Figure 8: DLS particle size distribution of 600°C template-extracted particles in ethanol. ... 25
Figure 9: DLS particle size distribution of 600°C template-extracted particles in Isopar G solvent. 25
Figure 10: Nitrogen sorption isotherms of: a) control, freeze-dried particles and b) 600°C calcined particles (graph and analysis performed by Micromeritics Analytical Services). 25
Figure 11: a) Photo of the GEGR pilot membrane coater; b) configuration of the coating station; and c) web path of the dip-knife coating process for RO membrane fabrication. 28
Figure 12: (a) Pre-chlorination and (b) post-chlorination performance (A value, B value, NaCl passage) of nanocomposite membranes with the indicated silica size fractions (US3440). Membranes were fabricated on P415 UF support. 31
Figure 13: (a) Pre-chlorination and (b) post-chlorination performance (A value, B value, NaCl passage) of membranes fabricated at line speeds of 4 and 8 ft/min (FPM). Membranes were fabricated on P415 UF support. 0.1%(w/v) silica (US3440), 1.25%(v) cyclohexanone (CHEX), or both were added to the organic phase for the non-control membranes. 33
Figure 14: (a) Pumping versus (b) gravity feeding the organic solution to the organic coating knife. 34
Figure 15: (a) Pre-chlorination and (b) post-chlorination performance (A value, B value, NaCl passage) of membranes fabricated using gravity and pump-delivered organic solutions. Membranes were fabricated on P415 UF support. 0.1%(w/v) silica (US3440), 1.25%(v) cyclohexanone (CHEX), or both were added to the organic phase for the non-control membranes. 35
Figure 16: (a) Pre-chlorination and (b) post-chlorination performance (A value, B value, NaCl passage) of nanocomposite membranes with the indicated GEGR-synthesized silica particles. Membranes were fabricated on P415 UF support. 1.25%(v) cyclohexanone (CHEX) was added to the organic phase for all membranes except

the control membrane; 0.1%(w/v) SiO_2 calcined at the indicated temperature was also added to the organic phase for the nanocomposite membrane formulations. Particle synthesis repeatability is demonstrated by two batches of particles made at the same conditions and used in nanocomposite membrane fabrication. 36
Figure 17: (a) Pre-chlorination and (b) post-chlorination performance (A value, B value, NaCl passage) of nanocomposite membranes with the indicated loadings of GEGR-made SiO_2 particles. Membranes were fabricated on P415 UF support. 1.25%(v) cyclohexanone (CHEX) was added to the organic phase for all membranes except the control membrane; 0.1% and 0.2% (w/v) silica nanoparticles calcined at 600 ^{o}C were also added to the organic phase for the nanocomposite membrane formulations. 38
Figure 18: Repeatability of pilot-scale nanocomposite membrane fabrication process, indicated by flat sheet coupon A values and NaCl passages. Membranes were fabricated on P415 UF support with 1.25%(v) cyclohexanone (CHEX), and 0.1%(w/v) SiO_2 particles in the organic phase. Red squares and blue circles indicate nanocomposite membranes made with commercially available SiO_2 particles and GEGR synthesized SiO_2 particles, respectively. The boxed region includes membranes that meet the performance criteria (A value greater than 16 with NaCl passage less than 0.5%)..... 39
Figure 19: Membrane element fabrication table and the lab-scale (2”x12”) AG RO membrane element fabricated at GEGR. 40
Figure 20: The lab-scale (2”x12”) RO element testing bench. Six elements can be tested simultaneously. 40
Figure 21: SEM images of the surfaces of the (a) polysulfone UF membrane, (b) a thin film composite control RO membrane (UF plus the polyamide thin film, without nanoparticles). 43
Figure 22: SEM images of the surface of a nanocomposite RO membrane fabricated with GEGR synthesized mesoporous silica nanoparticles. These nanoparticles are well dispersed on the surface of the polyamide RO membrane thin film. For comparison, the SEM image of as-synthesized bulk silica nanoparticles is inserted on the top left. 44
Figure 23: SEM image of the surface of a nanocomposite RO membrane fabricated with silica particles supplied by US Research Nanomaterials, Inc. (US3440). These nanoparticles form large surface aggregates on the surface of the polyamide RO membrane thin film..... 44
Figure 24: (a) SEM image of a nanocomposite RO membrane fabricated with silica particles supplied by US Research Nanomaterials, Inc. (US3440), and (b) Energy dispersive X-ray spectroscopy (EDS) map for silica nanoparticles on nanocomposite membrane surface. 45
Figure 25: SEM image of cross-section prepared by freeze fracture of a nanocomposite membrane showing “waves” and “folds” structure in the non-uniform polyamide layer and small agglomerate of nanoparticles on/at/in the polyamide layer..... 46
Figure 26: TEM of microtomed thin section of a nanocomposite RO membrane fabricated with silica particles supplied by US Research Nanomaterials, Inc. (US3440). Sample embedded in epoxy prior to microtoming. Silica particles have higher contrast. 46

Figure 27: Higher magnification image of a nanocomposite RO membrane fabricated with silica particles supplied by US Research Nanomaterials, Inc. (US3440). Green arrows indicate silica nanoparticles possibly entrapped in the PA film, and the red arrows indicate silica nanoparticles physically absorbed to the surface of the polyamide thin film. 47
Figure 28: a) The ZW-1 membrane bioreactor set-up at GE Global Research, and b) the ZW-1 MBR hollow fiber membrane module (membrane area=0.5 ft^2/0.047 m^2, length=17.5 cm, diameter=5.8 cm, and holdup volume=10 mL). 53
Figure 29: Schematic of the ZW-1 lab scale membrane bioreactor. 54
Figure 30: Hach portable DR3900 spectrophotometer and chemistry test-kits. 54
Figure 31: The turbidity of ZW-1 MBR influent, mixed liquor in the process tank, and effluent. 56
Figure 32: The BOD concentrations of ZW-1 MBR influent and effluent. 57
Figure 33: The COD concentrations of ZW-1 MBR influent and effluent. 57
Figure 34: The TOC concentrations of ZW-1 MBR influent and effluent. 57
Figure 35: The turbidity levels of ZW-1MBR influent and effluent. 58
Figure 36: The TSS levels of ZW-1 MBR influent and effluent. 58
Figure 37: The TDS levels of ZW-1 MBR influent and effluent. 58
Figure 38: The ZW-1 MBR influent and effluent ammonia concentrations. 59
Figure 39: The TKN concentrations of ZW-1 MBR influent and effluent. 59
Figure 40: The total phosphorous concentrations of ZW-1 influent and effluent. 60
Figure 41: The pH levels of ZW-1 MBR influent and effluent. 60
Figure 42: (a) The ZW-10 MBR system at GE Global Research, b) The ZW-10 MBR module (membrane area= 10 ft^2/0.93 m^2, length=69.2 cm, diameter =11 cm, holdup volume= 130 mL). 62
Figure 43: Re-configured ZW-10 MBR system. An additional tank and a pump were installed to house the ZW-10 membrane module and to re-circulate the activated sludge, respectively. 63
Figure 44: The BOD concentrations of influent and effluent and the BOD removal efficiency of the ZW-10 MBR system. 64
Figure 45: The COD concentrations of influent and effluent and the COD removal efficiency of the ZW-10 MBR system. 64
Figure 46: The TOC concentrations of influent and effluent and the TOC removal efficiency of the ZW-10 MBR system. 65
Figure 47: The ammonia concentrations of the ZW-10 MBR influent and effluent. 66
Figure 48: Percent ammonia removal and effluent pH monitored throughout the ZW-10 experimental study. 66
Figure 49: The TKN concentrations of ZW-10 MBR influent and effluent. 67
Figure 50: The total phosphorous concentrations of ZW-10 MBR influent and effluent. 67
Figure 51: The turbidity level of ZW-10 MBR influent and effluent. 68
Figure 52: The TSS of the ZW-10 MBR influent and effluent. 68
Figure 53: Variations of membrane flux and HRT during the ZW-10 MBR operation. 69
Figure 54: The transmembrane pressure profile during the ZW-10 MBR operation. 70
Figure 55: The membrane permeance and temperature of the ZW-10 MBR system. 71
Figure 56: The DO concentrations in the ZW-10 MBR processing tank. 71

Figure 57: Food to Microorganism (F:M) ratio for ZW-10 experiment. Average F:M over the entire study was 0.48. 73
Figure 58: Images of a) new ZW-10 module; b) fouled ZW-10 module; and c) recovered module following sodium hypochlorite and citric acid cleanings. 74
Figure 59: SEM images of a) new ZW-10 hollow fiber membranes; b) fouled ZW-10 membranes; c) recovered membranes following sodium hypochlorite; and d) recovered membranes following sodium hypochlorite and citric acid cleaning. 75
Figure 60: SEM images of fouled ZW-10 hollow fiber membranes. 75
Figure 61: Schematic of the integrated ZW-10 MBR and E2 RO system. 76
Figure 62: The BOD concentrations of influent and effluent and the BOD removal efficiency of the ZW-10 MBR system in treating real wastewater. 80
Figure 63: The COD concentrations of influent and effluent and the BOD removal efficiency of the ZW-10 MBR system in treating real wastewater. 81
Figure 64: The TOC concentrations of influent and effluent and the BOD removal efficiency of the ZW-10 MBR system in treating real wastewater. 81
Figure 65: The ammonia concentrations of influent and effluent and the ammonia removal efficiency of the ZW-10 MBR system in treating real wastewater. 82
Figure 66: The TKN concentrations of influent and effluent and the TKN removal efficiency of the ZW-10 MBR system in treating real wastewater. 82
Figure 67: Percent ammonia removal and effluent pH monitored throughout the ZW-10 experimental study. 83
Figure 68: The TP concentrations of influent and effluent and the TP removal efficiency of the ZW-10 MBR system in treating real wastewater 83
Figure 69: The turbidity level of ZW-10 MBR influent and effluent. 84
Figure 70: The TSS level of ZW-10 MBR influent and effluent. 84
Figure 71: Variations of flux, transmembrane pressure, and HRT during the real wastewater treatment study. 85
Figure 72: Dissolved oxygen levels in the ZW-10 process tank. 85
Figure 73: HRT and MLSS levels in the ZW-10 process tank. 86
Figure 74: Food to microorganism ratio calculated from influent BOD levels, MLSS, and flux for ZW-10 MBR. 86
Figure 75: Feed and permeate conductivities and salt rejection of E-2 RO unit. 87
Figure 76: GE deployable MBR/RO wastewater treatment system. 88

List of Acronyms

Acronym	Definition
A Value	Water Permeance. Water Transport Coefficient
AFM	Atomic Force Microscopy
ASP	Activated Sludge Process
B Value	Salt Permeance. Salt Transport Coefficient
BET	Brunauer, Emmett, Teller (Surface Analysis Technique)
BCIL	US Army Base Camp Integration Lab at Fort Devens, MA
BJH	Barrett-Joyner-Halenda (Pore Size Analysis Technique)
BOD	Biological Oxygen Demand
BOD_5	Five Day Biological Oxygen Demand
CAPEX	Capital Expenditure
CFU	Colony Forming Units
CHEX	Cyclohexanone
COD	Chemical Oxygen Demand
CSSL	Containerized Self-Service Laundry
CTAC	cetyltrimethylammonium chloride
DLS	Dynamic Light Scattering
DO	Dissolved Oxygen
DOD	United States Department of Defense
EDS	Energy-dispersive X-ray spectroscopy
EPA	Environmental Protection Agency
F:M	Food-To-Microorganism Ratio
FOB	Forward Operating Base
FT-IR	Fourier Transform Infrared Spectroscopy
GEGR	GE Global Research
GE W&PT	GE Water & Process Technologies
GFD	Gallons Per Square Foot Per Day
GPD	Gallons Per Day
GPM	Gallons Per Minute
HRT	Hydraulic Retention Time
LHS	Load Handling System
LMH	Liters Per Square Meter Per Hour
MBR	Membrane Bioreactor

MF	Microfiltration
MCL	Maximum Contaminant Levels
MLSS	Mixed Liquor Suspended Solids
mPD	Metaphenylene Diamine
NF	Nanofiltration
NPI	New Product Introduction
NTU	Nephelometric Turbidity Units
OPEX	Operational Expenditure
PDI	Polydispersity Index
PSI	Pounds Per Square Inch
RO	Reverse Osmosis
RPM	Revolutions Per Minute
SCFM	Standard Cubic Feet Per Minute
SDI	Silt Density Index
SEM	Scanning Electron Microscopy
SMCL	Secondary Maximum Contaminant Levels
SRT	Sludge Retention Time
SS-NMR	Solid-State Nuclear Magnetic Resonance
TEM	Transmission Electron Microscopy
TKN	Total Nitrogen
TMC	Trimesoyl Chloride
TP	Total Phosphorus
TSS	Total Suspended Solids
TDS	Total Dissolved Solids
TEOS	Tetraethyl Orthosilicate
TMC	Trimesoyl Chloride
TOC	Total Organic Carbon
UF	Ultrafiltration
ULE	Ultra-Low Energy
USEPA	United States Environmental Protection Agency
UV	Ultraviolet
WHO	World Health Organization
XPS	X-Ray Photoelectron Spectroscopy
ZW	ZeeWeed (A GE trademark)

Keywords

Gray Water
Wastewater
Wastewater Treatment
Water Reuse
Potable Water Reuse
Non-potable Water Reuse
Forward Operating Bases
Low Energy
Energy Efficient
Containerized
Military Deployable
Membrane Bioreactor
MBR
Reverse Osmosis
RO
Membrane
Nanocomposite
Techno-economic Analysis

Acknowledgments

The research described in this report was supported by the U.S. Department of Defense, through the Strategic Environmental Research and Development Program (SERDP). Dr. Andrea Leeson and other SERDP administrative and technical review staff are gratefully acknowledged for their invaluable project support and technical comments and suggestions. The authors would also like to thank Ryan Eckert at US Army Natick Soldier Systems Center, Joseph Findley at US Army Mobile District, and CPT Charles Decker and his team at U.S. Army Engineer Research & Development Center (ERDC), and Paul Bandstra, Carsten Owerdieck, John Peichel, Henk Koops, Minggang Liu, Jerome Daly, Lee-Anne Bresolin, Jeff Cumin, and Jeff Peeters at GE Water for insightful technical comments and suggestions.

Abstract

A. OBJECTIVE

Forward Operating Bases (FOBs) require 25-60 gallons of potable water per soldier per day for essentials including drinking, hygiene, and food preparation, and they produce 35-50 gallons of wastewater daily per soldier. Wastewater treatment methods in FOBs include burn-out latrines, chemical latrines, sewerage lagoons, removal to off-site facilities by contractors, and rarely, a conventional wastewater treatment plant. Currently, a 600 soldier FOB requires 22 trucks per day to supply the base with fuel and water and to remove wastewater and solid waste, creating significant security risk to convoy personnel and negative environmental impact.

The overall objective of this project has been to develop an innovative, easily deployable membrane bioreactor (MBR) and ultra-low energy (ULE) reverse osmosis (RO) system for on-site wastewater treatment to produces high-quality water for potable and non-potable reuse, thereby minimizing the need to transport water and wastewater to and from the FOBs.

B. TECHNICAL APPROACH

The approaches in this project include three integral components. The first is to develop ultra-low-energy (ULE), high permeance membrane technology by incorporating highly engineered nanomaterials. These ULE nanocomposite RO membranes operate at low pressures and have a low energy requirement. The second is to build a lab-scale MBR/RO wastewater treatment system to demonstrate its ability to produce high-quality water for reuse. The third is to perform a techno-economic feasibility assessment of a deployable MBR/RO system configuration based on lab-scale experimental data and suitable performance modeling.

C. RESULTS

GE Global Research has developed an advanced ULE RO membrane, incorporating engineered nanomaterials, and demonstrated a 2- to 3-fold permeance enhancement, while maintaining the 99.5% or higher salt rejection characteristic of current commercial RO membranes. MBR/RO wastewater treatment experiments were carried out using both synthetic wastewater and a mixture of on-site generated kitchen and laundry wastewater and tap water to simulate typical wastewater streams from FOBs. The integrated MBR/RO system was found to produce high quality effluents that met potable reuse requirements when the MBR was operated at low HRT (2-4 hours) and high SRT (20-25 days). In addition, rapid biological seeding and start-up procedures were successfully developed to start the MBR system and generate high quality effluent in less than 5 days. The system performance and water quality data were used next to design a low footprint, energy efficient, and deployable MBR/RO system for FOBs. The results indicate that the investment of the GE deployable, low energy MBR/RO wastewater treatment system pays back in less than 1 month after deployment in FOBs, offering tremendous cost savings for the US military and an improved base environment and security.

D. BENEFITS

The major benefits of the proposed MBR/ULE RO wastewater treatment system to the DoD and specifically its FOBs are:

- Greatly reduced potable water demand from off-base sources
- Greatly reduced need to transport wastewater away from the bases
- 80% less water traffic on roads (transport of potable water and wastewater)
- 50% less overall traffic on roads (transport of potable water, wastewater, and solid waste)
- Net annual cost savings of over $30 million per 600-soldier FOB
- Improved base environment, security, soldier health, and stewardship of foreign lands.

I. Introduction

Fresh water acquisition, treatment, and wastewater disposal have been identified by SERDP as key challenges of the Department of Defense's Forward Operating Bases (FOBs) [1–3]. In this program, GE Global Research has developed an innovative membrane bioreactor (MBR) and reverse osmosis (RO) system for onsite wastewater treatment for FOBs. The system produces high-quality water for potable and non-potable reuse, minimizing water demand from off-base sources. The benefits of the proposed wastewater treatment system include lower potable water and fuel demand from off-base sources, as well as improved base environment, security, soldier health, and stewardship of foreign lands.

The essential elements of the project are illustrated in Figure 1. FOB wastewater first undergoes sedimentation or crude filtration to remove large particles. The wastewater is then directed to the MBR unit to remove suspended solids, colloids, and biological material (cell tissue and microorganisms). The MBR effluent can then be used for non-potable applications, or fed to the RO unit to remove dissolved solids and ionic species. Finally, the RO-purified water is treated by UV disinfection as an additional treatment barrier before reuse for potable applications.

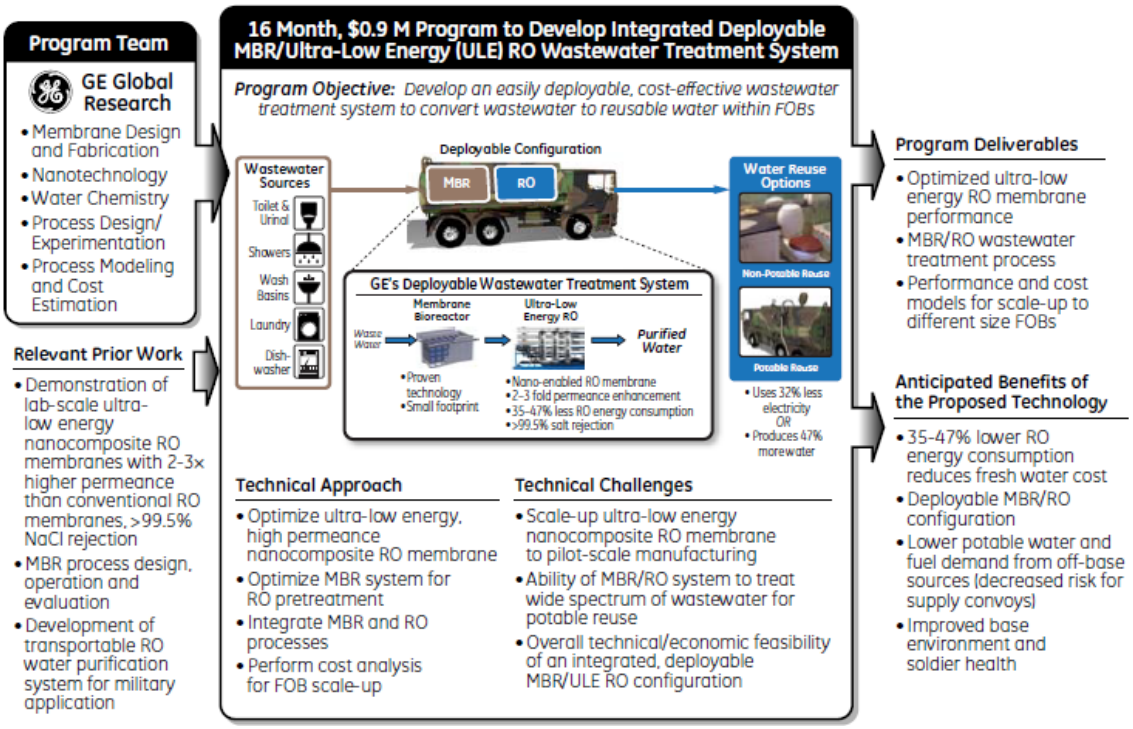

Figure 1: Program summary.

II. Project Objectives and Approach

The key objectives of this program are:

1. Develop ultra-low energy membrane technology

RO membranes are used worldwide for seawater and brackish water desalination, as well as municipal and industrial wastewater reuse[6–9]. Conventional polyamide RO membranes function by allowing water to permeate while rejecting dissolved solids and other contaminants. Unfortunately, these conventional RO membranes purify water by a solution-diffusion mechanism, so they suffer from an inherent "trade-off" between permeability and selectivity[10,11].

The RO membrane developed for the innovative wastewater treatment process needs to have high permeance (low energy consumption) and a small footprint, while maintaining high rejection of salts and other contaminants. As part of the MBR/RO system for treating gray water from FOBs for reuse, GE Global Research will develop an advanced ULE RO membrane incorporating highly engineered nanomaterials to demonstrate 2- to 3-fold permeance enhancement and reduce electrical consumption by 35% to 47% compared to current RO membrane processes, while maintaining the 99.5% or greater salt rejection characteristic of current commercial RO membranes. Enhanced water transport is afforded by the porous nanomaterials incorporated within the polyamide RO membrane matrix, while the polyamide matrix allows the nano-enabled membrane to maintain the required 99.5% salt rejection.

2. Validate lab-scale MBR/RO wastewater treatment system

For FOB wastewater treatment, a high permeance RO membrane with low energy demand and a small footprint that maintains high rejection of salts and other contaminants is essential for the design of a deployable wastewater treatment and reuse system. The ULE nanocomposite RO membrane and associated MBR pretreatment process will be evaluated experimentally using representative gray water samples. GE will build a lab-scale MBR/ULE RO prototype system to demonstrate MBR as a robust RO pre-treatment for gray water from FOBs, validate the system's ability to produce high-quality water for reuse, and determine the overall energy savings.

3. Develop deployable configuration

The final MBR/RO system must be able to fit inside a transportable container. The small footprint of the MBR unit (compared to that of conventional biological wastewater treatment systems) and the ULE, high permeance RO membrane make the MBR/ULE RO system amenable to a deployable configuration and minimize the area required for high quality wastewater treatment on-site. GE Global Research will evaluate the final MBR/ULE RO configuration footprint and obtain a cost estimate to determine the overall technical and economic feasibility of the proposed deployable wastewater treatment system.

III. Project Plan and Management

This project has been organized into three interrelated tasks, including:

1. Optimize ultra-low energy (ULE) nanocomposite RO membrane
2. Design and validate lab-scale MBR/ULE nanocomposite RO system
3. Project management plan

The project timeline is shown in Table 1:

Table 1: Program schedule, tasks, and final deliverables.

	Task	Start	Completion
1.	**Optimize ultra-low energy (ULE) nanocomposite RO membrane**	05/2012	04/2013
1.1	Optimize nanocomposite RO membrane formulation	05/2012	12/2012
1.2	Optimize nanocomposite RO membrane pilot-scale fabrication process	09/2012	01/2013
1.3	Test ULE RO membrane flat sheet performance with simulated water	09/2012	01/2013
1.4	Fabricate 2"x12" ULE RO membrane elements	12/2012	04/2013
1.5	Test 2"x12" ULE RO element performance with simulated waters	01/2013	04/2013
2.	**Design and validate lab-scale MBR/ULE nanocomposite RO wastewater treatment system**	09/2012	12/2013
2.1	Obtain representative wastewater samples and compositions	09/2012	06/2013
2.2	Evaluate MBR pretreatment of gray water	12/2012	05/2013
2.3	Evaluate range of MBR effluents on RO membrane performance	01/2013	06/2013
2.4	Design, fabricate, and validate lab-scale MBR/ULE RO prototype system	02/2013	11/2013
2.5	Develop deployable wastewater treatment system performance and cost models	06/2013	11/2013
3.	**Project management**	05/2012	05/2013
3.1	Submit quarterly progress reports	05/2012	01/2014
3.2	Submit draft final report		03/2014
3.3	Submit draft Interim report/Go No-Go decision point white paper		05/2013
3.4	Submit final report		05/2014
3.5	Final debrief		05/2014

VI. Results and Discussion

4.1 Task 1-Optimize Ultra-Low Energy (ULE) Nanocomposite RO Membranes

4.1.1 Objectives

- The key objectives of this task are:
- Synthesize mesoporous, colloidal silica nanoparticles with controlled characteristics (e.g., particle size, pore size, porosity)
- Conduct nanocomposite RO membrane pilot-scale fabrication experiments to determine the optimized formulation and process window
- Characterize nanoparticles and fabricated nanocomposite membranes using tools including scanning electron microscopy (SEM), transmission electron microscopy (TEM), and Brunauer, Emmett, and Teller (BET) surface area analysis
- Characterize water permeance and salt rejection of the nanocomposite RO membranes
- Fabricate lab-scale 1.8”x12” prototype spiral-wound RO membrane elements
- Make a go/no-go decision based on whether the nanocomposite membranes are capable of meeting the targets of water permeance ≥ 16 and sodium chloride rejection ≥ 99.5%

4.1.2 Mesoporous Silica Nanoparticles Synthesis and Characterization

4.1.2.1 Introduction

Porous silica nanoparticles of controlled size (<100nm) were synthesized for their incorporation into thin film composite reverse osmosis (RO) membranes as a means to improve membrane permeance, while still maintaining a high salt rejection (>99.5%).

The use of commercial silica nanoparticles presents several challenges, including a wide particle size distribution and an inability to keep the particles dispersed in organic solvents such as Isopar G, the solvent of choice to make the thin film RO membranes. The goal using this particular high yield synthesis method was to generate uniform-sized nanoparticles with high surface area and porous structure that could remain stable in Isopar G for several hours. A condensation reaction where the silica precursor tetraethyl orthosilicate (TEOS) is added to an aqueous alkaline solution containing a cationic surfactant as a growth-directing agent resulted in the formation of silica particles of the desired size range (50-80nm) that remained stable in the aqueous phase following a two-fold dilution in water for several weeks. Several batches of particles were made under the same conditions, demonstrating the reproducibility of the method. Additionally, scale-up batches (0.39g SiO_2 to 1.75g SiO_2) were made simply by proportionally increasing the amount of TEOS and reaction solution. These larger batches displayed similar particle size distribution.

Removal of the templating agent cetyltrimethylammonium chloride (CTACl) was carried out by first freeze-drying the aqueous solution in liquid nitrogen and drying under vacuum for 48-72 hours. Calcination in air for two hours at both 400°C and 600°C were performed on the freeze-

dried particles. Particles calcined at 400°C were black in color, likely the result of residual carbon that had yet to be burned off completely during the calcination. Increasing the temperature to 600°C burned off all of the carbon and generated a white powder typical of commercial silica products. TEM and SEM imaging of template-extracted particles re-suspended in ethanol and Isopar G revealed discrete particles, less than 50nm in size. The freeze-drying step prior to calcination may prevent increased agglomeration of the highly concentrated aqueous solution that can occur upon conventional drying methods.

Calcined particles could be temporarily (<60 min) dispersed in Isopar through the use of vigorous stirring and sonication. Several membrane coater trials were performed to incorporate GEGR silica nanoparticles into the RO membrane thin films produced on the GEGR pilot coater. Membrane performance was evaluated to determine if our mesoporous material could increase permeance and maintain high salt rejection. Initial results indicated an increase in membrane salt rejection and permeance (as compared to the control membrane) through the use of GEGR synthesized particles that was not previously observed. This preliminary data suggests that small particles (<50nm) could be more effectively incorporated in the thin film, resulting in enhanced membrane performance.

4.1.2.2 Experimental Section

Silica nanoparticles were synthesized following a modified form of the procedure from the literature[12,13] and then scaled up for higher yield syntheses accordingly. The reactions were performed at room temperature in an effort to control particle growth in solution. Particles were freeze-dried in liquid nitrogen in an effort to prevent particle agglomeration in the drying steps and then calcined at two different temperatures to successfully remove all of the templating agent and organic material to yield a mesoporous solid product.

Particle Synthesis

A stock solution containing 64 mL of deionized water (3.55 mol), 10.5 mL of ethanol (0.179 mol), and 10.4 mL of a 25 wt% CTACl solution (7.86 mmol) was stirred for 5-10 minutes (200-250 RPM). 4.1 mL of Triethanolamine (TEA, 0.031 mol) was then added and further stirred until dissolved. For small scale batches (0.39 g, 0.94 wt% Si02), 1.455 mL (6.5 mmol) of TEOS was added drop wise (in 1-2 minutes), under vigorous stirring (500 RPM). The mixture was allowed to react on the stir bar for two hours, after which 20 mL of deionized water was added to dilute the sample and prevent further hydrolysis and gelation. The entire solution was left to stir for 1-3 hours and resulted in a milky white mixture (Figure 2a). For higher synthesis yields (1.75 g, 0.94 wt% SiO_2), 6.47 mL of TEOS was added drop wise (less than 2 minutes) to the 89 mL stock solution, and 90 mL of deionized water was added to the final sample. The synthesized particles were found to remain stable in solution for up to two weeks.

Template Extraction

The aqueous particle solution (Figure 2a) generated from the synthesis procedure was freeze-dried using liquid nitrogen and then vacuum dried for 48-72 hours, leaving a fluffy white powder (Figure 2b). Calcination in air was selected as the method to remove the templating agent and all organics in solution, leaving behind porous silica nanoparticles in powder form. The calcination was initially performed at 400°C for two hours, and generated a black powder (Figure 2c). A second calcination was done on a new batch of particles, increasing the temperature to 600°C for

two hours in an effort to remove what appeared to be residual carbon left behind. Following the 600°C drying step, particles were left as a white dust-like powder, typically seen with commercial silica products (Figure 2d).

Particle Characterization

SEM and TEM images were collected at GEGR on a Hitachi SU-70 and FEI TF20 Tecnai 200KV instrument, respectively. Samples were prepared by evaporating a drop (usually 200µl) of the aqueous particle solution onto a holey carbon-coated 300 mesh nickel grid. For template extracted solid particles, a small amount of product (<10mg) was re-suspended in 10mL ethanol and a 200µl drop was evaporated on the grid. Surface area and pore size analyses were conducted externally at Micromeritics Analytical Services and at GEGR using a Micromeritics ASAP 2020 Accelerated Surface Area & Porosimetry System. Surface area measurements were obtained using nitrogen sorption isotherms and calculated from the Brunauer-Emmett-Teller (BET) equation. Pore size distribution and volume data were generated using the Barrett-Joyner-Halenda (BJH) method. Template extracted particles (600°C calcination) were suspended in ethanol or Isopar G to make a 0.1 wt% solution and then passed through a 0.2 µm filter to remove any large aggregates. Particle size distributions were obtained using a Brookhaven Dynamic Light Scattering instrument at 25°C and applying a Contin Fit algorithm to the correlation function. The average particle size and polydispersity index (PDI) were recorded.

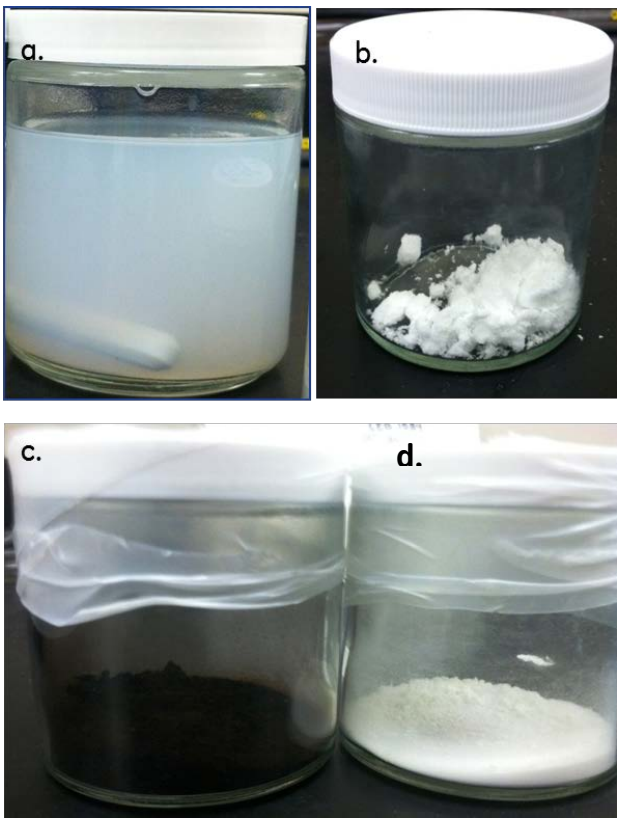

Figure 2: a) Silica nanoparticles synthesized in aqueous phase. b) Freeze-dried silica nanoparticles. c) and d) Template- extracted silica nanoparticles following calcination at 400°C (c) and 600°C (d).

4.1.2.3. Results and Discussion

Stable aqueous solutions of mesoporous silica nanoparticles were successfully synthesized following a modified procedure from the literature[12,13]. Performing the condensation reaction at room temperature with a final dilution in deionized water generated particles of uniform size (40-80 nm), that could remain in solution without further hydrolysis and gelation for 1-2 weeks. This synthesis method demonstrated strong reproducibility and scale-up capability. Particle size and morphology were characterized on several batches through the use of electron microscopy. TEM and SEM images of the first batch of aqueous particles synthesized at room temperature revealed discrete spherical particles that were less than 100nm in size and showed little agglomeration (Figure 3 and Figure 4). The average size of the particles in the aqueous phase was 40-80nm, well below the 100nm desired size range (Figure 3b, Figure 4b, and Figure 4d). SEM imaging performed on repeat synthesis batches of aqueous particles (following the same step-by-step procedure) confirmed that silica particles with controlled size could be generated repeatedly to yield uniform-sized particles (Figure 4c & d). Energy-dispersive X-ray spectroscopy (EDS) was an additional analytical technique used while imaging particles to confirm the presence of silica in the samples (Figure 3c and Figure 4e).

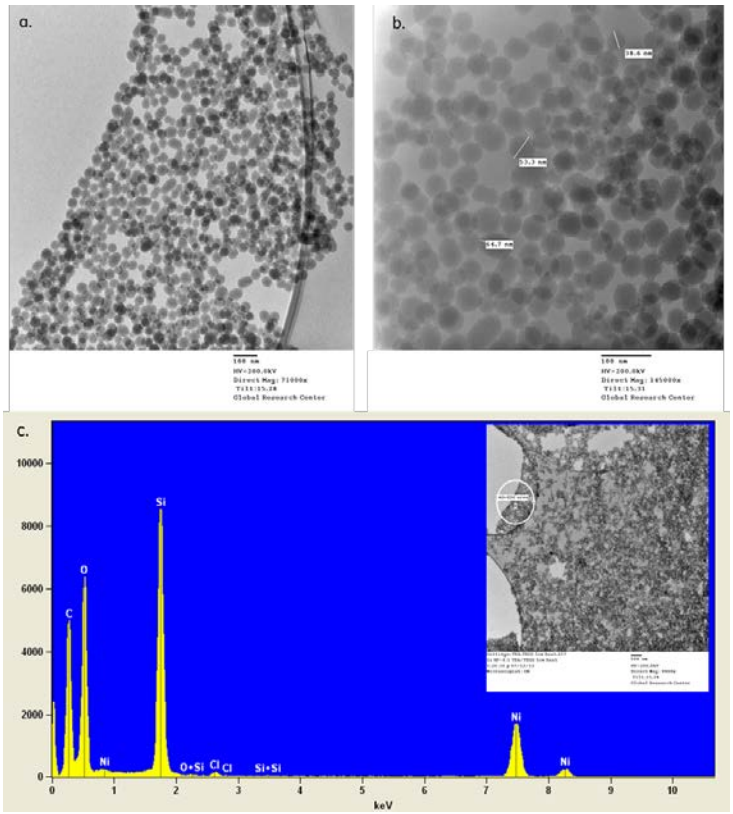

Figure 3: TEM images. a) Silica nanoparticles in aqueous phase at low magnification (71000x). b) Silica nanoparticles in aqueous phase at high magnification (145000x). c) EDS-analyzed region circled in white on accompanying TEM image.

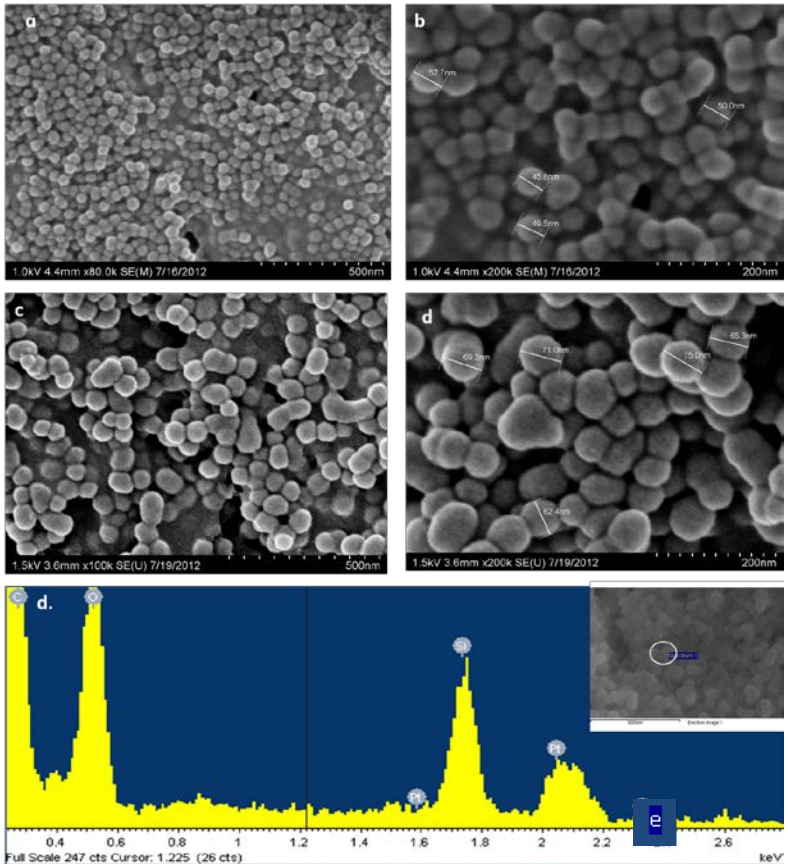

Figure 4: SEM images. a) and b) Silica nanoparticles in aqueous phase. c) and d) Repeat syntheses of particles in aqueous phase. e) EDS-analyzed region circled in white on accompanying SEM image.

Following template extraction, SEM and TEM images revealed particles of a slightly smaller size range (20-50 nm), indicating that some of the surfactant may have been surrounding the outside of the particles prior to removal (Figure 5 & Figure 6). Contrast in the TEM images appears to show visible pore structures in each of the particles, taking on a "honey-comb" like appearance (Figure 5), similar to literature results[12,13].

SEM images of 400°C and 600°C calcined particles revealed no significant changes with respect to particle morphology and size, however higher temperature calcination was used moving forward to generate white particles with no residual carbon left behind (Figure 6 & Figure 7). In addition, calcined particles could be re-suspended in both ethanol and Isopar G and remain stable for 30-60 minutes through the use of vigorous stirring and sonication. The presence of individual discrete particles following sample preparation (drying a drop of particle solution onto a grid) suggests that GEGR synthesized particles can be re-dispensed in a variety of solutions for further application (Figure 6 & Figure 7).

Dynamic light scattering (DLS) measurements were performed on template extracted particles re-suspended in ethanol or Isopar G. Results from this analysis revealed slightly larger particle sizes than observed using electron microscopy. The differences in particle size between these

two techniques have been noted in previous studies, and are likely a result of particle aggregation [13]. The mean diameter for the calcined particles in ethanol was 70 nm with a PDI of 0.307, displaying a narrow particle size distribution (Figure 8). DLS measurements taken on particles dispersed in Isopar G again exhibited a narrow size distribution (PDI = 0.213), however the mean particle diameter increased almost two-fold (Figure 9). Increased aggregation of non-functionalized particles in an organic solution such as Isopar G is expected and likely the cause of the differences seen in particle size compared to the ethanolic suspensions.

The surface area and pore diameter of the samples were determined by nitrogen adsorption. Figure 10 shows the N_2 adsorption–desorption isotherm by plotting the adsorbed volume as a function of the gas pressure (P) normalized by the adsorptive saturation pressure (P0). Furthermore, the experimental data were fitted using the BJH model to determine the pore sizes, and the BET method to determine the pore surface area. BET surface areas for freeze-dried particles ("control") and 400 °C and 600 °C calcined products are determined to compare changes in surface area following template removal. The results revealed an increase in surface area from 16.39 m^2/g in the control particles to 759.61 m^2/g after calcination at 400°C, indicating successful removal of organics. A repeat analysis was performed at both GEGR and Micromeritics on particles calcined at 600°C. In addition to BET surface area, pore size distribution and volume were obtained for these two samples. Micromeritics and GEGR data revealed surface area measurements of 714.10 m^2/g and 735.15 m^2/g respectively, for particles calcined at 600 °C. These results are comparable to particles calcined at 400 °C and demonstrate once again the repeatability of the synthesis and template extraction methods. 600 °C calcined particles displayed a large pore volume of 0.9374 cm^3/g (Micromeritics) and 1.001 cm^3/g (GEGR), with an average pore diameter of 6.5 nm (Micromeritics) and 6.8 nm (GEGR).

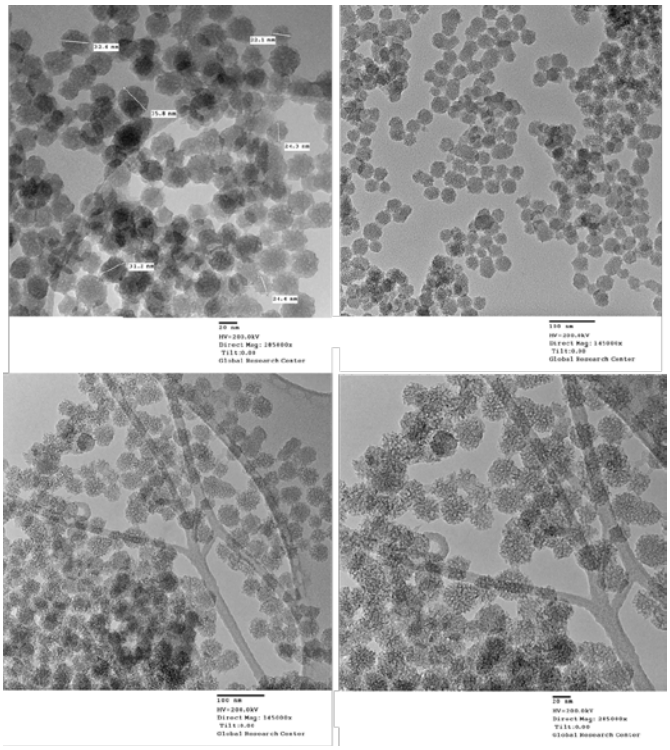

Figure 5: TEM images of silica nanoparticles calcined at 400°C.

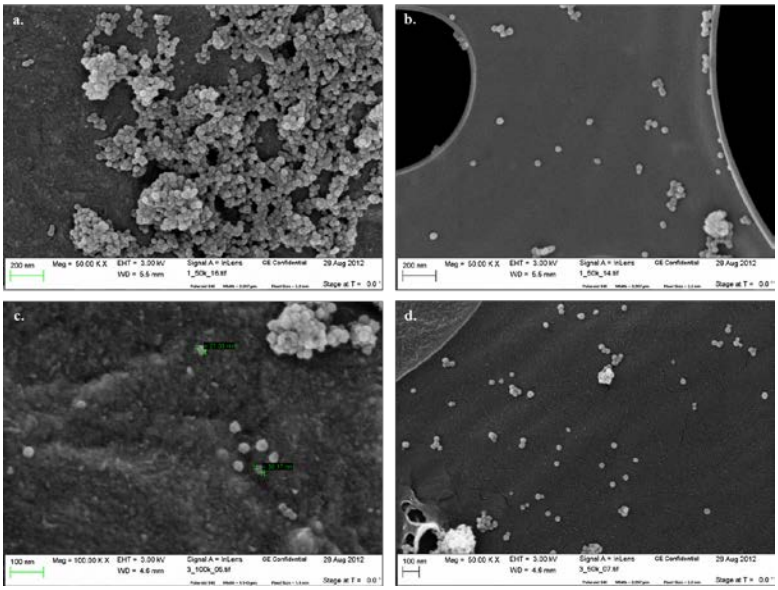

Figure 6: SEM images. a) and b) 400°C calcined silica nanoparticles re-suspended in ethanol. c) and d) 600 °C calcined silica nanoparticles re-suspended in ethanol.

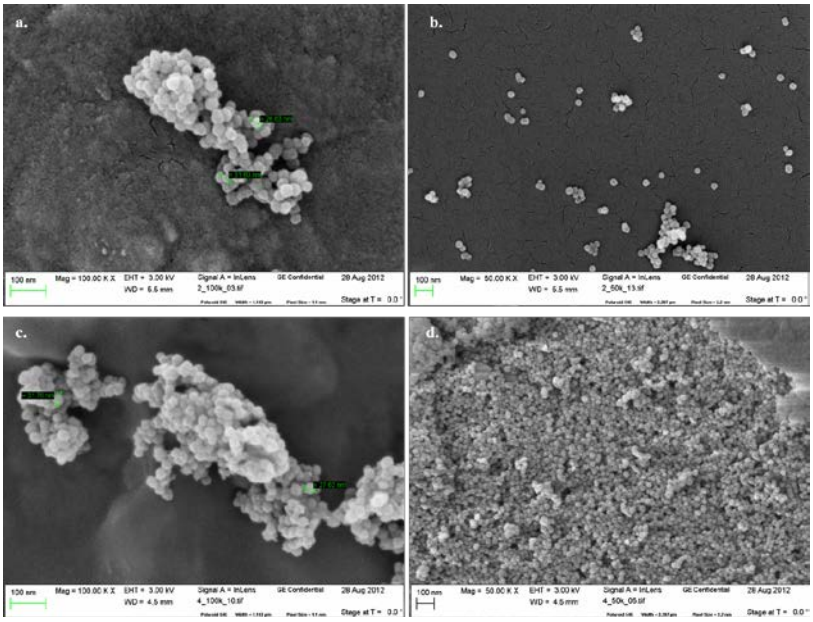

Figure 7: SEM images. a) and b) 400°C calcined silica nanoparticles re-suspended in Isopar G. c) and d) 600 °C calcined silica nanoparticles re-suspended in Isopar G.

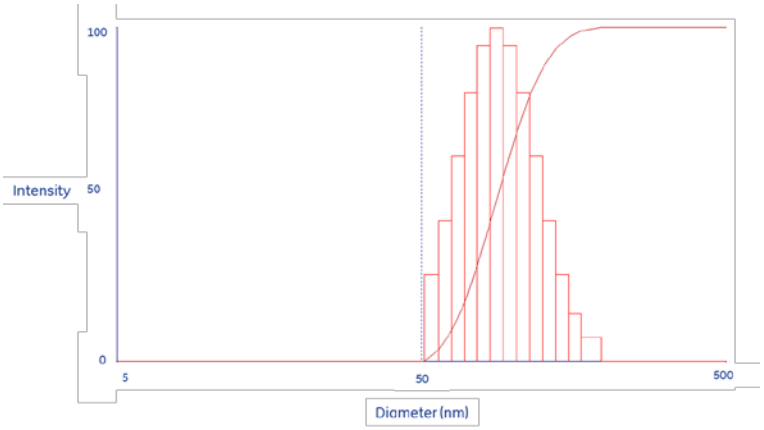

Figure 8: DLS particle size distribution of 600 °C template-extracted particles in ethanol.

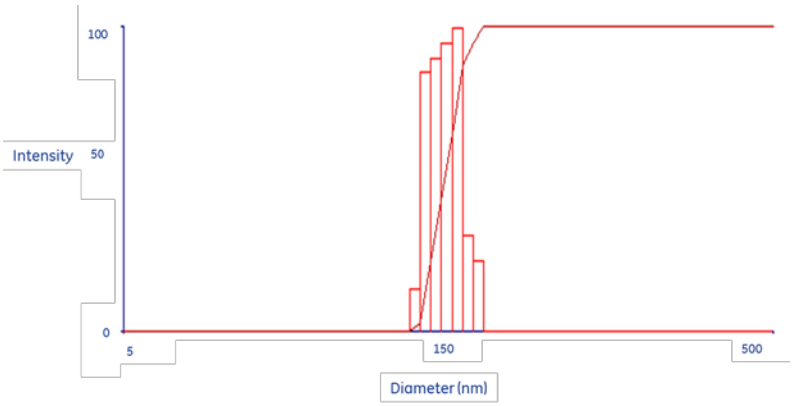

Figure 9: DLS particle size distribution of 600 °C template-extracted particles in Isopar G solvent.

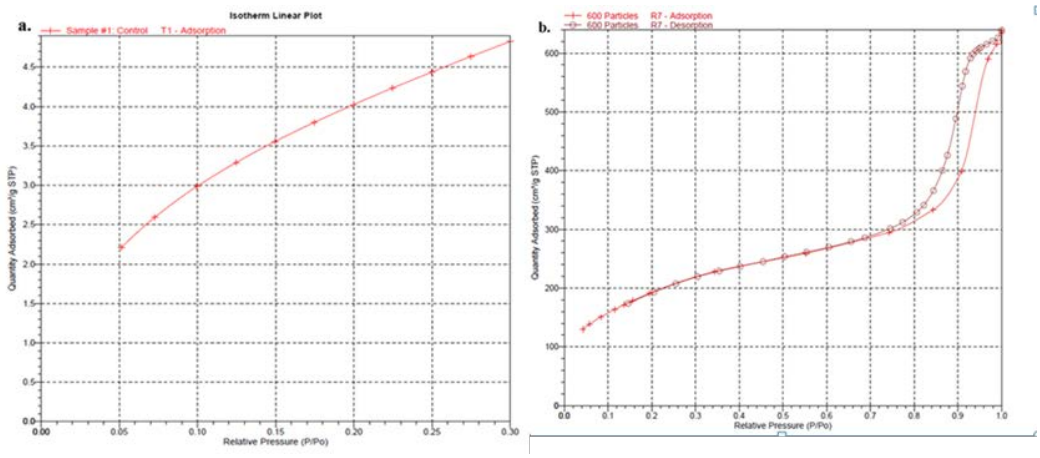

Figure 10: Nitrogen sorption isotherms of: a) control, freeze-dried particles and b) 600 °C calcined particles (graph and analysis performed by Micromeritics Analytical Services), plotted as a function of the gas pressure (P) normalized by the adsorptive saturation pressure (P0).

GEGR synthesized silica nanoparticles were used in a series of preliminary coater run trials in order to incorporate the mesoporous material into the RO thin film membranes. Prior to these trials, a variety of commercialized silica nanoparticles and other nanomaterials were tested in an effort to improve flux through the membrane (by way of small pore channels in the nanoparticles), while still maintaining high salt rejection. One of the major issues faced with commercial products is the wide particle size distributions, often with particles larger than the thin film layer itself (>100nm). The lack of controlled particle size with many of the commercial materials tested by GEGR prompted this particular particle synthesis experimental study. 400°C and 600°C calcined particles were used in an initial hand-pour coater run to determine: 1) if the particles could be incorporated into the thin films without creating any defects (i.e. passing a dye stain test), and 2) if the particles demonstrated any significant improvements in membrane flux or salt rejection. Additionally, any changes with respect to performance and/or membrane quality were noted for particles calcined at 400°C versus 600°C. The preliminary data on membrane performance and the morphology characterization for nanocomposite membranes made using GEGR synthesized silica nanoparticles are summarized in the subsequent sections. These performance and characterization results show improvements in membrane performance, in particular, increased salt rejection was observed with much higher flux rates compared to control membranes (without particles).

4.1.2.4 Conclusions

Mesoporous silica nanoparticles with controlled, uniform particle size of 30-50 nm and large surface area (>700 m^2/g) were repeatedly synthesized following a condensation reaction in an aqueous solution with the use of a cationic surfactant as a templating agent. Performing the synthesis at room temperature helped to controlled particle growth and a final dilution in water left highly stable particle suspensions. The use of an intermediate freeze-drying step prior to template extraction (via calcination) appears to be a crucial step in preventing increased agglomeration of the highly concentrated particle solution upon drying. Heating the dried particles to 400°C and 600°C removed the templating agent and all organic material, leaving behind silica nanoparticles in a solid powder form that could be re-suspended in ethanol and organic solutions, including Isopar G. The synthesized silica nanoparticles were successfully used in the fabrication of the thin film composite RO membrane. In addition to thin film production, this simple and high-yield synthesis method has the potential to be used across a wide range of applications.

4.1.3 Optimize Nanocomposite RO Membrane Pilot-Scale Fabrication

4.1.3.1 Introduction

Continuous roll-to-roll production of RO membranes containing nanomaterials requires additional process optimization compared to the standard RO membrane production process. For example, mixing and delivery of the nanomaterial-containing solution must be addressed in the nanocomposite RO production process in order to produce a repeatable, robust product with the desired performance. In this study, the impact of nanomaterials and process conditions were systematically studied to determine the optimal pilot-scale fabrication process.

4.1.3.2 Experimental Section

Nanocomposite membranes were fabricated by a dip-slot die coating process, using a modified air knife (i.e., organic coating knife) instead of a slot die to deliver the organic solution. In the dip-coating knife process of fabricating interfacially polymerized polyamide nanocomposite RO membranes, a wet UF support web enters a first coating tank where it is soaked with an aqueous metaphenylene diamine (mPD) solution. After the excess aqueous solution is metered off, a precise amount of trimesoyl chloride (TMC)/Isopar G solution containing nanomaterials is delivered to the mPD imbibed UF web by a coating knife. Knife coating is especially beneficial as the nanomaterial agglomeration and sedimentation issues commonly encountered in a dip coating tank is largely eliminated in the knife coating process, due to significantly reduced residence time of a nanomaterial dispersion in the slot die (Figure 11). The nanocomposite RO membrane formulation was optimized to give the highest possible water permeance without compromising salt rejection.

Membrane Permeation Test
Testing was conducted on the RO flat sheet crossflow test bench at GEGR. The test bench is equipped with 18 crossflow cells (Sterlitech model CF040) with an effective membrane area of 41.86 cm^2. The cells are plumbed three in series in each of 6 parallel lines. Each line of cells has a valve to turn feed flow on/off and regulate concentrate flow rate, which was set to 1 gallon per minute (gpm) in all tests. The bench is equipped with a temperature control system that includes a temperature probe, a heat exchanger which removes excess heat generated by pumping, and an air-cooled chiller which reduces the temperature of the coolant that circulates in the heat exchanger.

Composite membranes were first tested with a fluorescent red dye (rhodamine WT from Cole-Parmer) to detect defects. A dye solution comprising 1% rhodamine red dye was sprayed on the polyamide surface of the composite membrane and allowed to stand for 1 minute, after which time the red dye was rinsed off. Since rhodamine red dye does not stain polyamide, but stains polysulfone strongly, a defect-free membrane should show no dye stain after a thorough rinse. Conversely, dye stain patterns (e.g. red spots or other irregular dye staining patterns) indicate defects in the composite membranes.

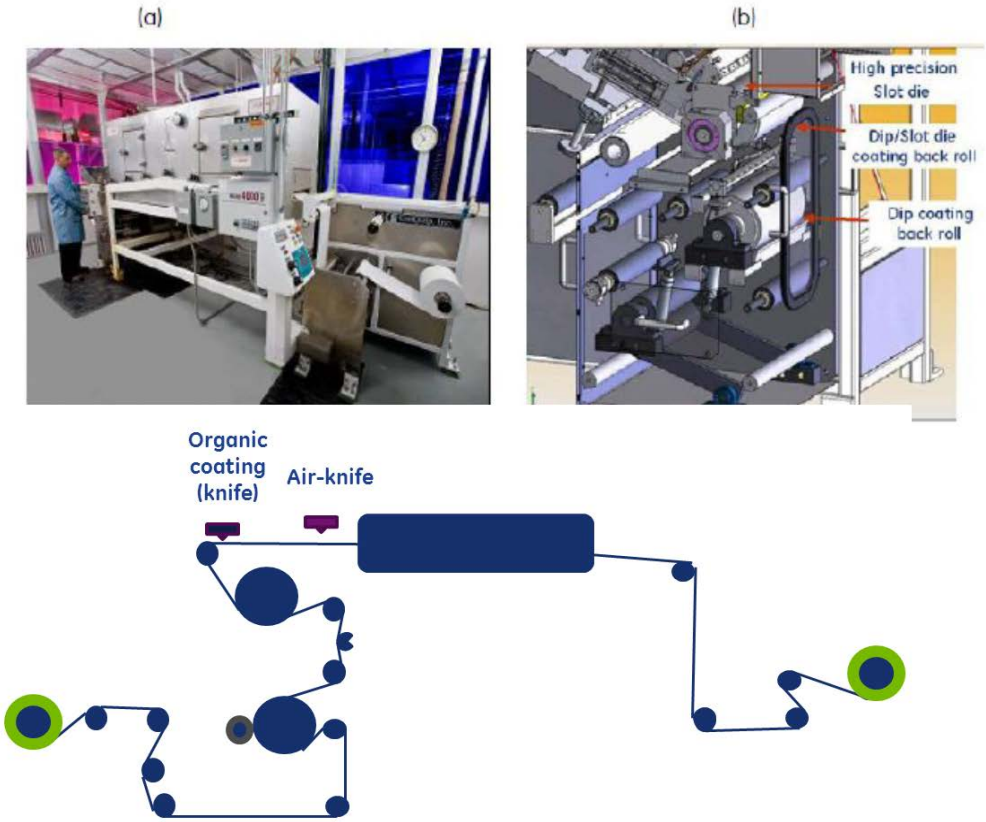

Figure 11: a) Photo of the GEGR pilot membrane coater; b) configuration of the coating station; and c) web path of the dip-knife coating process for RO membrane fabrication.

RO permeate water with conductivity less than 10 μS/cm was used to prepare the feed for the membrane performance test. The RO water was generated by passing Niskayuna city water through an RO unit. The membrane samples were cut into 2”x6” rectangular pieces, tested with the red dye to detect defects, and loaded into the crossflow testing cells. Three or more coupons from each experiment were tested under the same conditions and the results obtained were averaged to obtain the mean and standard deviation.

During testing of the brackish water RO membranes, the membrane samples were first cleaned by circulating water across the membranes in the test cells without recycling the permeate for 30 minutes to remove any residual chemicals and dyes. Afterwards, synthetic brackish water containing a specified amount of sodium chloride was circulated across the membranes at a specified operating pressure and 25 ^{o}C. Typically after one hour of operation, permeate samples were collected for 10 minutes. The crossflow rate for each line of cells was set to 1.0 gpm using the corresponding valves and flow meters.

After these test steps, the membranes were exposed to 70 ppm of sodium hypochlorite at 25 ^{o}C for 30 minutes; followed by rinsing with water for 15 minutes to remove the sodium hypochlorite, then tested again under the same synthetic brackish water conditions described in the previous paragraph.

The solution conductivities and temperatures were measured with a CON 11 conductivity meter (Oakton Instruments) which temperature compensates conductivity measurements to 25°C. The pH was measured with a Russell RL060P portable pH meter (Thermo Electron Corp).

Permeate was collected with a graduated cylinder. The weight of permeate was measured using a Navigator balance and a Fisher Scientific stopwatch was used for timing. Membrane A value was calculated based on permeate weight, collection time, membrane area, and transmembrane pressure. The salt concentrations in the feed and the permeate solutions were measured by conductivity which were in turn used to calculate salt rejection.

The permeate flux through the membrane is obtained from Eq. 1:

$$J_w = A \cdot TCF \cdot (\Delta P - \Delta\pi) \qquad \text{(Eq. 1)}$$

where J_w is the permeate flux, A is the water transport coefficient, or A value (with units of 10^{-5} $cm^3/(cm^2\text{-s-atm})$), at standard temperature of 25°C, TCF is the temperature correction factor for the water permeance[14], ΔP is the transmembrane pressure drop, and $\Delta\pi$ is the osmotic pressure difference across the membrane.

Salt flux, J_s, is given by Eq. 2:

$$J_s = B \cdot TCF \cdot (C_{sf} - C_{sp}) \qquad \text{(Eq. 2)}$$

where B is the salt transport coefficient, or B value (with units of 10^{-5} $cm^3/(cm^2\text{-s})$), and C_{sf} and C_{sp} are the salt concentrations in the bulk feed and permeate solutions, respectively.

Salt passage and rejection are calculated by Eqs. 3 and 4:

Salt passage $$SP = \frac{C_{sp}}{C_{sf}} \times 100\% \qquad \text{(Eq. 3)}$$

Salt Rejection $$R = (1 - \frac{C_{sp}}{C_{sf}}) \times 100\% \qquad \text{(Eq. 4)}$$

Salt rejection values calculated using the bulk feed concentration are commonly referred to as apparent salt rejection. They generally fall below the true salt rejections of the membrane due to concentration polarization, which increases the salt concentration at the membrane surface above the bulk solution concentration[15–18]. All salt rejection data reported here are apparent salt rejections.

The following equations are used for converting conductivity, measured in microsiemens per centimeter ($\mu S\ cm^{-1}$), to the concentration of NaCl[19]:

if $K > 10^4$,

$$C = 6.05\times10^{-3} + 2.20\times10^{-5}\times k + 3.394\times10^{-6}\times k\times \ln(k) + 6.29\times10^{-11}\times k^2 \qquad \text{(Eq. 5)}$$

If $K \le 10^4$,

$$C = 4.63\times10^{-5}\times k + 9.44\times10^{-8}\times k^{1.5} - 1.40\times10^{-11}\times k^2\times \ln(k) \qquad \text{(Eq. 6)}$$

where C is the wt% of NaCl and k (or K) is conductivity of the NaCl solution in μS cm^{-1}.

Materials

Both commercially available silica particles and GEGR synthesized mesoporous silica nanoparticles were used. Silica particles supplied by US Research Nanomaterials, Inc. (US3440) are specified to have a particle size of 15-20 nm. However, dynamic light scattering (DLS) data as well as observations of organic knife plugging during pilot coating demonstrate that there is actually a wide particle size distribution. While the primary particle size is 15-20 nm, particle agglomeration occurs when the particles are dried into powder form (i.e., form shipped to customer), and the size distribution of these agglomerates is captured by DLS measurements.

4.1.3.3 Results and Discussion

Particle Size

In order to determine the performance of nanocomposite membranes fabricated with known sizes of silica particles/agglomerates, the dry silica powder (US3440) was sieved through a series of decreasing mesh sizes and each fraction was used in the organic phase to fabricate nanocomposite membranes with silica of a known size range. Cyclohexanone was also added to the organic phase (1.25%(v)) as a flow enhancer. Six size fractions of silica were used: <38 μm, 38-75 μm, 75-106 μm, 106-150 μm, 150-300 μm, and >300 μm. Figure 12 shows the performance of the control , control with 1.25%(v) cyclohexanone added to the organic phase, and the six nanocomposite membranes with 0.1%(w/v) of the sieved silica fractions and 1.25%(v) cyclohexanone added to the organic phase. Both pre-chlorination (Figure 12a) and post-chlorination (Figure 12b) data are presented, however, elements are chlorinated before shipment to customers, so the post-chlorination data are more representative of the expected element performance.

As shown in Figure 12b, nanocomposite membrane performance is independent of silica size range. The addition of cyclohexanone alone to the organic phase yields an 85% increase in A value (14.3 vs. 7.7), while the addition of silica further increases A value to around 16.5. NaCl passage increases with the addition of cyclohexanone (0.61% vs. 0.26%), but silica does not cause further increase in NaCl passage.

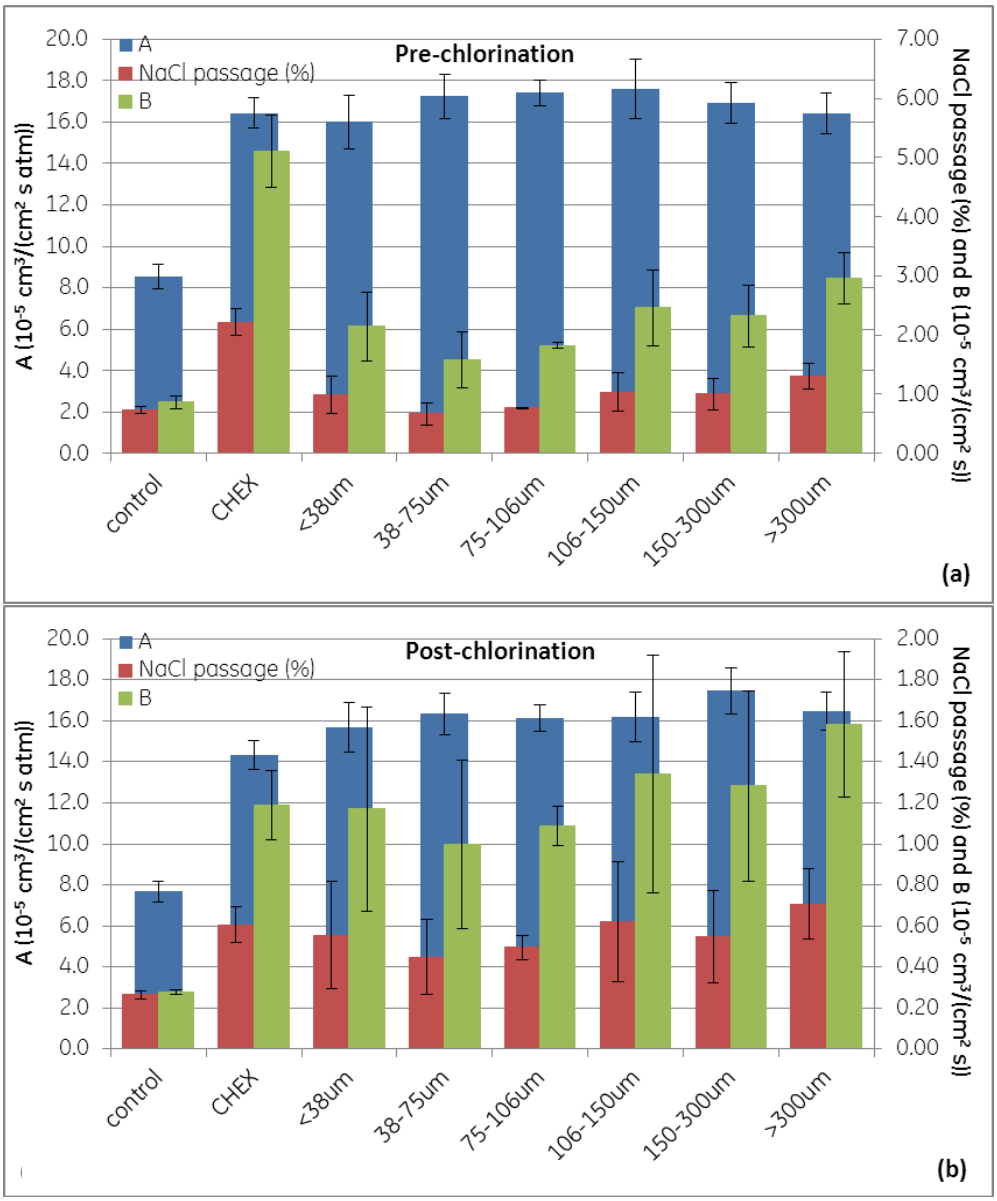

Figure 12: (a) Pre-chlorination and (b) post-chlorination performance (A value, B value, NaCl passage) of nanocomposite membranes with the indicated silica size fractions (US3440). Membranes were fabricated on P415 UF support.

Process Conditions-Line Speed
Figure 13 illustrates the performance (A value, B value, NaCl passage) obtained for several membranes fabricated at line speeds of 4 and 8 ft/min. The post-chlorination data indicate that while line speed does not impact A value, higher line speed yields higher NaCl passage and B value, as expected. Dryer residence time may not be the only issue; saturation of the post-aqueous coating nip roller at higher line speeds may prevent complete removal of aqueous solution from the UF membrane surface, leading to defects in the thin polyamide film. The GEGR pilot coater was operated at 4 ft/min subsequently, and the organic solution delivery was monitored for any potential flowback. Flowback only happened when the organic knife became clogged with large agglomerates of particles during nanocomposite membrane coating. Frequent changing and cleaning of the organic knife during coating runs was found to prevent flowback from becoming an issue, allowing smooth operation at 4 ft/min.

Gravity-fed vs. Pump-fed Organic Solution Delivery
Two methods have been explored for delivery of the organic solution to the organic knife: gravity (i.e., organic feed tank placed directly above the organic knife) and pumping (i.e., organic solution pumped from feed tank to organic knife). The two methods are illustrated in Figure 14. Gravity feeding replaced pump feeding due to concerns about nanomaterial settling during pumping of the organic solution to the organic knife. However, the organic feed solution was pumped from some distance in production coating, so the effect of pumping the organic solution versus using the gravity feed method must be determined.

Figure 15 illustrates the performance (A value, B value, NaCl passage) obtained for several membranes fabricated using gravity and pumping to deliver the organic solution to the organic coating knife. The post-chlorination data indicate that while delivery method does not affect A value, pumping the organic solution yields higher NaCl passage and B value for membranes made with cyclohexanone added to the organic phase. The reason for this phenomenon is unclear, but a similar trend may be expected on scale up to production.

GEGR Synthesized Mesoporous SiO_2 Nanoparticles
Nanomaterial dispersion instability is thought to be caused, at least in part, by agglomeration of nanoscale primary particles into micron-sized agglomerates during the drying step in particle synthesis. Commercial nanomaterials are supplied as dry powders, whose particle sizes are much larger than the primary particle size specified by the manufacturer. Breaking large, dry agglomerates down into primary particles upon dispersion in the organic coating solvent is challenging due to the particles' affinity for each other and their insolubility in the organic coating solvent. In-house synthesis of SiO_2 particles was explored as a means of exercising better control over particle formation and possibly particle agglomeration. If particles could be synthesized, functionalized (to repel each other and increase solubility in the organic coating solvent) and dispersed in the organic coating solvent without ever being in a dry state, small, uniformly dispersed particles could possibly be obtained.

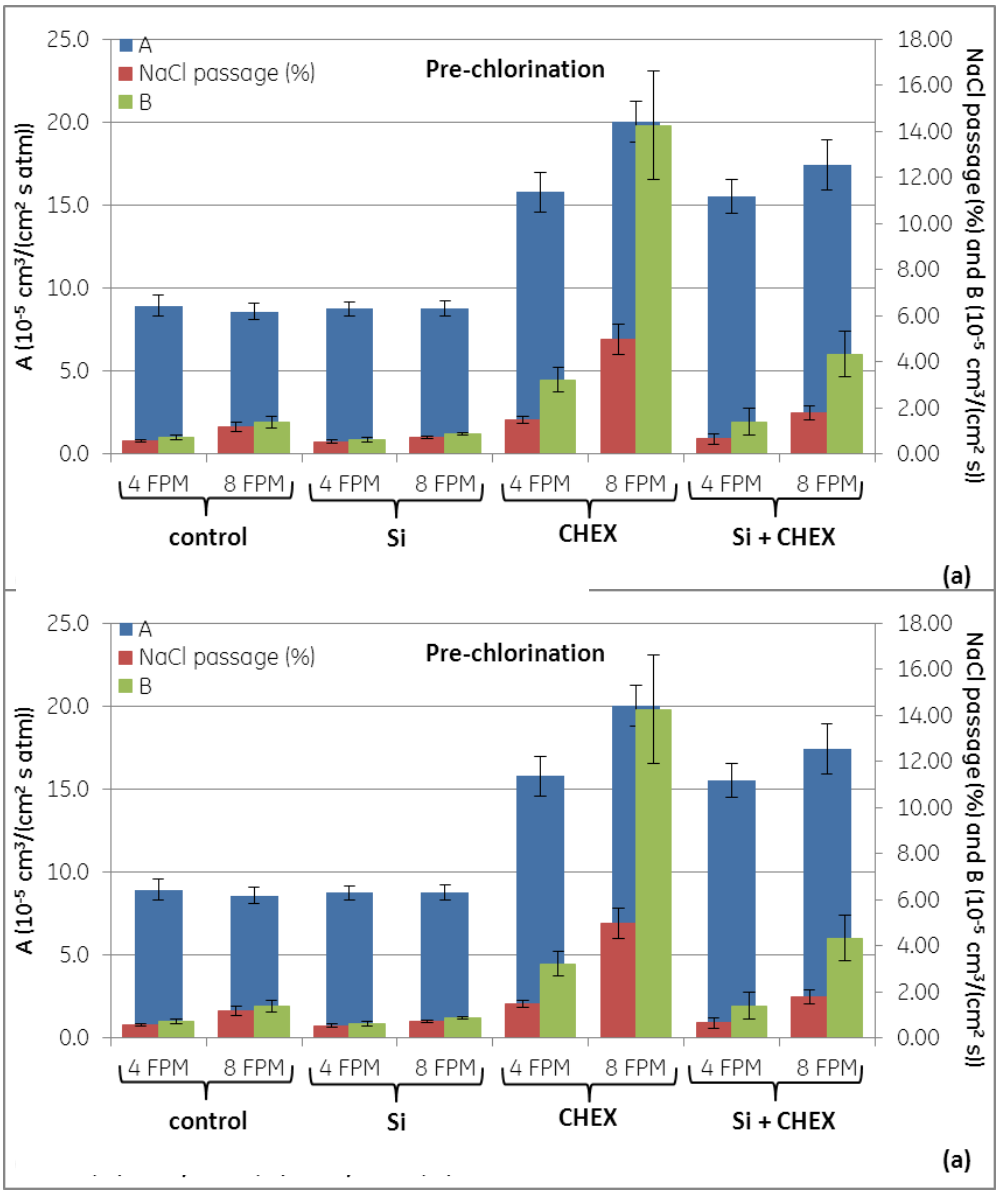

Figure 13: (a) Pre-chlorination and (b) post-chlorination performance (A value, B value, NaCl passage) of membranes fabricated at line speeds of 4 and 8 ft/min (FPM). Membranes were fabricated on P415 UF support. 0.1%(w/v) silica (US3440), 1.25%(v) cyclohexanone (CHEX), or both were added to the organic phase for the non-control membranes.

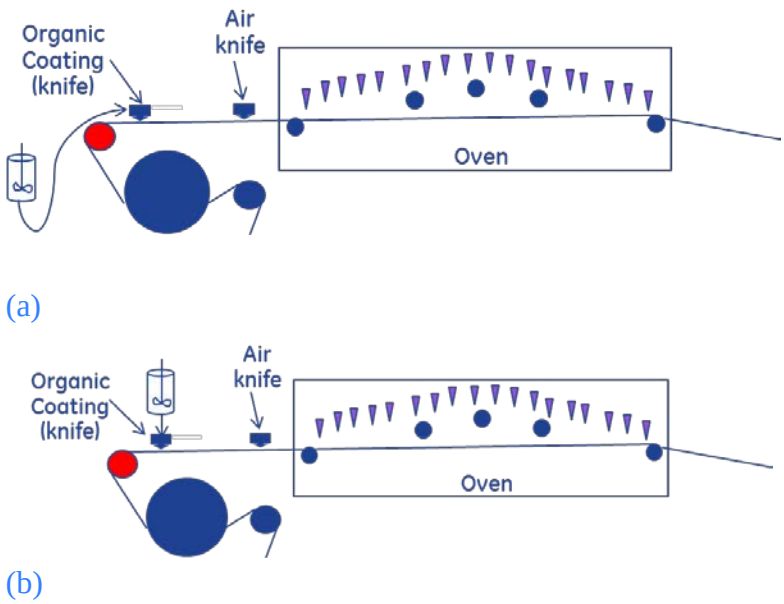

Figure 14: (a) Pumping versus (b) gravity feeding the organic solution to the organic coating knife.

Initial work on mesoporous silica particle synthesis focused on developing a repeatable process to synthesize sub-100 nm particles. Nanocomposite membranes were then fabricated using particles made by the same process, but at different calcination temperatures. Figure 16 shows the performance of the control membrane, control membrane with 1.25%(v) cyclohexanone (CHEX) added to the organic phase, and nanocomposite membranes with 0.1%(w/v) of the GEGR-made SiO_2 particles and 1.25%(v) CHEX added to the organic phase. The SiO2 particles were calcined at 400 or 600 ^{o}C, and the repeatability of the particle synthesis is demonstrated by the performance of nanocomposite membranes made with two different batches of particles calcined at 600 ^{o}C. The pre-chlorination data (Figure 16a) shows similar A values for membranes made with either CHEX or CHEX and SiO_2 particles, although the nanocomposites (i.e., made with CHEX and SiO_2 particles) have lower NaCl passage than membranes made with CHEX alone. However, after chlorination (see Figure 16b), the A value of the membranes made with CHEX alone decreases, giving the nanocomposite membranes higher A value as well as lower NaCl passage. Thus, improvements were observed in membrane performance, in particular, increased salt rejection was observed compared to control membranes (without particles). It appears that the small particle sizes (<50nm) observed in the GEGR-made particles may be more effective than previously used commercial products that often display wide particle size distributions.

Nanocomposite membrane performance is independent of particle calcination temperature. Nanocomposites made with the second batch of 600 ^{o}C calcined particles had higher A value and NaCl passage than those made with the first batch of similarly calcined particles, however, direct analysis of the particles has shown good batch-to-batch repeatability of particle size and surface area.

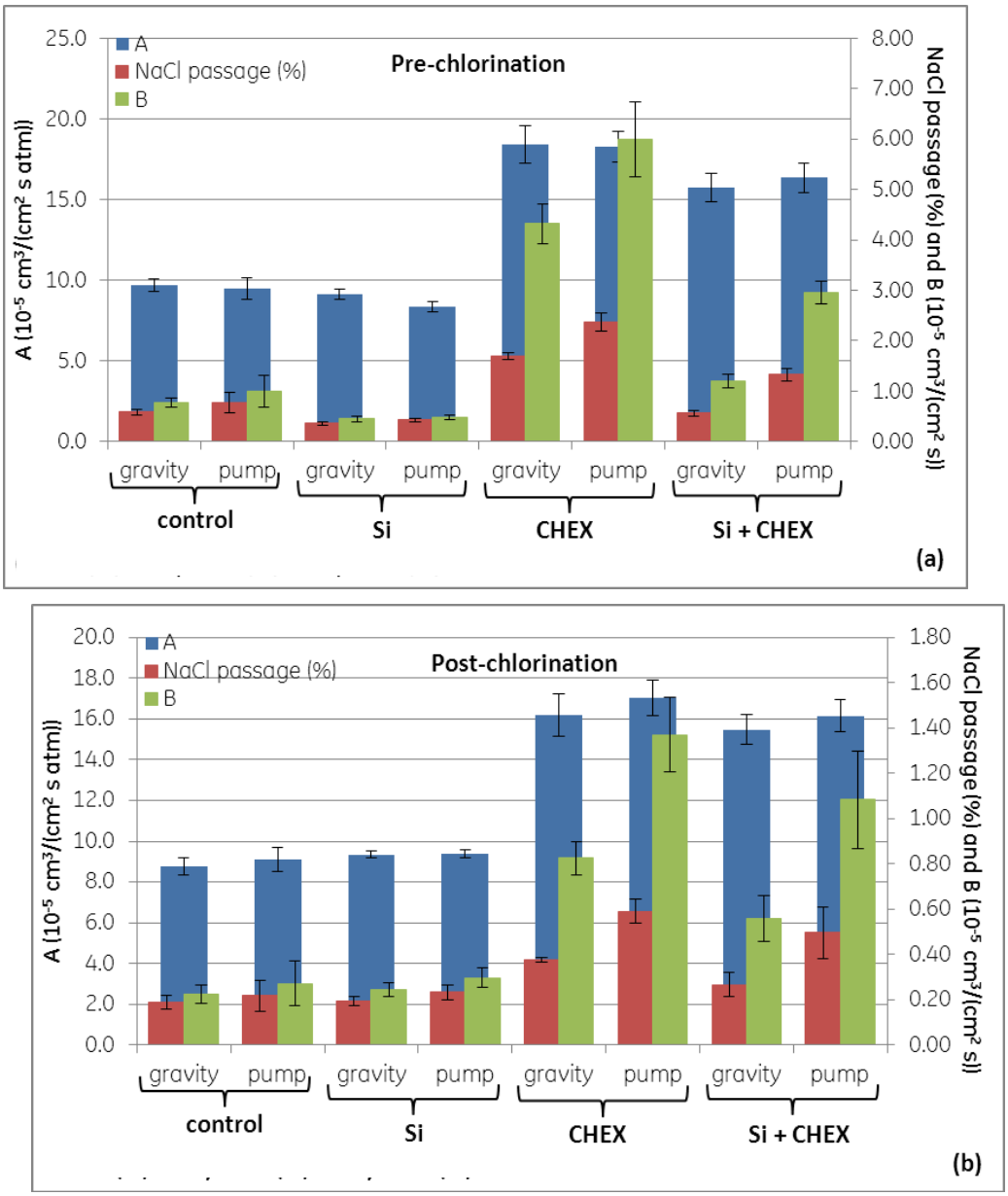

Figure 15: (a) Pre-chlorination and (b) post-chlorination performance (A value, B value, NaCl passage) of membranes fabricated using gravity and pump-delivered organic solutions. Membranes were fabricated on P415 UF support. 0.1%(w/v) silica (US3440), 1.25%(v) cyclohexanone (CHEX), or both were added to the organic phase for the non-control membranes.

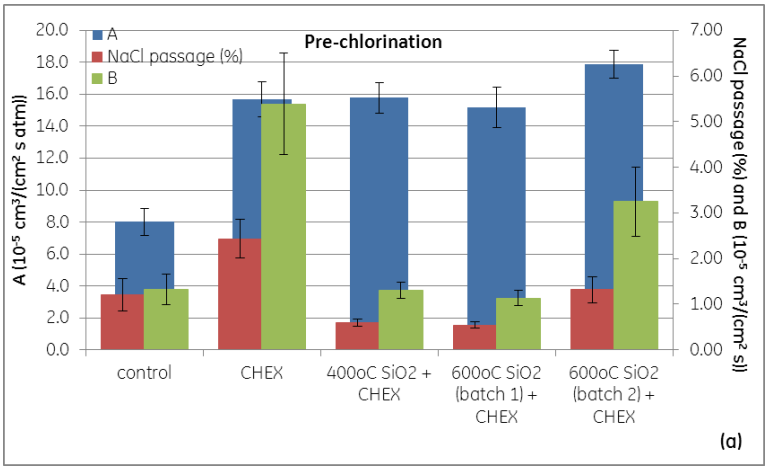

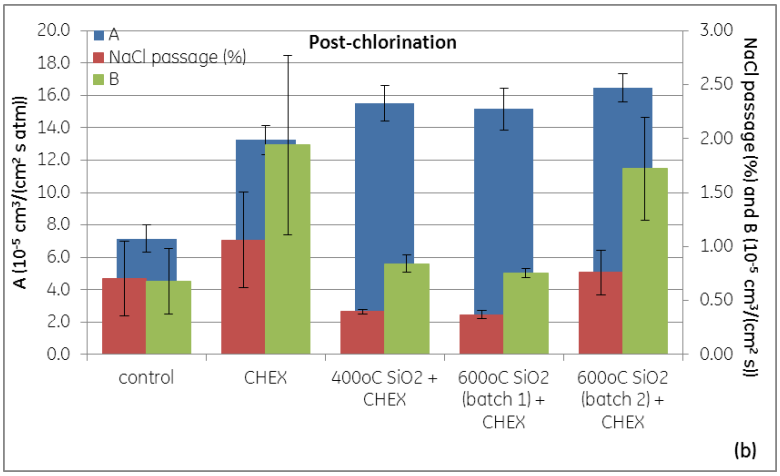

Figure 16: (a) Pre-chlorination and (b) post-chlorination performance (A value, B value, NaCl passage) of nanocomposite membranes with the indicated GEGR-synthesized silica particles. Membranes were fabricated on P415 UF support. 1.25%(v) cyclohexanone (CHEX) was added to the organic phase for all membranes except the control membrane; 0.1%(w/v) SiO_2 calcined at the indicated temperature was also added to the organic phase for the nanocomposite membrane formulations. Particle synthesis repeatability is demonstrated by two batches of particles made at the same conditions and used in nanocomposite membrane fabrication.

Effect of SiO_2 nanoparticle loading

Figure 17 shows the performance of the control membrane, control membrane with 1.25%(v) cyclohexanone (CHEX) added to the organic phase, and nanocomposite membranes with 0.1% and 0.2% (w/v) of the GEGR-made SiO_2 particles and 1.25%(v) CHEX added to the organic phase. The SiO_2 particles were calcined at 600°C. The pre-chlorination data (Figure 17a) shows higher A values for nanocomposite membranes made with CHEX and SiO_2 particles than control membranes or membranes made with CHEX alone, and the nanocomposites (i.e., made with CHEX and SiO_2 particles) have lower NaCl passage than membranes made with CHEX alone. After chlorination (see Figure 17b), the nanocomposite membranes showed higher A value as well as lower NaCl passage than membranes made with CHEX alone. Figure 17 also shows that the membrane A value increases when the mesoporous silica nanoparticle loading increases from 0.1% (w/v) to 0.2% (w/v). Thus, improvements were observed in membrane permeance and salt rejection performance compared to control membranes (without particles). Nanocomposite membranes with 0.2% (w/v) of the GEGR-made SiO_2 particles and 1.25%(v) CHEX added to the organic phase showed a post-chlorination A-value of 16.6 and salt passage of 0.4%, meeting the performance criteria (A value greater than 16 with NaCl passage less than 0.5%).

Repeatability

The commercially available SiO_2 particles (US3440, US Research Nanomaterials, Inc.) have been used to demonstrate the pilot scale repeatability of nanocomposite membrane fabrication. Multiple trials were conducted over a three-month period, all using P415 UF support and the same formulation with 1.25%(v) cyclohexanone (CHEX), and 0.1%(w/v) US3440 SiO_2 particles in the organic phase. Variation in measured A values and NaCl passage are reported in Figure 18, which demonstrates the repeatability of the nanocomposite membrane fabrication process. The performance of nanocomposite membranes made with the GEGR synthesized SiO_2 particles (same particle loading and membrane formulation used for nanocomposite membranes made with commercially available SiO_2 particles) is also included for comparison (blue circles in Figure 18). There is a significant amount of variability in nanocomposite membrane performance, but the ability to fabricate nanocomposite membranes with A value greater than 16 and NaCl passage less than 0.5% has been demonstrated. It should be noted that nanocomposite membranes made with GEGR synthesized SiO_2 particles have also demonstrated the target performance (A = 16, 99.5% NaCl rejection) with 0.2%(w/v) particle loading, but Figure 18 only includes nanocomposite membranes with 0.1%(w/v) particle loading (commercial or GEGR synthesized), since this was the loading used for repeatability studies. Some potential causes of performance variability include particle agglomeration resulting in coating nonuniformity, particle interaction with organic solution components (i.e., TMC and CHEX), or coupon-to-coupon variability. Fabrication and testing of nanocomposite membrane elements give a clearer picture of process capability, since elements contain ~75x the membrane area of a flat sheet coupon.

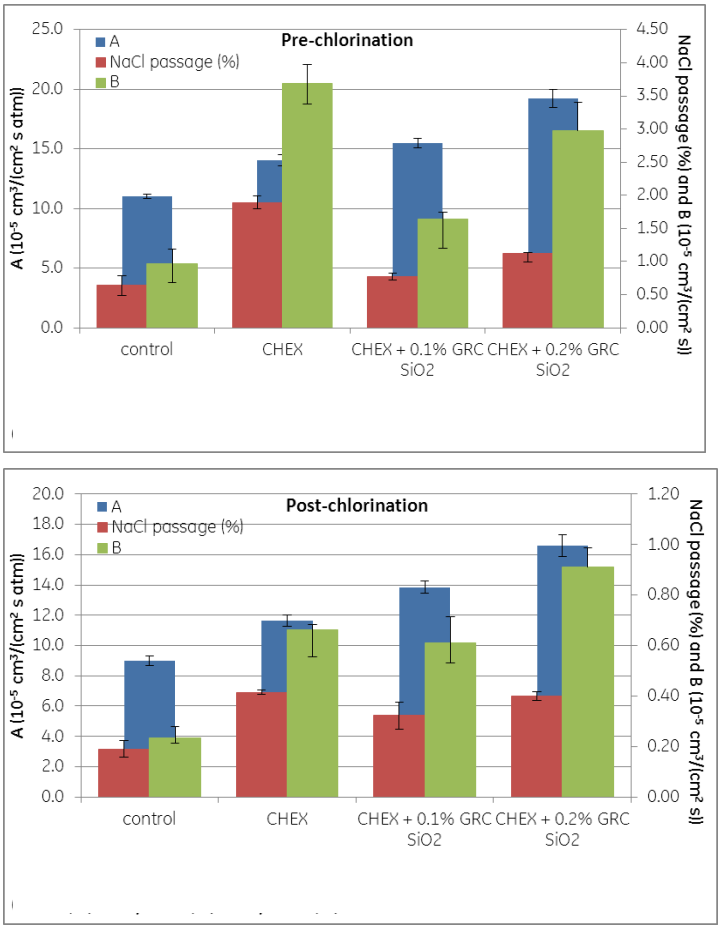

Figure 17: (a) Pre-chlorination and (b) post-chlorination performance (A value, B value, NaCl passage) of nanocomposite membranes with the indicated loadings of GEGR-made SiO_2 particles. Membranes were fabricated on P415 UF support. 1.25%(v) cyclohexanone (CHEX) was added to the organic phase for all membranes except the control membrane; 0.1% and 0.2% (w/v) silica nanoparticles calcined at 600 ^{o}C were also added to the organic phase for the nanocomposite membrane formulations.

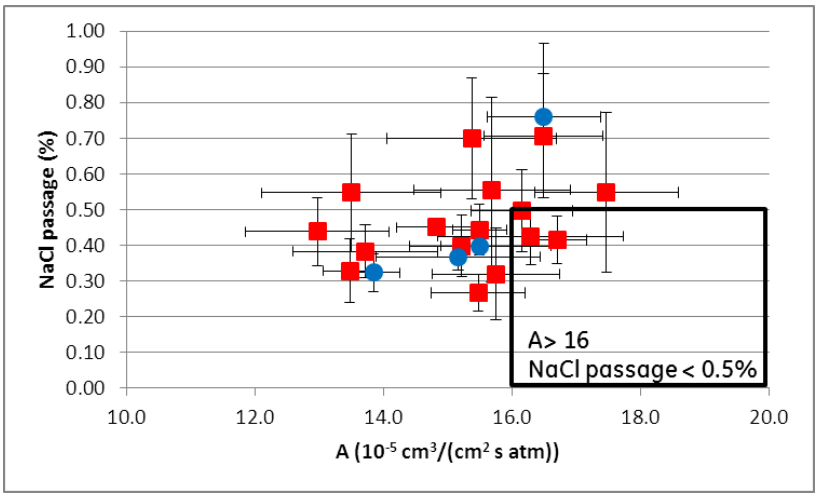

Figure 18: Repeatability of pilot-scale nanocomposite membrane fabrication process, indicated by flat sheet coupon A values and NaCl passages. Membranes were fabricated on P415 UF support with 1.25%(v) cyclohexanone (CHEX), and 0.1%(w/v) SiO_2 particles in the organic phase. Red squares and blue circles indicate nanocomposite membranes made with commercially available SiO_2 particles and GEGR synthesized SiO_2 particles, respectively. The boxed region includes membranes that meet the performance criteria (A value greater than 16 with NaCl passage less than 0.5%).

4.1.3.4 Conclusions

Nanocomposite RO membrane pilot coating trials have been conducted to understand the effects of formulation and process variables on separation performance. The effects of material (e.g. particle size, particle loading) and operating (line speed, organic delivery method) parameters have been systematically studied. Results demonstrated the entitlement of the initial targets of water permeance (A) = 16 and sodium chloride rejection = 99.5% by using silica nanoparticles and organic additives.

4.1.4 Prototype RO Element Fabrication

One of the goals of Task 1 was to demonstrate the high permeance of nanocomposite RO membranes in prototype elements. Thus, lab-scale (2”x12”) ULE RO elements were fabricated from flat sheet membranes and their performance were tested with simulated waters. As a first step, the standard commercial brackish water RO membranes (AG) from GE Water were used to establish element fabrication capability at GE Global Research. A membrane element rolling table was built and 2”x12” RO membrane elements were made with AG membranes (Figure 19).

Table 2 shows the performance (post-chlorination, 225 psi, 2000 ppm NaCl) of the GEGR-made element compared to the performance of the flat sheet AG membrane used to make it. The membrane element testing was conducted using a GEGR membrane test bench (Figure 20). The element A value and salt rejection agree with the product specification (A = 8 (+25%/-15%),

minimum NaCl rejection = 99.3%, average NaCl rejection after 24 hours of operation = 99.7%) and flat sheet crossflow cell test data for AG standard brackish water RO membranes.

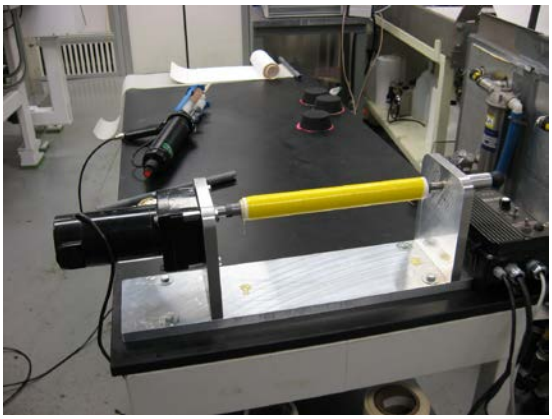

Figure 19: Membrane element fabrication table and the lab-scale (2”x12”) AG RO membrane element fabricated at GEGR.

Table 2: Performance of standard brackish water RO membrane (AG)

	Element (w/ AG membrane)	Flat sheet AG membrane
A (10^{-5} cm^3/cm^2-s-atm)	9.6	7.5
NaCl rejection (%)	99.7	99.6
B	0.4	0.4

Figure 20: The lab-scale (2”x12”) RO element testing bench. Six elements can be tested simultaneously.

Table 3 summarizes the performance of GE’s standard and ultra-low energy brackish water RO membranes. These ultra-low energy membranes will be evaluated in Task 2 as part of the integrated MBR/RO wastewater treatment system.

Table 3: Performance of GE's standard and ULE RO membranes.

Membrane Technology	Membrane Permeance (10^{-5} cm^3/cm^2-s-atm)	Membrane Salt Rejection
Standard Brackish Water RO membrane	8	99.75%
ULE Brackish Water RO Membrane (with nano/organic additives) 1	16	99.5%
ULE Brackish Water RO Membrane 2	25	99+%
ULE Brackish Water RO Membrane 3	35	98%

4.1.5 Nanocomposite membrane characterization

Characterization of the nanocomposite membranes is important for developing a fundamental understanding of the structure and transport mechanism of this new class of membranes. There has been an ongoing effort to characterize the morphology of the nanocomposite membranes by a number of techniques to gain an understanding of how the nanomaterials enable the observed improvements in membrane performance and thereby facilitate the design of more effective membranes. High resolution scanning electron microscopy (Hi-res SEM) and transmission electron microscopy (TEM), coupled with elemental analysis with energy dispersive spectroscopy (EDS), have been the primary characterization tools used to characterize the nanocomposite RO membranes. We employed two sample preparation methods to access the cross-section of the polyamide layer: (1) freeze fracture of the membrane (for SEM) and (2) ultramicrotomy of the membrane (embedded in epoxy for stability) which produces ~ 500 nm thin sections (for TEM) and a remaining block face (for SEM).

SEM

The Zeiss' Supra 55 VP FE SEM was used to document the microstructure of the RO membranes and supports. Images were generated using a variety of energies including 1kV, 3kV, and 5kV. Samples included the surface and cross sections of the polysulfone UF membrane, UF support membrane plus the polyamide thin film layer and UF support plus nanocomposite polyamide thin film coated with mesoporous Si particles and were imaged with the InLens detector.

Sample preparation typically includes air drying, vacuum drying and then platinum coating to render the sample conductive to the electron beam. Often the sample surface was beam sensitive, and damage occurred during imaging. More Pt coating along with varying energies helped to minimize beam damage. Cross sections were prepared by freezing the membrane in liquid nitrogen and subsequently fracturing the sample.

SEM is a very effective tool to probe nanoscale surface morphologies. SEM images of the surfaces of the (a) polysulfone UF membrane, (b) UF plus the control polyamide layer (without

nanoparticles) are shown in Figure 21. Figure 22 & Figure 23 show SEM images of the surfaces of the nanocomposite polyamide RO membranes using GEGR synthesized mesoporous silica nanoparticles and silica particles supplied by US Research Nanomaterials, Inc. (US3440), respectively. It is clear from these SEM micrographs that the GEGR synthesized silica nanoparticles have excellent dispersibility in the coating solution and remained well dispersed during and after the coating operation. On the other hand, the US3440 silica particles form large surface aggregates on the surface of the polyamide thin film. Thus, the GEGR synthesized nanoparticles have superior dispersibility and dispersion stability. SEM and EDS of another area containing larger surface agglomerates was used to confirm the composition of the surface agglomerates as silica, as shown in Figure 24.

A more challenging question than the surface dispersion of the nanoparticles is if they are dispersed within the polyamide layer. Freeze fracture of the nanocomposite membrane provides a cross-section amenable for SEM observation (Figure 25). The polyamide roughness and non-uniformity that was observed in the SEM top-down views (Figure 22 & Figure 23) are now seen as 'waves' and 'folds' of the polymer. While the surface agglomerates are also visible in this cross-section there is no conclusive evidence of nanoparticles within the polyamide layer because of poor contrast.

TEM

As is often the case, the information obtained from multiple imaging techniques helps to fit the 'puzzle' pieces together. TEM of microtomed thin sections allows for a different perspective of the polyamide morphology and the dispersion of the nanoparticles. The thickness of a microtomed thin section is ~ the thickness of the polyamide layer and 2-3 times the thickness of the primary particle size of the nanoparticles. It should be noted that the sampling size by TEM is even smaller than that by SEM; a microtomed thin section probes ~ 100 nm x 3 mm of the sample surface.

Figure 26 & Figure 27 shows representative TEM cross-sections at different magnifications. In both figures, the 'waves' and 'folds' structure of the rough polyamide surface layer are consistent with the polyamide features imaged by SEM (Figure 25). The dispersion of the nanoparticles is most clearly seen at the higher magnification shown in Figure 27. Here, for the first time, there appear to be silica nanoparticles possibly entrapped in the PA film (green arrows). The red arrows indicate silica nanoparticles physically absorbed to the surface of the polyamide thin film.

Conclusions

The chemical and material characteristics of the nanocomposite RO membranes have been assessed using a variety of characterization techniques, including high resolution SEM, TEM, and EDS. High resolution SEM shows that GEGR synthesized mesoporous silica nanoparticles have superior dispersibility and dispersion stability as compared to commercially obtained nanoparticles. TEM of microtomed membrane cross-sections showed that small agglomerates of silica nanoparticles may be fully incorporated into the polyamide layer, although the volume fraction of such nanoparticle incorporation is difficult to quantify.

4.1.6 Conclusions from Task 1

The nanocomposite RO membrane formulation and associated membrane flat-sheet manufacturing process were optimized on the pilot scale, using the GE Global Research pilot coater. Lab-scale (2”x12”) ULE RO elements were fabricated from the flat sheet membranes and their performance was tested with simulated waters. The results of the nanocomposite RO membrane fabrication, characterization and testing demonstrated the success of nanocomposite RO membranes in meeting the performance targets.

(a)

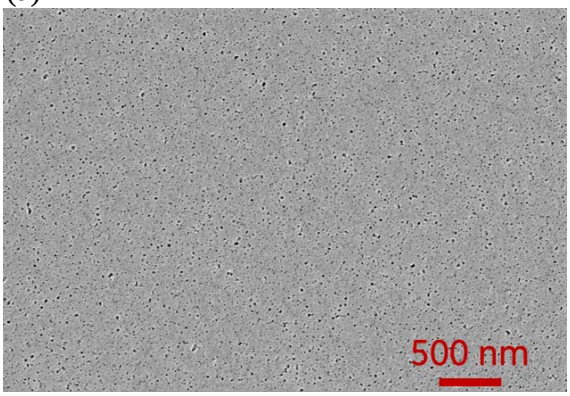

(b)

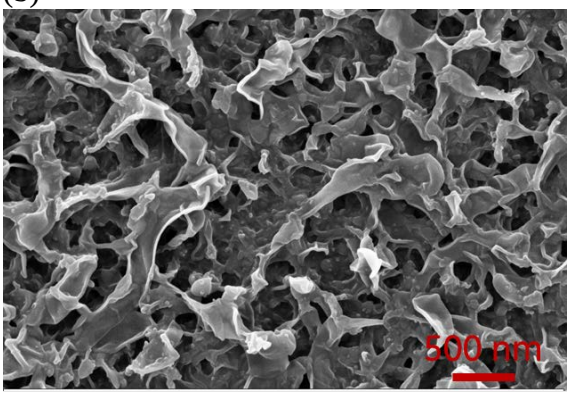

Figure 21: SEM images of the surfaces of the (a) polysulfone UF membrane, (b) a thin film composite control RO membrane (UF plus the polyamide thin film, without nanoparticles).

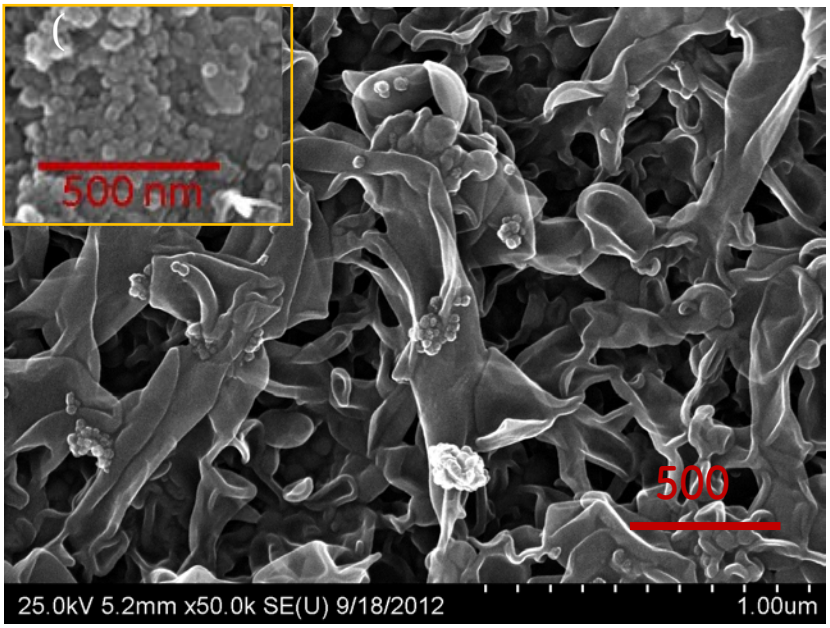

Figure 22: SEM images of the surface of a nanocomposite RO membrane fabricated with GEGR synthesized mesoporous silica nanoparticles. These nanoparticles are well dispersed on the surface of the polyamide RO membrane thin film. For comparison, the SEM image of as-synthesized bulk silica nanoparticles is inserted on the top left.

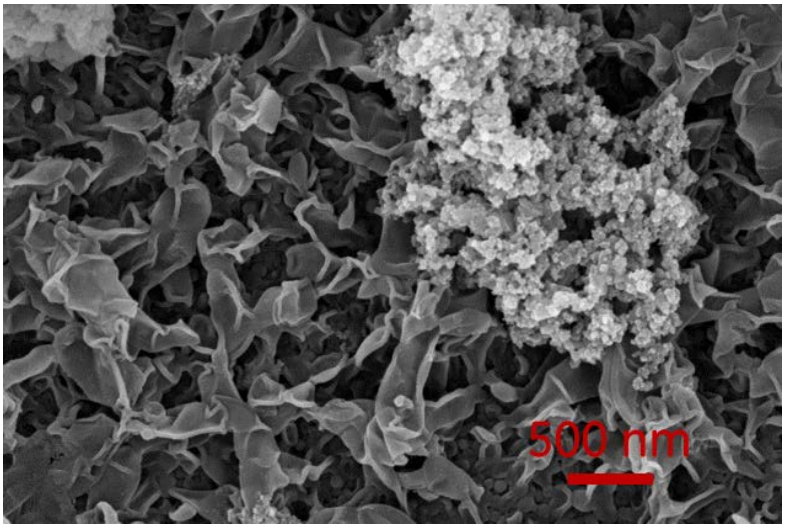

Figure 23: SEM image of the surface of a nanocomposite RO membrane fabricated with silica particles supplied by US Research Nanomaterials, Inc. (US3440). These nanoparticles form large surface aggregates on the surface of the polyamide RO membrane thin film

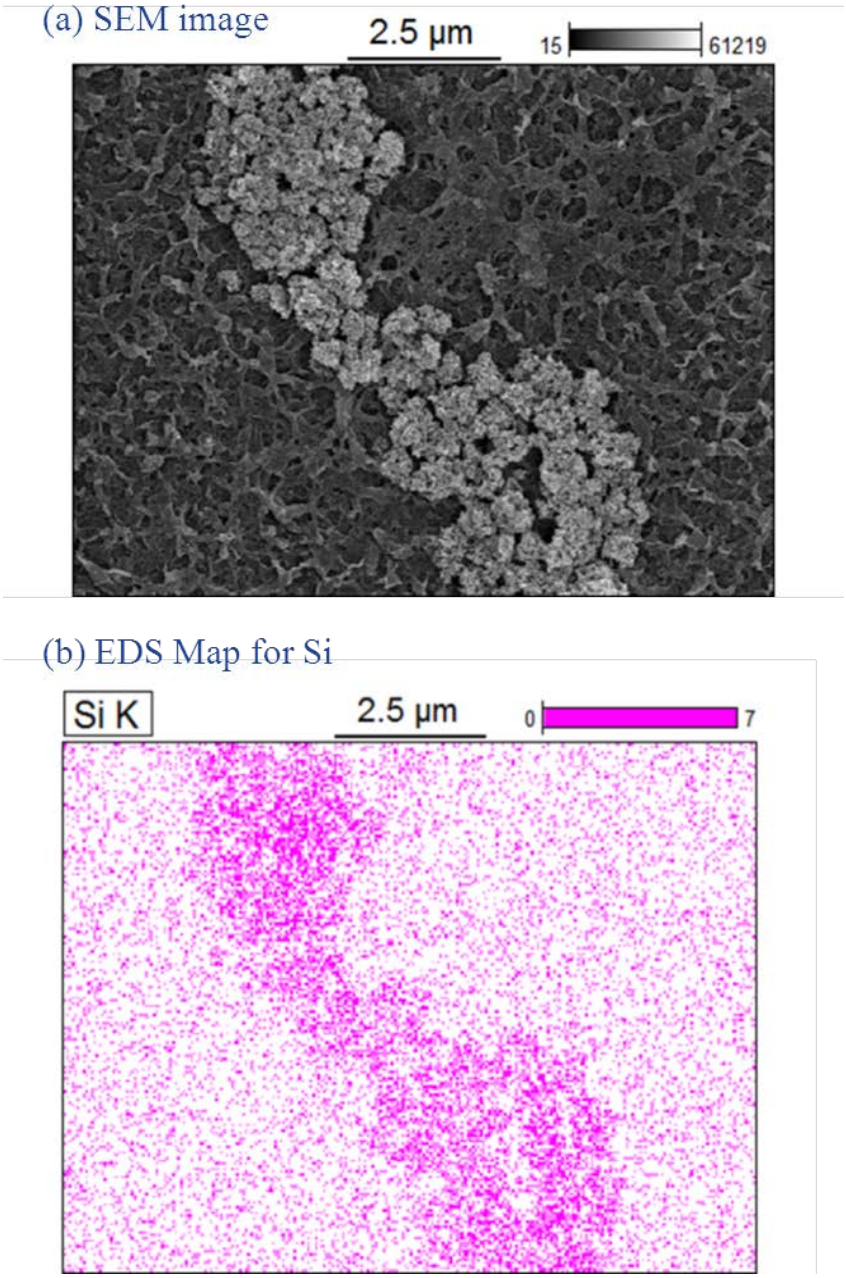

Figure 24: (a) SEM image of a nanocomposite RO membrane fabricated with silica particles supplied by US Research Nanomaterials, Inc. (US3440), and (b) Energy dispersive X-ray spectroscopy (EDS) map for silica nanoparticles on nanocomposite membrane surface.

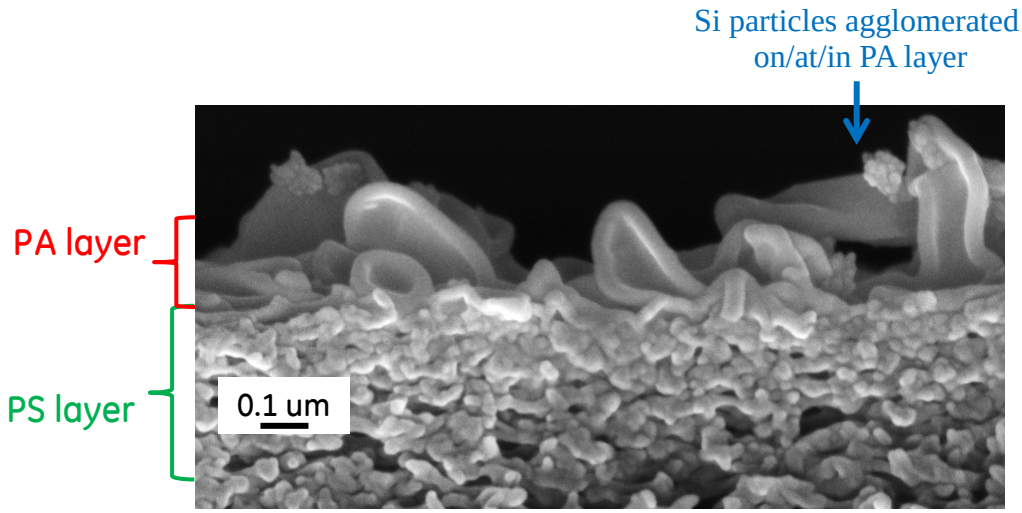

Figure 25: SEM image of cross-section prepared by freeze fracture of a nanocomposite membrane showing "waves" and "folds" structure in the non-uniform polyamide layer and small agglomerate of nanoparticles on/at/in the polyamide layer.

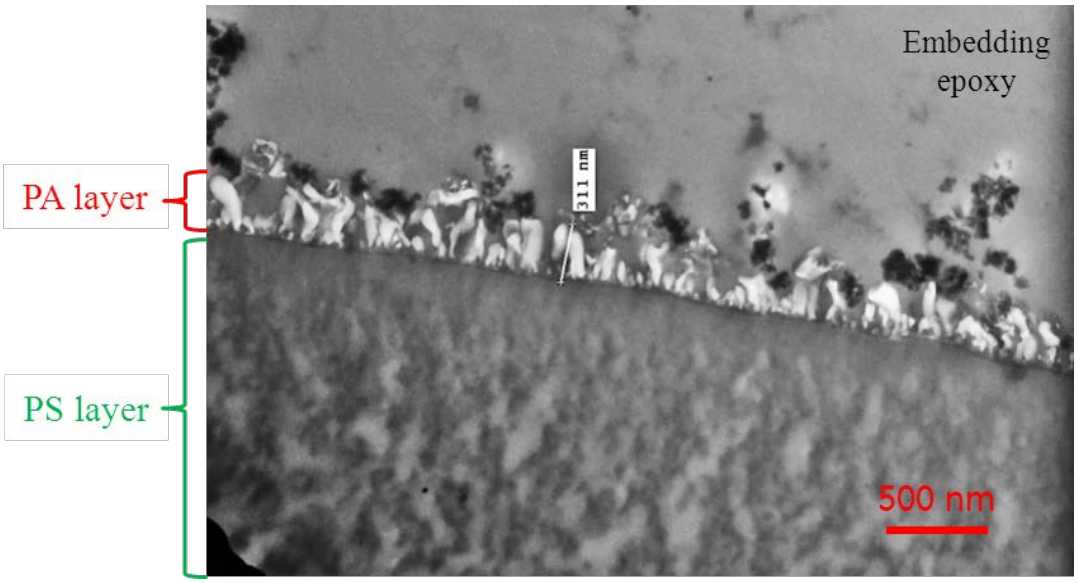

Figure 26: TEM of microtomed thin section of a nanocomposite RO membrane fabricated with silica particles supplied by US Research Nanomaterials, Inc. (US3440). Sample embedded in epoxy prior to microtoming. Silica particles have higher contrast.

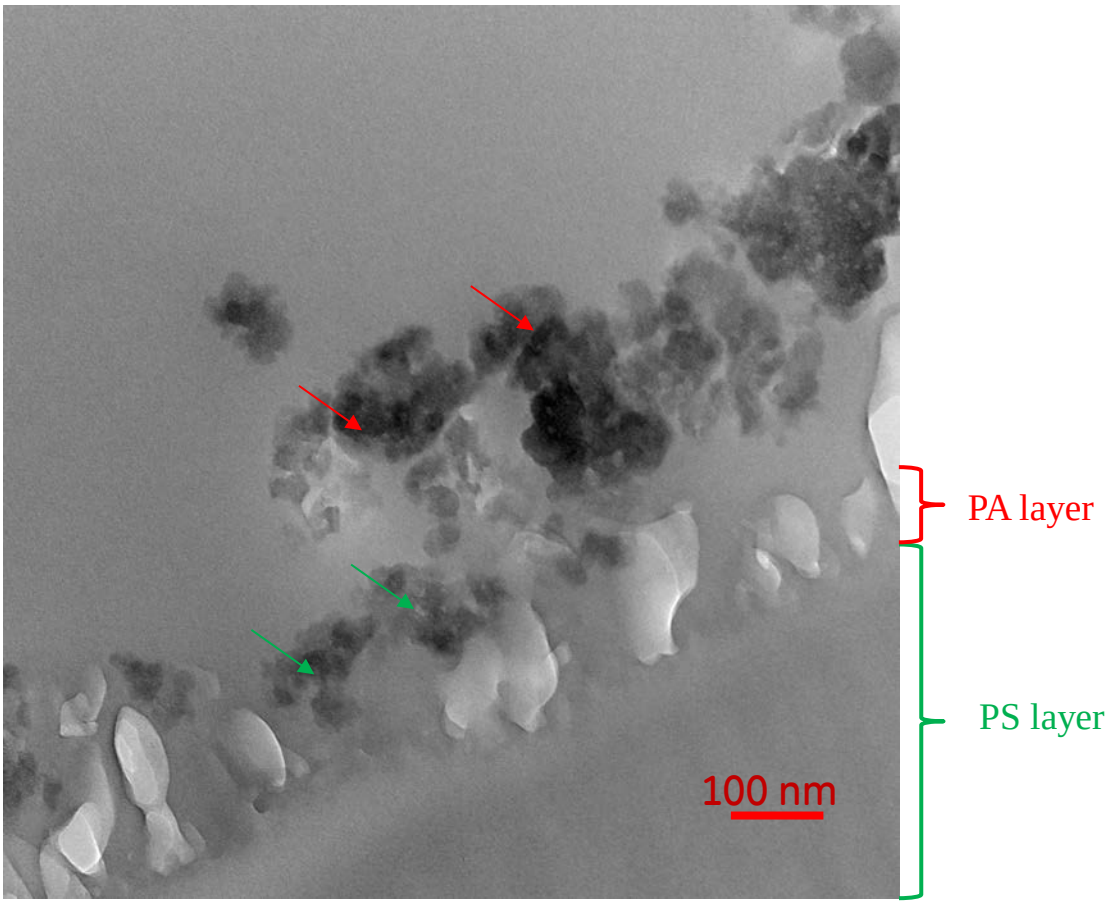

Figure 27: Higher magnification image of a nanocomposite RO membrane fabricated with silica particles supplied by US Research Nanomaterials, Inc. (US3440). Green arrows indicate silica nanoparticles possibly entrapped in the PA film, and the red arrows indicate silica nanoparticles physically absorbed to the surface of the polyamide thin film.

4.2 Task 2- Design and Validate Lab-Scale MBR/Ultra-Low Energy RO Wastewater Treatment System

4.2.1 Objectives and Approaches

The key objectives and approaches of this task are:

- Perform gray water benchmarking. Understand the characteristics of a wide range of gray waters, especially those relevant to FOBs.
- Demonstrate MBR as a robust RO pre-treatment for gray water from FOBs using lab-scale ZW-1 MBR unit, with MBR effluents meeting RO feed water quality specifications (Table 4). Optimize MBR operation and performance using automated pilot-scale ZW-10 MBR system.
- Build an integrated MBR (ZW-10) and ULE RO (E-2) prototype system and evaluate a range of gray water feeds to demonstrate stable and robust performance of the integrated MBR/ULE RO system. The purified water from the MBR/ULE RO system needs to meet the water quality specifications for potable reuse applications (Table 5)[20-21].
- Design FOB wastewater treatment system and build system performance and cost models. The design case will be based on a containerized, military deployable MBR/ULE RO wastewater treatment system capable of treating gray water generated by a FOB with 600 soldiers. The designed MBR/ULE RO wastewater system will have the following key characteristics:
    - Robust performance, capable of treating a wide range of gray waters and load conditions
    - Highly automated, low operator attendance and maintenance
    - Rapid system start-up of the biological system
    - Reduced system footprint and pack out volume
    - Low waste generation
    - Reduced system energy demand

Table 4: RO feed water quality specifications.

Parameter	RO Feed Requirements
COD	<60 mg/L
BOD	<20 mg/L*
TOC	<10 mg/L
Turbidity	<0.4 NTU

*wastewater with BOD>20 mg/L must be evaluated further to determine the constituents of BOD.

Table 5: Water quality specifications for MBR/RO purified water.

Parameter	Specification
Maximum contaminant levels (MCL)	Below levels specified by EPA primary drinking water regulation[21]
Secondary maximum contaminant levels (SMCL)	Below levels specified by EPA secondary drinking water standard[21]

The primary objective of the program is to demonstrate and validate an innovative, energy-efficient, and cost-effective membrane bioreactor (MBR) and ultra-low energy (ULE) reverse osmosis (RO) membrane system for gray water treatment at DoD FOBs. It should be noted that the units can be operated separately, in the event that additional purification by RO membrane is not required (i.e. treating water for disposal only).

4.2.2. Characteristics of gray water

We have obtained gray and black water data from Base Camp Integration Lab (BCIL) at Fort Devens, MA. Table 6 & Table 7 show water quality data for the gray and black water sampled from December 2000 to January 2001 from on-base containerized self-service laundry (CSSL) and toilets, respectively [22]. In addition, characteristics of black, gray, and combined wastewater from other military (e.g. ship board) and domestic applications are available in the literature [23-28].

Table 8 & Table 9 summarize water quality data for various gray water streams from three US Navy vessels and from various domestic gray water streams. These tables show that the gray water streams from shower and wash basin contain relative low concentrations of organic contaminants, as indicated by biological oxygen demand (BOD) and chemical oxygen demand (COD). They also contain relative low level of nutrients, as indicated by total Kjeldahl nitrogen (TKN) and total phosphorus (TP), and low levels of total suspended solids (TSS) and total dissolved solids (TDS). On the other hand, the gray water streams from kitchen, laundry, and dishwasher contain high concentrations of organic contaminants and nutrients.

Table 6: Characteristics of gray water from containerized self-service laundry at Base Camp Integration Lab at Fort Devens, MA[22].

	Date									
Parameter	**26-Dec**	**27-Dec**	**28-Dec**	**29-Dec**	**2-Jan**	**3-Jan**	**4-Jan**	**5-Jan**	**Average**	**Stdev**
BOD (mg/L)	16	20	17	36	33	37	58	36	**32**	14
COD (mg/L)	32	92	119	272	201	134	181	237	**159**	79
TOC (mg/L)	69	32	37	33	33	38	21	25	**36**	15
Turbidity (NTU)	15	78	68	105	117	92	65	80	**78**	31
TSS (mg/L)	24	57	51	127	58	73	167	63	**78**	46
TDS (mg/L)	252	238	344	396	348	282	350	278	**311**	56
Color (CU)	107	90	110	104	107	65	53	57	**87**	24
Ammonia (mg/L)	0.1	1	3.2	2.8	3.6	1.8	0.4	4.5	**2**	2
T. Phosphate (mg/L)	0.5	0.2	8	5	4	4	0.2	6.3	**4**	3
TKN (mg/L)	0.5	4	12.3	10.6	7.8	6	8	9	**7**	4
Chloride (mg/L)	107	90	110	104	107	65	53	57	**87**	24
Sulfates (mg/L)	0	8	27	0	0	0	7	28	**9**	12
pH	8.38	7.48	6.6	7.33	7.45	8.08	9.09	7.24	**8**	0.8

Table 7: Characteristics of black waters from on-base toilets at Base Camp Integration Lab at Fort Devens, MA[22].

	Date											
Parameter	**11-Dec**	**12-Dec**	**13-Dec**	**14-Dec**	**15-Dec**	**18-Jan**	**19-Jan**	**22-Jan**	**23-Jan**	**24-Jan**	**Average**	**Stdev**
BOD (mg/L)	377	184	109	63	56	436	175	178	167	-	**194**	131
COD (mg/L)	1300	1140	884	689	504	953	560	520	769	446	**777**	289
TOC (mg/L)	310	140	88	68	56	190	76	110	99	-	**126**	80
Turbidity (NTU)	235	263	230	214	101	589	204	114	129	60	**214**	148
TSS (mg/L)	388	295	288	608	220	790	160	118	216	112	**320**	221
TDS (mg/L)	519	450	500	608	620	740	500	580	564	536	**562**	82
Color (CU)	206	220	200	200	180	120	100	40	40	40	**135**	75
Ammonia (mg/L)	137	117	110	119	115	86.3	56.2	82.9	57.1	62.9	**94**	29
T. Phosphate (mg/L)	14	14	15	12	7	15	8	11	4	8	**11**	4
TKN (mg/L)	165	155	152	138	135	196	89	109	81	91	**131**	38
Chloride (mg/L)	-	171	-	167	162	144	128	142	136	128	**147**	17
Sulfates (mg/L)	27	18	40	42	45	15	14	39	38	-	**31**	12
pH	8.46	8.51	8.45	8.43	8.45	8.39	8.59	8.81	8.55	8.65	**9**	0.1

Table 8: Characteristics of various gray water streams from three US Navy vessels: USS O'Hare (DD 889), USS Seattle (AE 3), and USS Sierra (AD 18)[23-27].

Parameter	DD 889 Wash Basins and Showers[14]	DD 889 Comb. Food Prep[14]	DD 889 Laundry[14]	AOE 3 Wash Basins and Showers[13]	AOE 3 Dishwasher and Deep Sink[13]	AOE 3 Laundry[13]	AD 18 Wash Basins and Showers[12]	Galley Weighted Average	Sink and Shower Weighted Average	Laundry Weighted Average	Flow Weighted Average**
No. Samples	*114*	*134*	*28*	*7*	*60*	*20*	*91*				
pH	7.3	6.88	9.99	7.12	6.74	8.33	6.86				
TSS	404	4,695	221	94	194	176	119	3303	271.4	202.3	802
TDS	1,445	8,064	1,006	237	752	583	225	5803	881.4	829.8	1756
BOD	230	2,618	419	226	503	190	144	1964	193	323.6	540
COD	348	7,839	721	509	2,380	469	304	6150	334.4	616	1443
TOC	70	1,133	165	82	251	59	-	860	70.7	120.8	224
Oil & grease	12.06	1,210	8.11	20.65	82.46	4.56	-	861.3	12.6	6.6	164
MBAS *	0.96	0.09	0.84	0.12	0.14	4.12	-	0.11	0.9	2.2	1.1
N-ammonia	15.4	669	80.48	0.58	0.64	0.17	-	462.3	14.5	47	102.3
N-nitrate	2.73	10.85	1.16	0.89	2.08	0.29	-	8.1	2.6	0.8	3.2
N-nitrite	-	-	-	0.09	0.11	-	-	-	-	-	-
N-Kjeldahl	187	99.84	164	4.31	4.84	0.43	-	70.5	176.4	95.8	140
P (phosphate)	1.36	20.78	1.3	1.03	6.34	28.25	-	16.3	1.3	12.5	6.5
Total coliforms (microorg/100mL)	707,000	257,000	178	8,300	2,360,000	3,890	60,600	907,412	406,466	1725	407,593
Fecal coliforms (microorg/100mL)	178,000	103,000	-	200	1,250,000	21,000	7,900	457,742	99,115	-	141,862

Table 9: Characteristics various domestic gray water streams [28].

Parameter		Bath		Shower		Washing Basin		Kitchen Sink		Washing Machine	Dish Washer
	Units	Avg	Std	Avg	Std	Avg	Std	Avg	Std	Avg	Avg
Volume	liter/use	53	27.5	28	18.8	1.9	1.7	12	5.96	85	33.4
BOD	mg/l	173	218	424	219	205	42.5	890	480	462	699
COD	mg/l	230	195	645	289	386	230	1340	1076	1339	1296
TOC	mg/l	91	89.1	120	69.6	119	44.3	582	214	361	234
TSS	mg/l	78	105	303	205	259	130	625	518	188	525
EC	mmho/cm	1220	409	1565	485	1200	401	1040	294	2457	2721
pH	-	7.14	0.04	7.43	0.36	7.0	0.3	6.48	0.6	7.5	8.2
NH_4-N	mg/l	0.89	1.49	1.2	0.83	0.39	0.29	0.6	0.81	4.9	5.4
PO_4-P	mg/l	4.56	1.49	10	13.7	15	13.8	22	27	169	537
Faecal Chliforms	cfu/100 ml	4.0E 6	6.9E 6	4.0E 6	8.5E 6	3.5E 3	7.4E 3	1.2E 6	2.4E 6	4.0E6	6.0E6

In summary, gray water from different sources have a wide range of contaminant loadings. Thus, it is very important to design a robust MBR/RO wastewater treatment system capable of treating a wide range of influent wastewater. The GE project team initially used synthetic gray water for a feasibility study and initial process optimization. Next, the project team used mixtures of kitchen and laundry gray water streams and varied the influent wastewater composition to test the robustness of the MBR/RO system.

4.2.3 Synthetic gray water characterization

Four different synthetic gray water recipes were chosen initially from literature data (Table 10) and a detailed water quality analysis was conducted. Table 11 shows the characteristics of these synthetic gray waters. The contaminant levels of these synthetic gray waters (e.g. BOD, COD, and TOC, as shown in Table 11) were within the range of those typically observed in actual military and domestic gray waters, as shown in Table 8 & Table 9.

Table 10: Synthetic gray water compositions.

Synthetic Gray Water Recipe 1 (SynGW1) [29]		Synthetic Gray Water Recipe 2 (SynGW2) [30]		Synthetic Gray Water Recipe 3 (SynGW3)		Synthetic Gray Water Recipe 4 (SynGW4) [31]	
Ingredient	mL/L	Ingredient	Mg/L	Ingredient	Mg/L	Ingredient	Mg/L
Toothpaste	21	Dextrin	85	Dextrin	170	Glucose	800
Shower gel	0.175	NH4Cl	75	NH_4Cl	150	Peptone	150
cleaner	0.3	Yeast Extract	70	Yeast Extract	140	KH_2PO_4	35
Shower oil	0.025	Soluble Starch	55	Soluble Starch	110	$MgSO_4$	35
Shampoo	0.025	Na2CO3	55	Na_2CO_3	110	$FeSO_4$	20
Bubble bath	0.125	NaH2PO4	11.5	NaH_2PO_4	23.0	Sodium Acetate	450
Urea	30	KH2PO4	4.5	KH_2PO_4	9.0		
Na_2CO_3	27.5						
K_2HPO_4	2.5						
NH_4Cl	17.5						

Table 11: Characteristics of synthetic gray water.

Parameter	Concentration	Synthetic Gray Water Recipe 1 (SynGW1)	Synthetic Gray Water Recipe 2 (SynGW2)	Synthetic Gray Water Recipe 3 (SynGW3)	Synthetic Gray Water Recipe 4 (SynGW4)
Total Suspended Solids (TSS)	Mg/L	17.5	67	134	<1
Total Dissolved Solids (TDS)	Mg/L	215	235	470	1,000
Total Organic Carbon (TOC)	Mg/L	29.1	40.2	80.4	514
Biological Oxygen Demand (BOD)	Mg/L	78.0	95.0	190	>802
Chemical Oxygen Demand (COD)	Mg/L	183	173	346	1,360
pH		8.3	7.4	14.8	7.4
Turbidity	NTU	17.0	22.0	44	6.6
Total Kjeldahl Nitrogen (TKN)	Mg/L	25.2	37.0	74	19.0
Ammonia	Mg/L	4.2	19.7	39.4	0.3
Total Phosphorus (TP)	Mg/L	0.72	2.4	4.8	6.2

4.2.4 Evaluate MBR pre-treatment of synthetic gray water using lab-scale ZW-1 MBR units

4.2.4.1 ZW-1 Lab Scale Membrane Bioreactor

Initial screening experiments were carried out utilizing GE's small lab scale ZW-1 MBR module in order to determine the effectiveness of gray water treatment by MBR. The goal was to produce high quality MBR effluent that meets the RO feed water specification. To minimize system footprint and solid waste generation, ZW-1 experiments were performed at various hydraulic retention times (HRTs) and sludge retention times (SRTs) in order to demonstrate wastewater treatability and membrane operation stability at low HRT and high SRT, before scaling up to a pilot scale ZW-10 MBR system.

Figure 28 & Figure 29 show the ZW-1 MBR system that was built in January 2013. The unit consists of a 3,000 mL process tank, a small hollow fiber membrane module with an area of 0.50 ft^2, feed and permeate tanks, two pumps, a flow meter, and a pressure gauge.

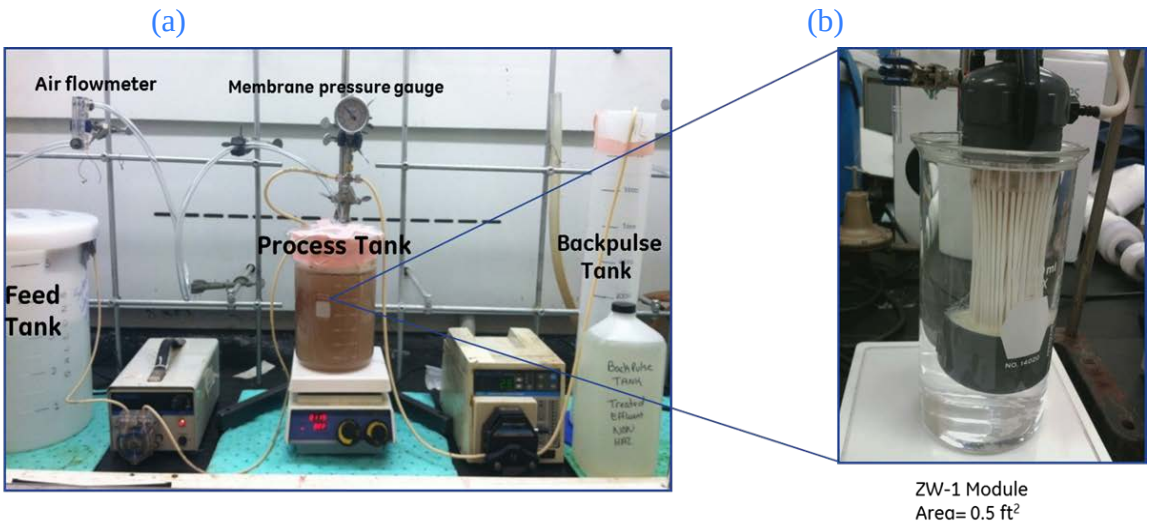

Figure 28: a) The ZW-1 membrane bioreactor set-up at GE Global Research, and b) the ZW-1 MBR hollow fiber membrane module (membrane area=0.5 ft^2/0.047 m^2, length=17.5 cm, diameter=5.8 cm, and holdup volume=10 mL).

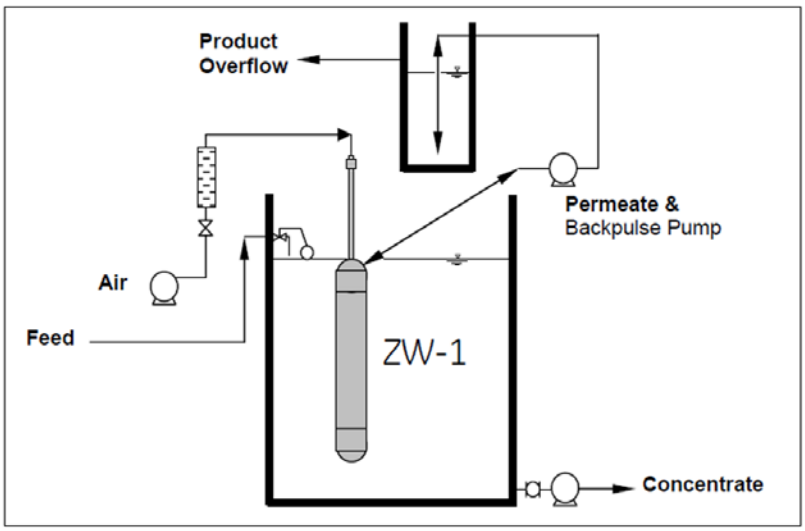

Figure 29: Schematic of the ZW-1 lab scale membrane bioreactor.

4.2.4.2 Water Quality Characterization

Water quality characterization (BOD, COD, TOC, TDS, TSS, TKN, TP, pH, turbidity, and fecal coliforms) was performed both internally using a portable DR3900 spectrophotometer (DR3900 from Hach) and by an external partner, Adirondack Environmental Services, Inc. The spectrophotometer has the capability to test over 35 different parameters, including COD, TOC, ammonia, total nitrogen, and total phosphorus (Figure 30).

Figure 30: Hach portable DR3900 spectrophotometer and chemistry test-kits.

4.2.4.3 Results and Discussion of Lab-Scale ZW-1 MBR Study

The ZW-1 unit was seeded with one pound of BioQuick™ 5130 seed stock from Novozymes and synthetic wastewater (SynGW3) for rapid start-up of a population of a broad range of microorganisms without having to import sludge from an outside waste water treatment plant. Continuous wastewater flow and permeation of the MBR unit began after an initial seeding period of 3 days where 0.35 scfm (standard cubic feet per minute) of air was supplied to the process tank in order to grow the bacteria (the seed stock contains a readily available carbon source, nitrogen, and phosphorus for rapid and balanced growth of microorganisms). The ZW-1 unit was started at a modest 16 hour HRT with a low average flux of 2.3 gfd (gallon per square feet of membrane area per day). The influent feed gray water was created using a synthetic waste water recipe (SynGW3). Influent and effluent from the reactor were analyzed on a weekly basis for the following parameters typically measured to assess wastewater treatment efficiency and water quality: BOD, COD, TOC, ammonia, TP, TKN, TDS, TSS, turbidity, and pH. In addition to water quality data, MBR operating parameters were also monitored on a daily or weekly basis to ensure stable unit operation and to evaluate system performance over time, including mixed liquor suspended solids (MLSS), dissolved oxygen (DO) levels, flow rate and flux, process tank temperature, and trans-membrane pressure. The ZW-1 system was back-pulsed manually 1-2 times per day because the system was not automated. For the ZW-1 lab scale MBR unit, the sludge in the reactor was not extracted except for occasional MLSS sampling, similar to the procedure used in Ref. 32.

The small ZW-1 unit demonstrated excellent contaminant removal efficiency and gray water treatability throughout the entire study period. The bioreactor was operated continuously for the first 60 days at an HRT of 16 hours. Liquid DO level was maintained well above 8 mg/L and was found to be more than adequate to support the microorganism community. Effluent was analyzed on Day 3 and very high levels of all major contaminants were found, presumably due to the carbon source, nitrogen, and phosphorus formulated in the Bioquick™ 5130 seed stock. By day 11, the ZW-1 MBR unit appeared to be operating efficiently and drastic improvements in water quality were observed, suggesting that an MBR system could begin producing on-spec treated water within 1-2 weeks after start-up (Table 12 Table 13). At a 16 hour HRT, a very conservative operation, excellent pollutant removal was observed on a regular basis with no system disturbances (Figure 31-39). On days 61 and 73, the HRT was reduced to 7 hours and 4.5 hours respectively, and the system continued to produce high quality MBR effluent.

Table 12: Characteristics of the feed water and ZW-1 MBR effluent, including turbidity, COD, BOD, TOC, and pH.

Day	Turbidity		Chemical Oxygen Demand (COD)		Biological Oxygen Demand (BOD)		Total Organic Carbon (TOC)		pH	
	NTU		mg/L		mg/L		mg/L		pH units	
	Influent	Effluent	Influent	Effluent	Influent	Effluent	Influent	Effluent	Infuent	Effluent
3	14	1.5	62	6,500	32	866	15.9	25,700	7.9	5.3
11	14	1.4	42	45	16	5	10.0	15.8	8.2	8.5
18*	24	1.3	77	22	20	<4	18.3	7.2	8.0	8.7
25	300	0.37	1,270	18	238	<4	48.8	6.1	7.8	8.5
32	78	0.46	443	22	235	<4	55.5	7.3	8.0	8.6
39	150	0.3	541	13	296	<4	47.9	4.6	7.7	8.7
46	430	0.44	1,590	38	745	3	34.2	8.6	7.8	8.7
53	32	0.96	154	18	85	<4	38.9	5.7	8.0	8.7
61	130	0.24	670	55	302	<6	64.0	5.5	7.2	8.6
68	99	0.33	773	9	469	<4	91.6	6.5	5.8	8.4
73	120	0.12	650	9	334	<4	66.9	3.9	6.9	8.2
75	120	0.29	670	13	481	2	110.0	3.9	6.4	8.4
82	220	0.38	1,420	9	805	<4	96.8	4.6	6.6	8.4
89	13	0.31	233	9	103	<4	67.3	6.4	8.0	8.4

*Influent recipe doubled in concentration from Day 18

Table 13: Characteristics of the ZW-1 MBR influent and effluent, including TDS, TSS, ammonia, total nitrogen, and total phosphorous.

Day	Total Dissolved Solids (TDS)		Total Suspended Solids (TSS)		Ammonia		Total Kjeldahl Nitrogen (TKN)		Total Phosphorus (TP)	
	mg/L		mg/L		mg/L		mg/L		mg/L	
	Influent	Effluent	Influent	Effluent	Influent	Effluent	Influent	Effluent	Influent	Effluent
3	380	37,000	15.5	20	21.0	2,040	26.3	2,760	2.8	740
11	490	375	7	2	19.9	23.9	28.0	26.9	3.8	3.3
18*	1,340	300	12	<1	30.7	27.6	43.7	31.4	4.1	2.6
25	480	490	20.5	2	47.2	44.2	60.5	64.4	12.8	4.2
32	560	530	281	<1	37.9	35.6	52.6	39.2	9.7	4.4
39	495	460	506	<1	38.2	33.6	44.8	42.6	9.5	4.9
46	530	490	1,290	<1	43.8	40.9	49.3	38.1	13.4	7.0
53	440	390	40	<1	36.4	34.5	51.5	39.2	8.4	5.3
61	770	630	388	<1	43.5	39.5	47.0	34.7	10.6	5.2
68	440	335	665	4	47.6	68.1	59.4	65.0	11.4	10.9
73	415	205	61	1.5	42.4	43.9	65.0	47.0	10.2	7.8
75	500	390	281	<1	65.9	40.4	63.8	54.9	12.2	6.6
82	530	385	712	<1	49.4	36.2	72.8	40.3	14.5	5.9
89	565	490	42.5	<1	47.1	53.4	59.4	54.9	7.8	7.5

*Influent recipe doubled in concentration from Day 18

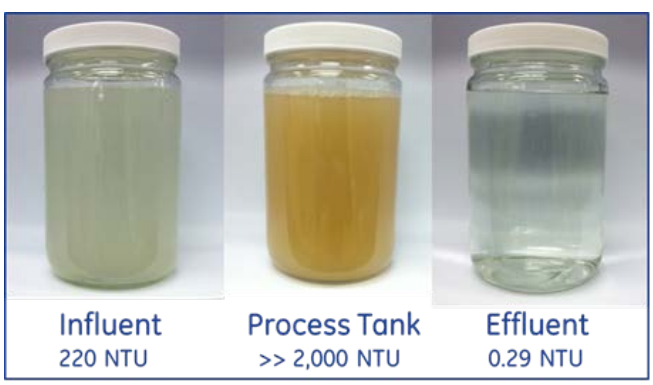

Figure 31: The turbidity of ZW-1 MBR influent, mixed liquor in the process tank, and effluent.

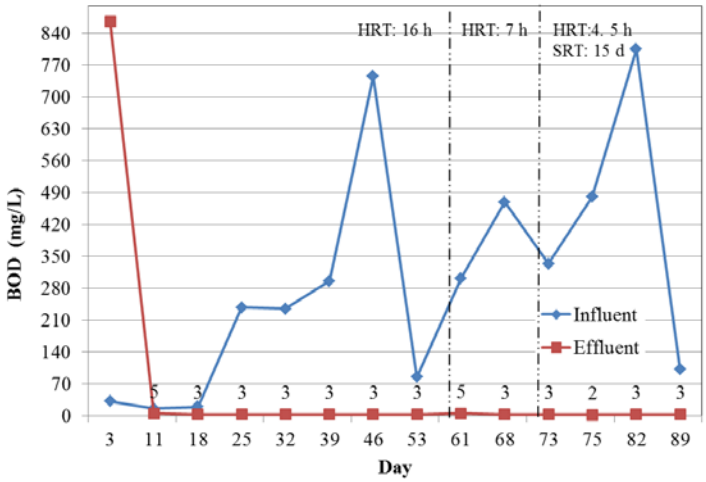

Figure 32: The BOD concentrations of ZW-1 MBR influent and effluent.

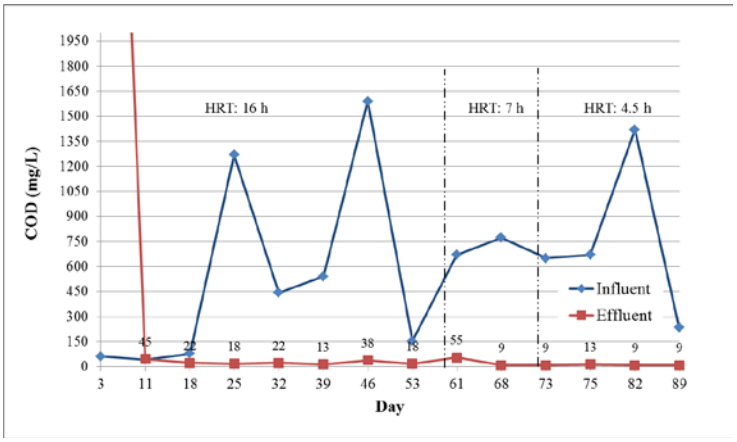

Figure 33: The COD concentrations of ZW-1 MBR influent and effluent.

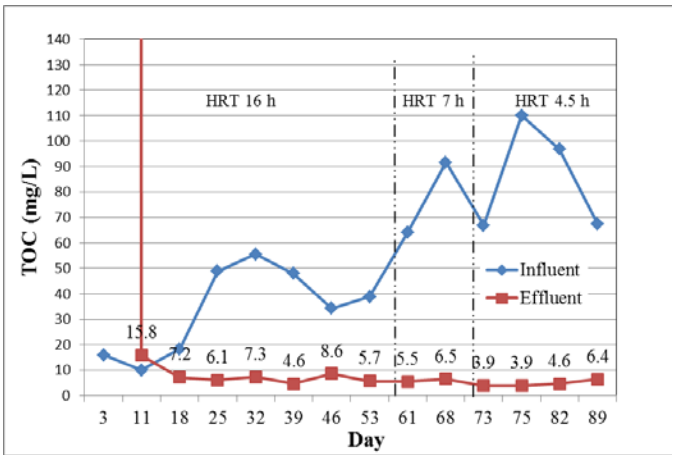

Figure 34: The TOC concentrations of ZW-1 MBR influent and effluent.

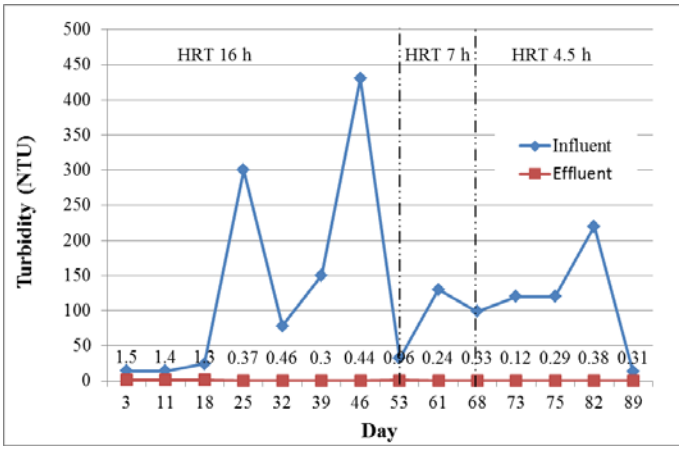

Figure 35: The turbidity levels of ZW-1MBR influent and effluent.

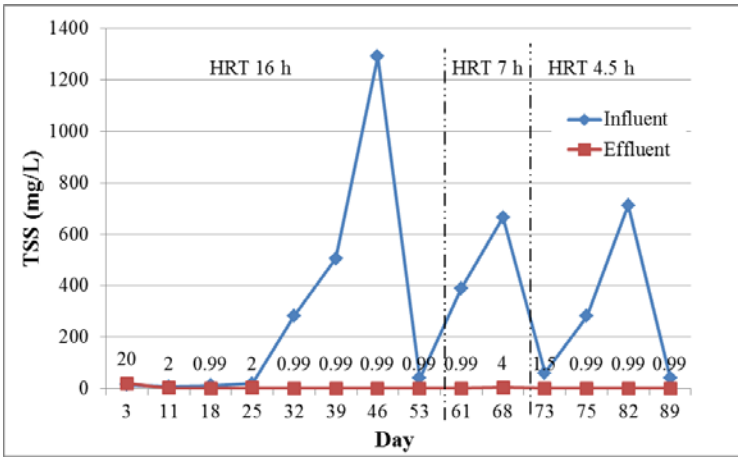

Figure 36: The TSS levels of ZW-1 MBR influent and effluent.

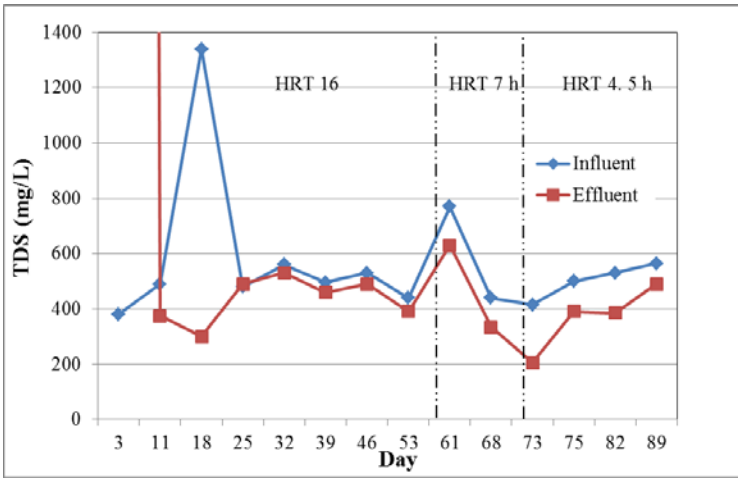

Figure 37: The TDS levels of ZW-1 MBR influent and effluent.

Removal of ammonia and TKN was low during the experiments (Figure 38-Figure 40). However, this was expected given that there was no seeding of nitrifying bacteria. Without seeding of slow-growing nitrifying bacteria, their population likely would not become established in a bioreactor as fast as the more common bioreactor organisms. To accelerate nitrification in MBR wastewater treatment, a nitrifying microorganism seed (BioRemove™ 5805 from Novozymes) was added into the pilot-scale ZW-10 MBR processing tank. Very effective removal of ammonia and TKN was achieved by the MBR system with the addition of nitrifying microorganism seeds (section 4.2.5.2). The pH of the influent and ZW-1 MBR treated effluent are shown in Figure 41.

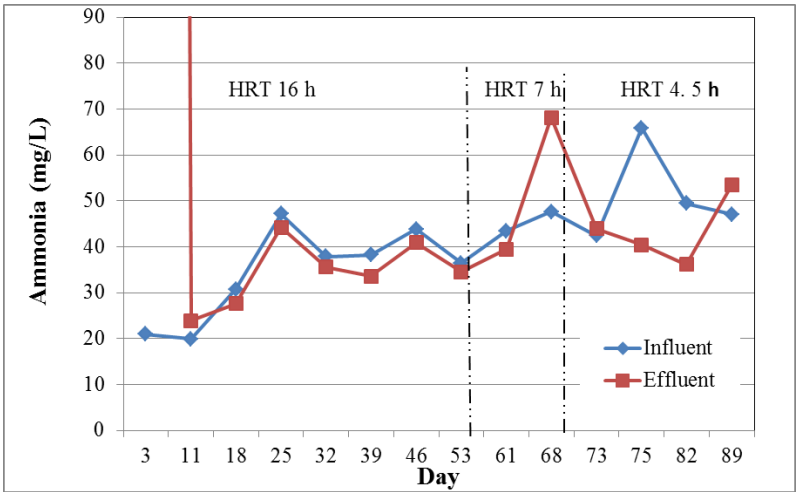

Figure 38: The ZW-1 MBR influent and effluent ammonia concentrations.

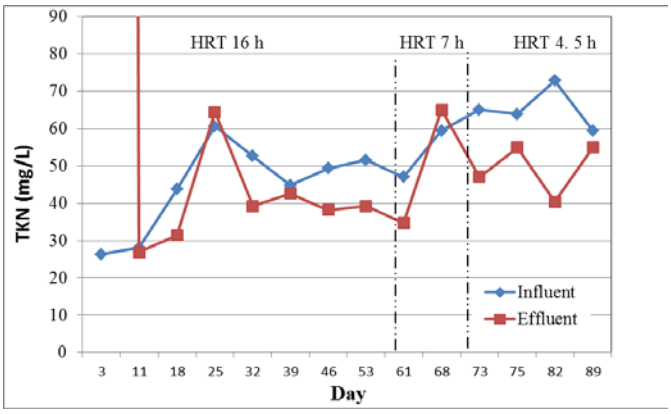

Figure 39: The TKN concentrations of ZW-1 MBR influent and effluent.

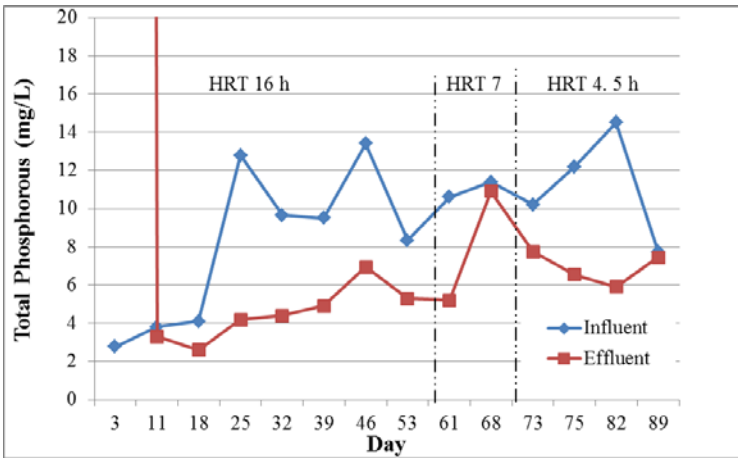

Figure 40: The total phosphorous concentrations of ZW-1 influent and effluent.

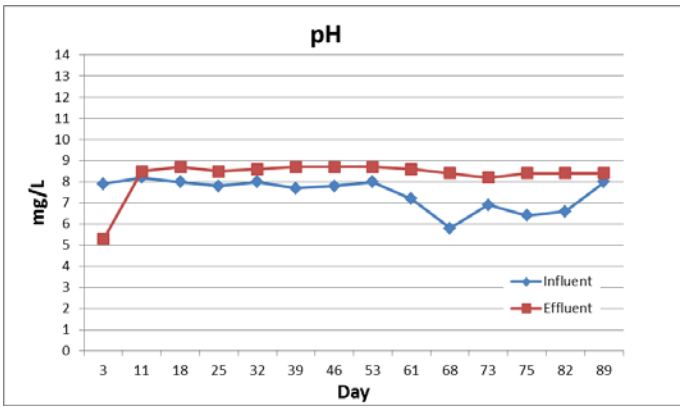

Figure 41: The pH levels of ZW-1 MBR influent and effluent.

Mixed liquor suspended solids were measured during the experiment to observe the build-up of solids and biomass in the MBR process tank. MBR systems can readily treat wastewater at MLSS level >8,000 mg/L, making them more efficient with smaller footprints than conventional activated sludge plants, which are typically operated at a MLSS range of 1,500 – 5,000 mg/L . The average MLSS value during the 16 hour HRT, 60 day experiment was less than 5,000 mg/L. At this condition, the ZW-1 consistently treated incoming synthetic wastewater to acceptable levels for further RO purification. The effluent from the ZW-1 reactor met all of the feed limit requirements for RO purification and in most cases approached the lower detection limits of the test methods (Table 12 & Table 13).

The incoming wastewater feed was also monitored on a weekly basis to calculate the percent removal of contaminants (Table 14). Variability of COD, BOD, TSS, and turbidity in the synthetic feed water was often observed and was attributed mainly to the settling of suspended solids and perhaps incomplete dissolution of certain wastewater components such as starch due to inadequate mixing in the 275 gallon totes used to make and store large batches of synthetic wastewater. Depending on the sampling date, a freshly made batch of synthetic water could differ significantly from water that had been in the large totes for several days. It was observed that more water soluble nutrients such as ammonia, TP, and TKN remained very consistent from batch to batch (Figure 38-Figure 40; Table 12 & Table 13). Changes in feed water occur

naturally in real wastewater treatments plants and are not a concern here, as the small-scale MBR system was found to treat all incoming wastewaters with high efficiency (Table 12 &Table 13) and consistency.

The ZW-1 unit was gradually reduced to an HRT of 7 hours, followed by an HRT of 4.5 hours over the course of several weeks in order to monitor water quality before scaling up to the pilot scale reactor. The ZW-1 continued to generate high quality effluent without system upsets or disturbances (Figure 32-Figure 41). Once a 4-5 hour HRT was reached, solids were wasted on a 15 day SRT in order to evaluate a low HRT/ high SRT design case scenario. The unit continued to operate under these conditions. However, very low HRTs (less than 4 hours) were not demonstrated with the current ZW-1 configuration as the MBR system reached its maximum flux.

Table 14: Average removal efficiency for COD, BOD, TOC, TDS, TSS, and turbidity by ZW-1 MBR (excluding day 3 data).

Parameter	Average Removal Efficiency
BOD	95.0%
COD	86.5%
TOC	76.0%
TSS	96.0%
Turbidity	98.2%
TDS	22.0%

4.2.4.4 Conclusions

Lab-scale MBR experiments using a GE ZW-1 lab MBR unit to treat synthetic gray water were carried out to generate initial water quality data and establish MBR process capability for treating gray water such that the MBR effluent can be further treated using an RO unit. The ZW-1 MBR experiments were conducted over the course of 89 days. During that time, water quality data was collected on the synthetic gray water influent as well as the MBR treated effluent, with a hydraulic retention time (HRT) in the range of 4-18 hours. The data showed the promise of MBR in treating gray water, as the BOD, COD, TOC, and TSS of the MBR effluent were found to meet RO feed water requirements.

4.2.5 Synthetic Gray Water Treatment Using ZW-10 Pilot Scale Membrane Bioreactor and E-2 RO Wastewater Treatment System

4.2.5.1 ZW-10 Pilot Scale MBR System

After initial screening experiments utilizing a GE ZW-1 lab system, the MBR experiments were scaled up using a ZW-10 MBR unit (260-1050 mL/min, or 100-400 gallons/day). The larger unit enables more precise control and more detailed monitoring of membrane operating parameters (e.g., flux, TMP) and was used to verify the findings from the smaller ZW-1 units. Flux data from units of this size can be used as guidance for design and performance evaluation of a full scale system. The ultimate goals of the pilot-scale MBR/RO experiments were as follows: i) generating permeate that meets RO design feed limits for further RO treatment to meet potable water specifications; ii) maintaining stable operation of the reactor at the lowest possible hydraulic retention time (HRT) and relatively long solids retention time (SRT) to reduce the overall footprint and energy costs, as well as waste generation and disposal costs; and iii) optimizing the bioreactor to run continuously with RO treatment as an integrated system with minimal maintenance and membrane fouling.

Initially, the ZW-10 unit consisted of a 60 gallon process tank (40 gal operating volume) and a larger ZeeWeed® hollow-fiber module with a nominal surface area of 10 ft^2 (Figure 42). Three large totes (275 gallons) were used to make and store large batches of synthetic wastewater (using synthetic gray water recipe 3 in Table 10 & Table 11). The synthetic wastewater was fed into the reactor tank using a diaphragm pump. A 6-gallon backpulse tank was used to collect permeate and pulse water back through the membrane every 15 minutes for 60 seconds to prevent membrane fouling and solids build-up.

(a)	(b)
a	

Figure 42: (a) The ZW-10 MBR system at GE Global Research, b) The ZW-10 MBR module (membrane area= 10 ft^2/0.93 m^2, length=69.2 cm, diameter =11 cm, holdup volume= 130 mL).

Flow rate and transmembrane pressure were measured daily to determine flux through the membrane and to monitor changes in flow and membrane fouling while progressively decreasing the HRT. Mixed liquor suspended solids (MLSS) levels were monitored throughout the entire experiment and used to determine the approximate food-to-microorganism (F:M) ratio. One of the goals of the MBR experiment was to operate the system efficiently at the lowest possible HRT (i.e., <4 hours) and generate the least amount of waste from sludge disposal (i.e., high SRT)

while still maintaining superior treatment and water quality. The synthetic gray wastewater treatment experiments were finished at an HRT of just below 4 hours before severe membrane fouling occurred, resulting in membrane replacement and recovery cleaning.

Toward the end of the study, The ZW-10 MBR unit was reconfigured to reduce the volume of the process tank in order to operate the MBR at a desired HRT of less than 4 hours while maintaining a flux of less than 24 gfd, the maximum recommended operating flux of the GE Zenon MBR membrane system. The reconfigured ZW-10 MBR system is shown in Figure **43**. The smaller process volume was used for the second round of experiments using laundry and kitchen wastewater with a wide range of HRT.

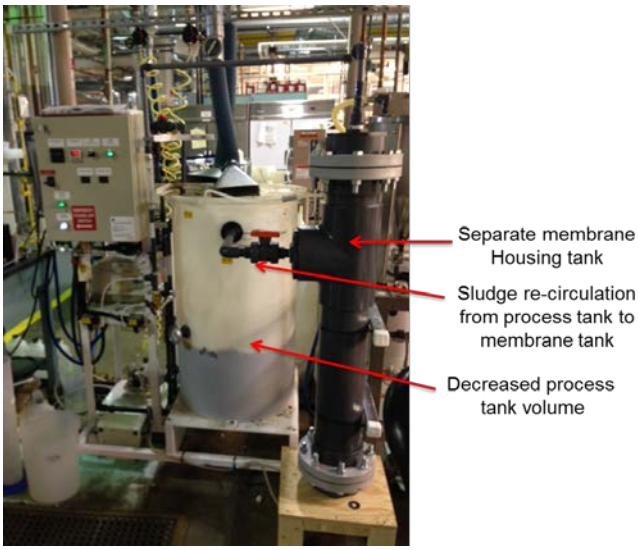

Figure 43: Re-configured ZW-10 MBR system. An additional tank and a pump were installed to house the ZW-10 membrane module and to re-circulate the activated sludge, respectively.

4.2.5.2. Results and Discussion of ZW-10 Pilot-Scale MBR Study

1. Water Quality Parameters

BOD, COD, and TOC BOD is a measurement of the amount of dissolved oxygen that is required to meet the metabolic needs of the microorganisms in order to degrade the organic matter in wastewater. Figure 44 shows the BOD profile of the raw wastewater and MBR effluent. The average BOD values of the raw gray water and MBR effluent, after a 15 day stabilization period, were 417.4 mg/L and 7.0 mg/L, respectively. The average removal efficiency of BOD by the MBR was 98.4%. The BOD of the effluent was found to be consistently below the RO feed water quality requirement of 20 mg/L throughout the experimental period.

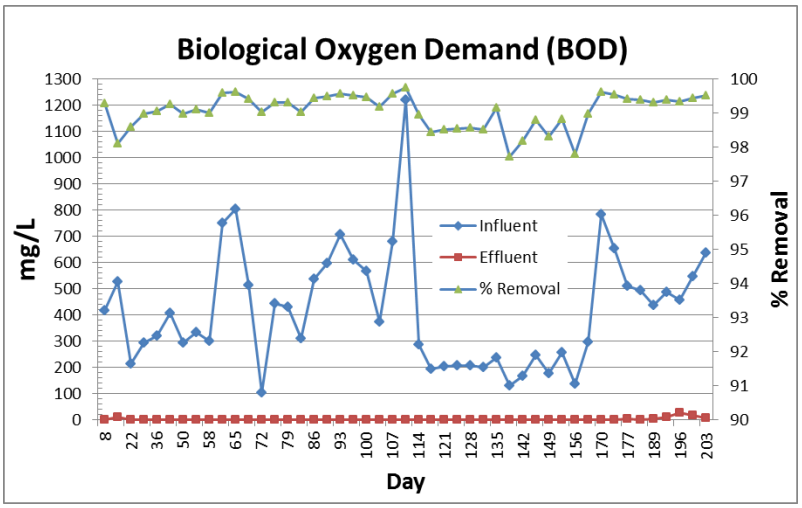

Figure 44: The BOD concentrations of influent and effluent and the BOD removal efficiency of the ZW-10 MBR system.

COD is a measurement of the amount of contaminants that can be oxidized chemically in a water sample. Figure 45 shows the COD levels of the MBR influent and effluent. The average COD values of the raw gray water and MBR effluent were 747.8 mg/L and 18.7 mg/L, respectively. The average removal efficiency of COD by the MBR was 97.0%. COD levels in the effluent dropped below the 60 mg/L RO feed water specification following a 15 day stabilization period. Spikes in permeate COD levels were observed on days 15, 43, and 100. These sporadic COD spikes did not cause noticeable fouling of the membrane or negatively impact the performance of the RO membrane system

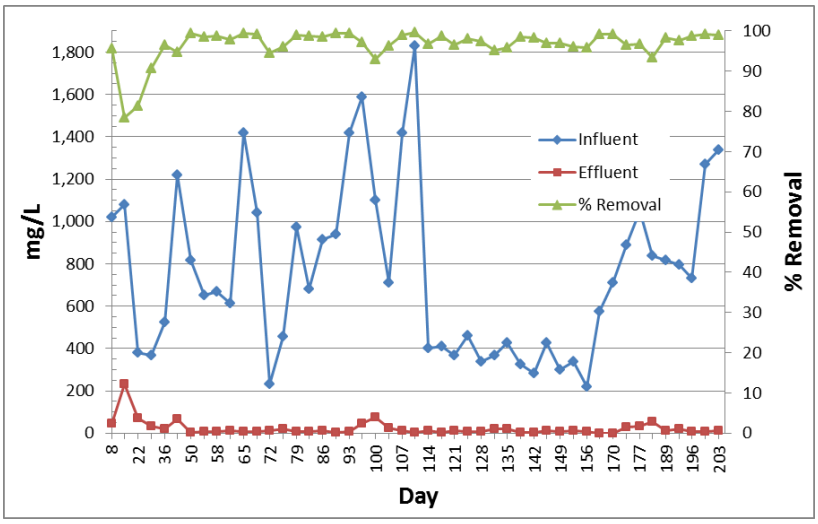

Figure 45: The COD concentrations of influent and effluent and the COD removal efficiency of the ZW-10 MBR system.

TOC is a measure of the amount of carbon covalently bonded in organic compounds, and thus is another key water quality parameter. The average TOC values of the raw gray water and MBR effluent, after a 15 day stabilization period, were 109.8 mg/L and 5.8 mg/L, respectively. The average removal efficiency of TOC by the MBR was 92.0%. Figure 46 shows that the TOC level mostly stabilized to 2-6 mg/L after the initial start-up period, well below the 10 mg/L requirement for RO feed water.

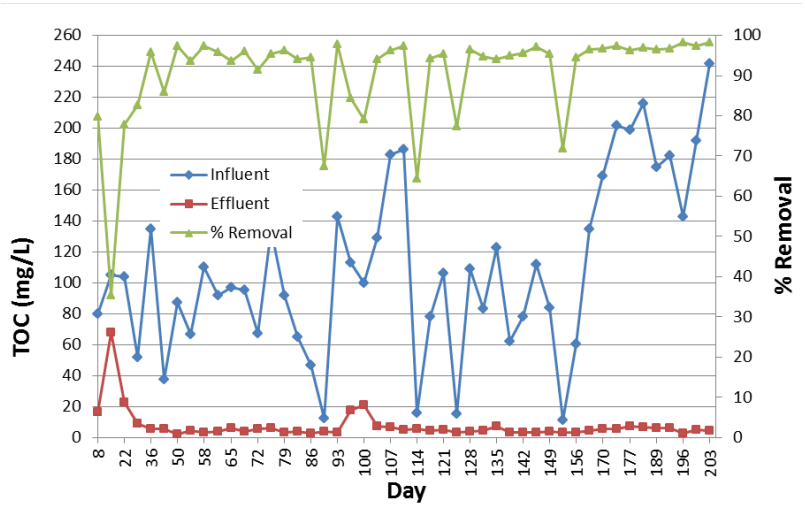

Figure 46: The TOC concentrations of influent and effluent and the TOC removal efficiency of the ZW-10 MBR system.

<u>Nitrogen and phosphorus species</u> Similar to ZW-1 experiments, removal of ammonia, TP, and TKN was minimal during the experiment (Figure 47-51) without seeding of nitrifying bacteria, as their population takes significantly more time to establish in a bioreactor. In order to initiate ammonia removal in the ZW-10 reactor, a nitrifying bacterial culture was introduced into the process tank on day 83 of the experiment. Approximately 5 pounds of GE Bio plus BA2912, a blend of proprietary bacterial culture for removal of nitrogen compounds, was added to the MBR tank and nitrification occurred almost immediately, as indicated by a near 50% increase in ammonia and TKN removal just 24 hours after addition of the cultures (Figure 47 & Figure 48). The 15 day SRT was increased to 20 days in order to ensure the establishment of a nitrifying population for ammonia removal. The following is the complete nitrification oxidation reaction[35]:

$$NH_4^+ + 2O_2 \rightarrow NO_3^- + 2H^+ + H_2O \qquad \text{(Eq. 7)}$$

Nitrification causes a pH drop over time with the addition of H^+ ions to the system as a result of the above nitrification oxidation reaction, eventually creating a poor water condition to support further nitrification. As a result, a noticeable decline in ammonia removal was recorded in the effluent following the pH drop from days 93-120 (Figure 48). This cycle of increased nitrification-pH drop-decreased nitrification-pH increase will continue unless the pH is maintained at or just above 6.5, an optimal condition for nitrification. Nevertheless, the nitrifying stock was instrumental in rapidly establishing a growing nitrifying bacteria population to effectively remove ammonia from the wastewater. This enhanced ammonia removal can be

sustained by taking the appropriate steps to control the pH and keep a reasonable SRT to balance the heterotrophic organism population with the nitrifying bacteria population.

Figure 50 shows that the total phosphorous concentrations of ZW-10 MBR influent were in the range of 5 to 18 mg/L, and the total phosphorous concentrations of the MBR effluent were in the range of 4 to 14 mg/L. The average removal efficiency of total phosphorous by the MBR was approximately 30%.

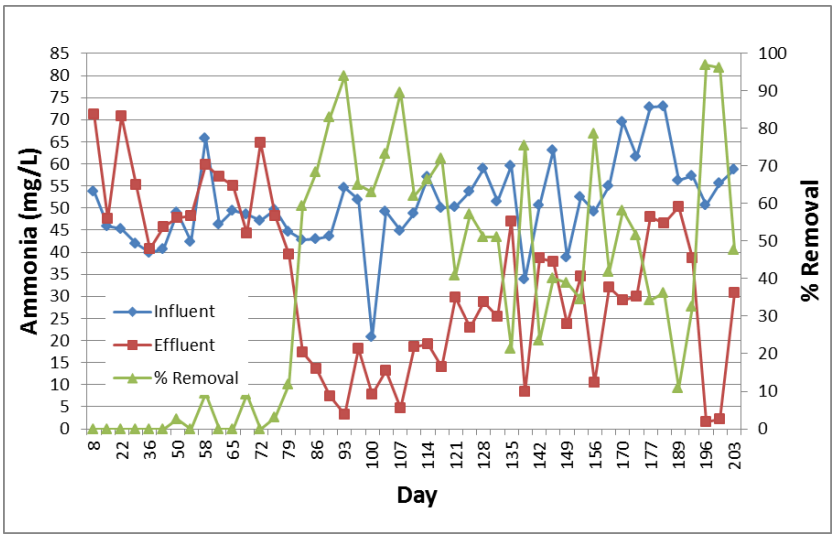

Figure 47: The ammonia concentrations of the ZW-10 MBR influent and effluent.

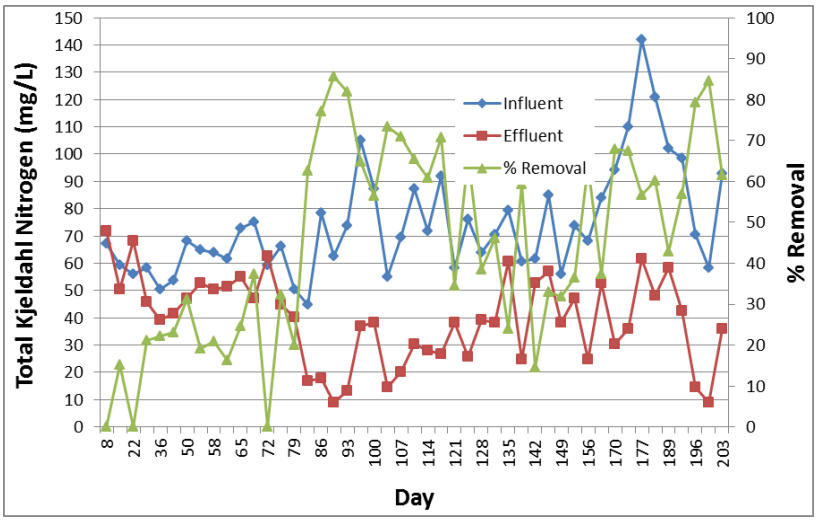

Figure 48: The TKN concentrations of ZW-10 MBR influent and effluent.

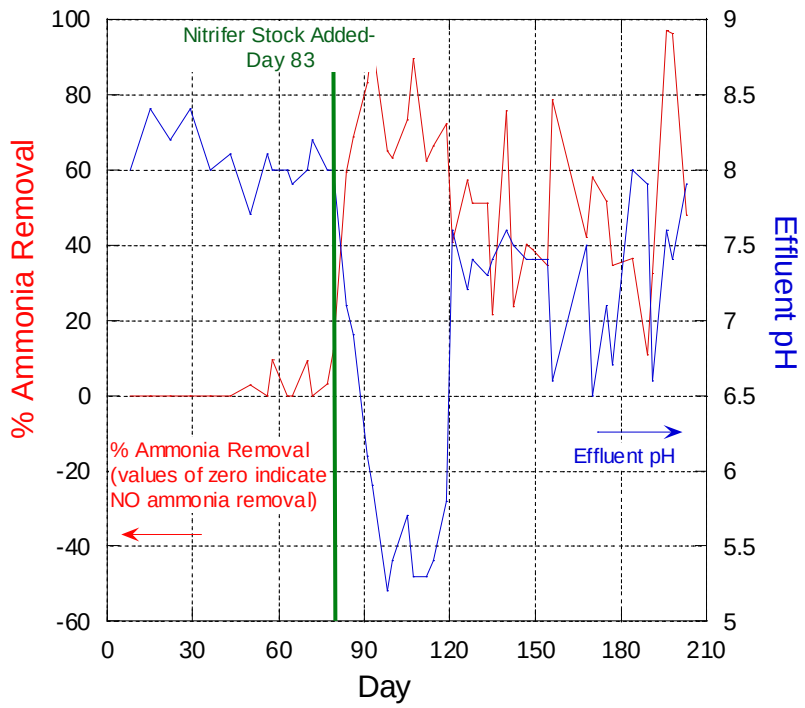

Figure 49: Percent ammonia removal and effluent pH monitored throughout the ZW-10 experimental study

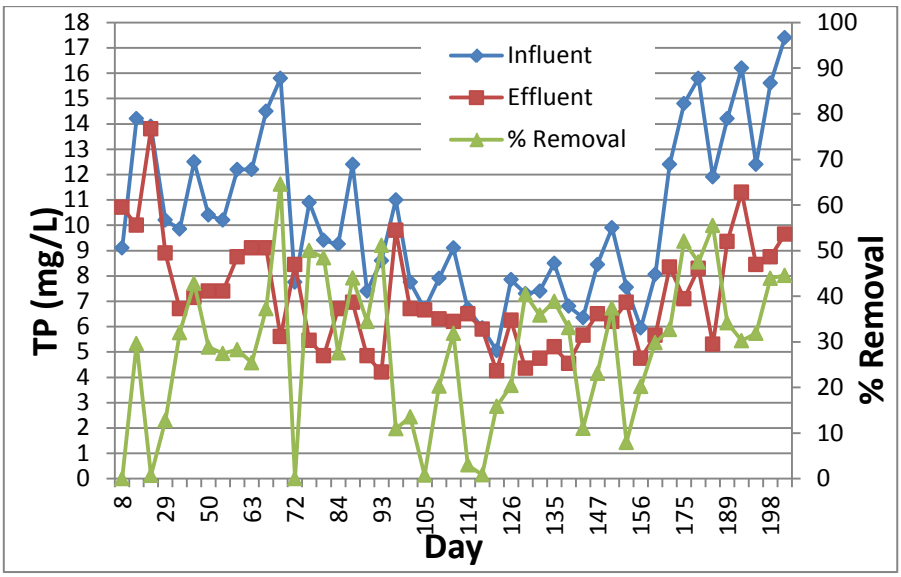

Figure 50: The total phosphorous concentrations of ZW-10 MBR influent and effluent.

<u>Turbidity and TSS</u> The turbidities and TSS levels of the influent gray water and the MBR permeate are shown in Figure 51 & Figure 52. Permeate turbidity remained at 0.3 NTU (nephelometric turbidity unit) or less during the entire operation period, below the 0.4 NTU

specification for RO feed water. Similarly, the TSS level for the MBR permeate was in the range of 1-2 mg/L, reaching the lower detection limit.

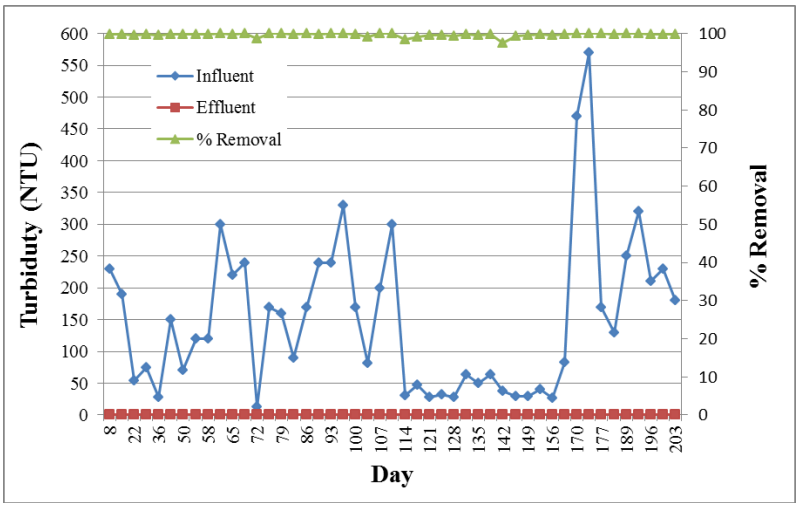

Figure 51: The turbidity level of ZW-10 MBR influent and effluent.

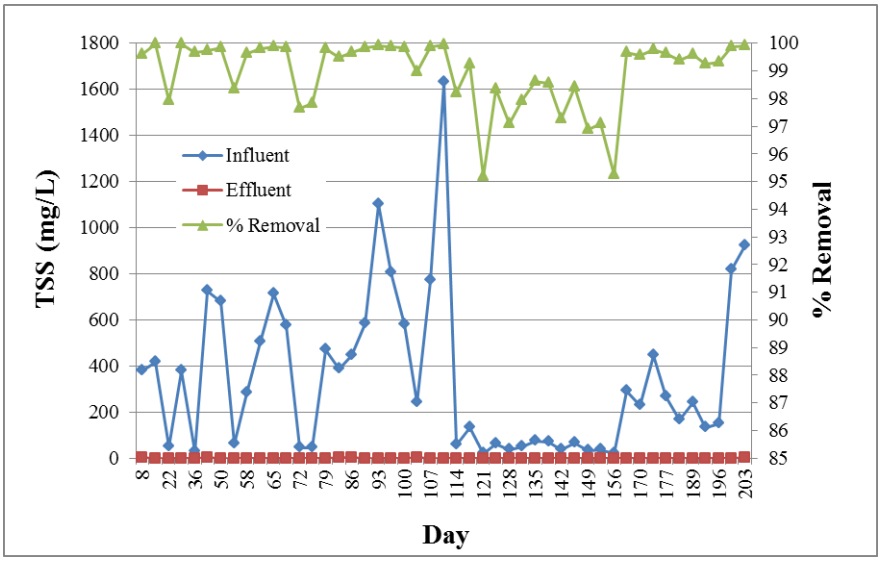

Figure 52: The TSS of the ZW-10 MBR influent and effluent.

2. Operational Parameters

The operational parameters for evaluating the performance of the MBR system include permeate flux, transmembrane pressure, permeability, backpulse, and air scouring. These parameters are described below.

ZW-10 MBR Start-Up The ZW-10 MBR process tank was seeded over the course of 5 days using BioQuick™ 5130 seed stock from Novozymes. Initially, 8 pounds of seed packs were added to the process tank containing synthetic wastewater (SynGW3) and aerated at 3 scfm. On

days 4 and 5, an additional three and two pounds of seed stock, respectively, were added to the tank. Continuous flow of synthetic wastewater and permeate collection began on day 6.

Membrane Flux Flux is a measure of the rate at which the permeate passes through the membrane per unit area of the membrane surface, with units of U.S. gallons per square foot per day (gfd) or liters per square meter per hour (lmh). Membrane flux selection is a balance between cost and risk. A lower design flux results in higher initial cost but in general less maintenance and lower risks of membrane fouling, whereas a higher design flux generally results in lower initial cost but higher maintenance and a potentially high risk of membrane fouling. Factors affecting the selection of design flux include temperature, MLSS concentration, and type and composition of wastewater (municipal, industrial, commercial, etc.). GE's ZeeWeed® hollow fiber membrane typically operates in the range of 10 to 24 GFD to effectively manage membrane fouling.

Figure 53 shows the water flux through the membrane over the period of 208 days. Since one of the key objectives was to evaluate effluent quality while operating the MBR system at low HRTs (<4 hr) and high SRTs (>20 days), the membrane flux inevitably exceeded the recommended maximum flux (24 GFD) for the ZW-10 module with the original MBR reactor volume (40 gallons). Figure 53 shows that water flux increases as the HRT decreases. The ZW-10 operated at a reasonable TMP and flux for a period of approximately 110 days without any membrane cleaning before a noticeable decline in flux was observed. The fouled membrane was removed and replaced with a new module and the experiments were continued. Membrane cleanings using citric acid and sodium hypochlorite were performed to evaluate flux improvement after chemical washes, and will be discussed in more detail in the next section. Following membrane replacement, a dramatic improvement in flux was observed. As the HRT was lowered further throughout the course of the experiment, increases in flux were observed accordingly. Membrane flux reached 30-40 GFD from days 127-162,well above the maximum recommended flux for the ZW-10 module (24 GFD), in order to achieve an HRT of 2.5 hrs. The MBR effluent was found to meet the RO pre-treatment requirements during the entire experimental period. However, membrane fouling occurred, as expected.

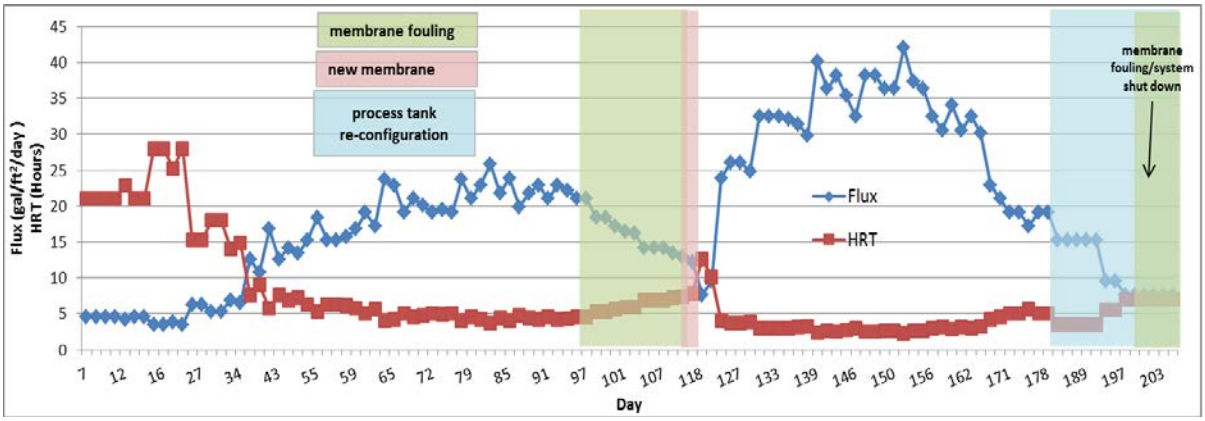

Figure 53: Variations of membrane flux and HRT during the ZW-10 MBR operation.

Transmembrane Pressure (Vacuum) ZeeWeed ultrafiltration membranes are immersed in an aeration tank, in direct contact with mixed liquor. Through the use of a permeate pump, a vacuum is applied to a header connected to the membrane lumens. The vacuum draws the treated water through the hollow fiber ultrafiltration membranes. The MBR pilot system is typically operated to maintain a constant flux. Thus, as membrane fouling occurs, transmembrane pressure increases in order to maintain the flux. Membrane cleaning was required if the vacuum exceeded 8 psi over an extended period of time. Figure 54 shows that the average vacuum pressures before and after backpulse were around 1.5 to 2 psi, and the values were consistently below 8 psi when the membranes were operated below the critical flux of 24 gfd (i.e., for the first 106 days of operation). For days 127 to 150, when the MBR was operated at 30-45 gfd, the transmembrane pressure increased to 14 psi, indicating unsustainable membrane flux and membrane fouling.

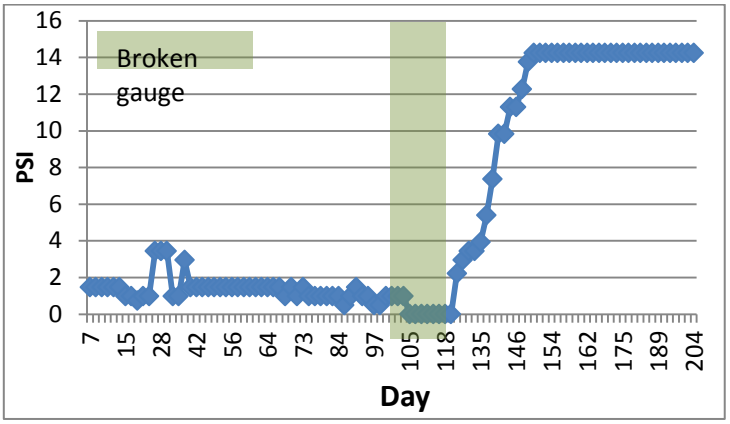

Figure 54: The transmembrane pressure profile during the ZW-10 MBR operation.

<u>Membrane Permeance</u> Permeance is the transmembrane pressure normalized flux, in gfd/psi, calculated by dividing the membrane flux by the transmembrane pressure. It is used to indicate the level of membrane fouling and/or filterability of the mixed liquor and whether membrane cleaning should be scheduled. Generally membrane cleaning is initiated when permeability is <4 gfd/psi. Figure 55 shows that the permeance was generally between 2 and 20 gfd/psi, with the initial low permeance likely due to the low flux used during initial operation, and the low permeance near the end of the experimental period due to very high membrane flux and membrane fouling. The ZeeWeed MBR processing tank temperature ranged from 17 to 22 ^{o}C during the course of the experiment.

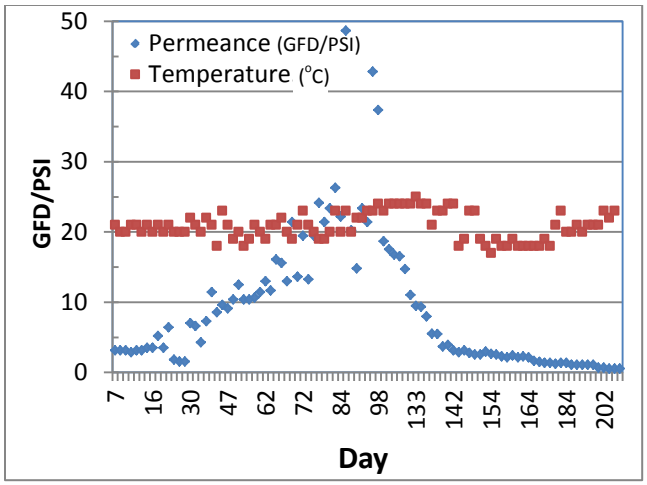

Figure 55: The membrane permeance and temperature of the ZW-10 MBR system.

Backpulse Backpulse refers to a short period of time where the flow of permeate is reversed through the membrane so that the permeate flows from the inside of the membrane fibers to the outside, to remove solids and other foulants from the membrane surface. In this study, fully automated backpulse occurred for 60 seconds every 15 minutes of permeation.

Air Scouring During MBR operation, continuous airflow is introduced to the bottom of the membrane module, producing turbulence that scours the external surface of the hollow fibers. This scouring action removes rejected solids away from the membrane surface and provides mixing of the mixed liquor in the tank to prevent over-concentration or 'sludging' in the membrane fibers. Aeration also serves to sustain the minimum DO concentration of 1.0 mg/L in the processing tank necessary to maintain a healthy bacteria population. In the current study, the airflow in the tanks was maintained at 3.5 scfm. Figure 56 shows that the DO concentration in the ZW-10 process tank was well above 1 mg/L.

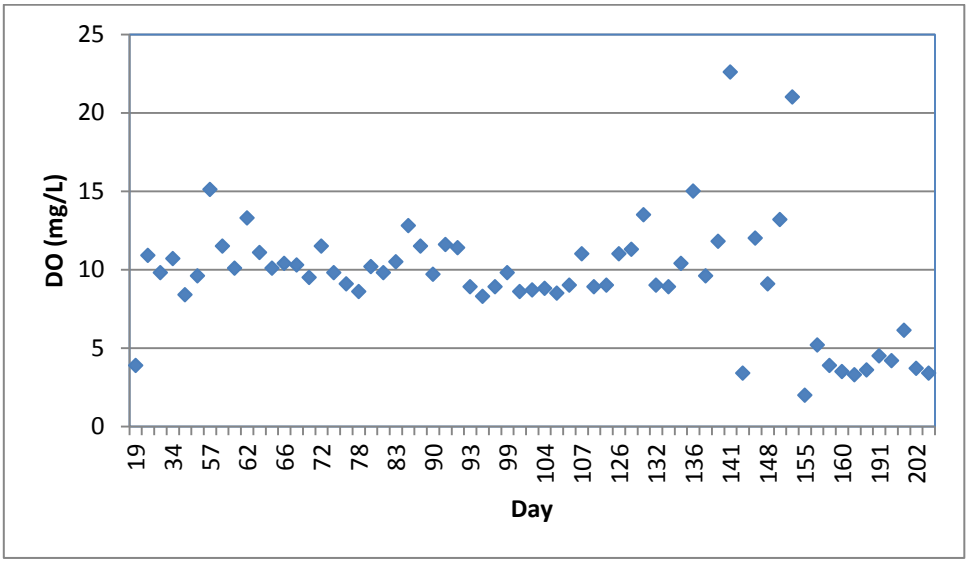

Figure 56: The DO concentrations in the ZW-10 MBR processing tank.

Mixed liquor suspended solids (MLSS) Mixed liquor suspended solids (MLSS) values were typically measured and recorded twice a week to monitor increases in the activated sludge population in response to changes in HRT and SRT (Table A-3 in Appendix). The MLSS value was also used to estimate the food to microorganism (F:M) ratio in the process tank as an indication of potential upsets in the biological population that could result in foaming events. An F:M ratio of approximately 0.2-0.4 in a system with an SRT of 5-15 days is typical, and an increase in MLSS often occurs as the SRT increases [36]. The MLSS value throughout the course of the experiment was rather low for what the ZW-10 MBR can typically support (8-10,000 mg/L), however the water quality data did not show any indication of population failure and the MLSS value gradually increased to close to 9,000 mg/L by the end of the experiment as the SRT increased from 13 to 22 days and the HRT decreased to less than 4 hours (Figure 57). The higher SRT allowed the seeded nitrifying organisms to maintain a growing population, and also supported the COD and BOD-removing organisms.

The F:M ratio is calculated by the following equation:

$$F:M = \frac{\text{Pounds BOD to aeration tank}}{\text{Pounds MLSS in aeration tank}}$$

$$= \frac{\text{Influent Flow (MGD)} \times \text{Influent BOD Concentration (ppm)} \times 8.34 \left(\frac{\text{lb}}{\text{gal wastewater}}\right)}{\text{Aeration Tank Volume (MGal)} \times \text{MLSS (ppm)} \times 8.34 \left(\frac{\text{lb}}{\text{gal wastewater}}\right)}$$

$$= \frac{\text{Influent Flow (GPD)} \times \text{Influent BOD Concentration (ppm)}}{\text{Aeration Tank Volume (Gal)} \times \text{MLSS (ppm)}} \qquad \text{(Eq. 8)}$$

Because the F:M ratio is a function of the incoming BOD, variations of BOD in the feed causes F:M ratio to fluctuate. On average, the F:M ratio was within a reasonable range for the ZW-10 operating conditions (Figure 57). Because the incoming BOD levels vary depending on how long the wastewater was inside the feed tanks and when a new batch of synthetic gray water was made, the F:M ratio shows high spikes throughout the course of the study. As the MLSS value continued to increase with a higher SRT of 20 days, the F:M value stabilized to a range of 0.2 to 0.6 (Figure 57). Despite the variability in the F:M ratio, the system operated efficiently and consistently produced high quality effluent (see next section for water quality data).

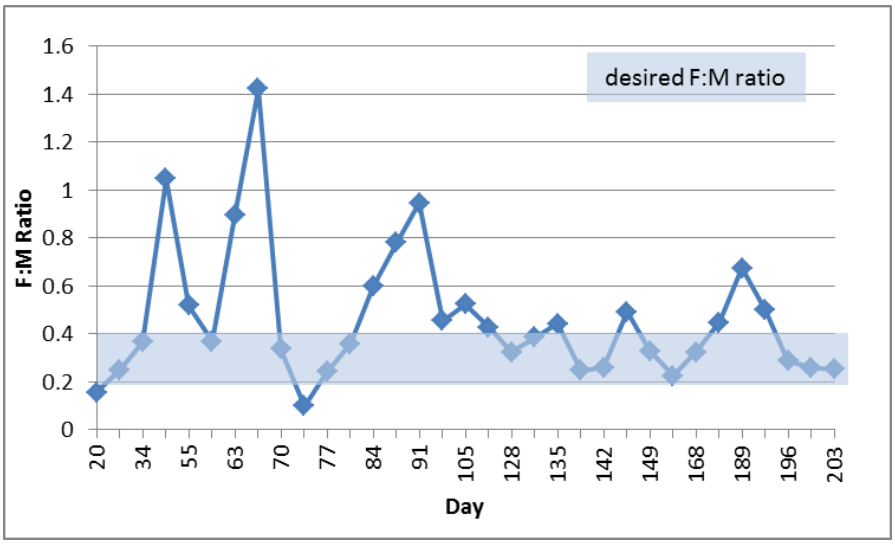

Figure 57: Food to Microorganism (F:M) ratio for ZW-10 experiment. Average F:M over the entire study was 0.48.

Foaming Control On day 21, foaming was observed in the ZW-10 process tank, coinciding with a noticeable decline in effluent water quality. 190 ml of FOAMTROL AF2050, an anti-foaming agent from GE Water and Process Technologies, was dosed into the process tank. This antifoaming agent is designed to operate with MBR systems without any detrimental effects on the microorganisms or the membranes, and appeared to be a fast-acting approach to controlling foaming issues in the bioreactor. By day 24 the foaming had completely subsided and no additional foaming issues occurred after that time. The water quality data on day 29 showed a decrease in COD levels in the effluent from 233 mg/L during the foaming event, to 71 mg/L, as well as a significant decrease in TOC levels, from 67.9 mg/L to 23 mg/L.

Membrane Fouling and Cleaning Membrane cleaning is an integral part of MBR operation. Under normal operating and cleaning conditions, membrane life for the current generation of GE's ZeeWeed hollow fiber membrane products should be greater than 10 years [37]. As part of the current study, membrane fouling and the effectiveness of cleaning experiments were carried out.

Operational data for the ZW-10 reactor were recorded on a daily basis to monitor for increases in transmembrane pressure and potential membrane fouling. Backpulse and air scouring were used to un-block constricted membrane pores and to minimize floc formation and caking on the outside of the membrane. The ZW-10 operated at normal TMP and flux for a period of approximately 110 days without any membrane cleaning before a noticeable decline in flux was observed (Figure 58). The fouled membrane was removed and cleaned using citric acid and sodium hypochlorite to evaluate flux improvement after chemical washes, while a new module was used to continue the experiment.

At the end of the ZW-10 experiments, a complete membrane recovery cleaning using sodium hypochlorite and citric acid was performed. The ZW-10 module was first submerged in a 1000 ppm bleach in water solution for 24 hours. Aeration was maintained throughout the entire

cleaning process. Forward flow and backpulsing were performed periodically in an effort to remove solids build-up in the membrane pores. Following the 24 hour bleach soak, the membrane and process tank were flushed completely with water and then treated with a 500 ppm citric acid soak for 24 hours. The same aeration and flow protocol was followed using citric acid. Following bleach and citric acid cleans, an over 90% membrane flux recovery was observed (>90% flux recovery in tap water). Images of the fouled membrane before the cleanings show sludge cake formation on the outside of the membrane as well as what appears to be a biofilm layer over the fibers (Figure 59b & Figure 60). After membrane cleaning, the sludge cake and biofilm were removed (Figure 58c, Figure 59c and Figure 59d), and the cleaned membrane surface (Figure 59d) appeared very similar to that of the new membrane (Figure 58a & Figure 59a).

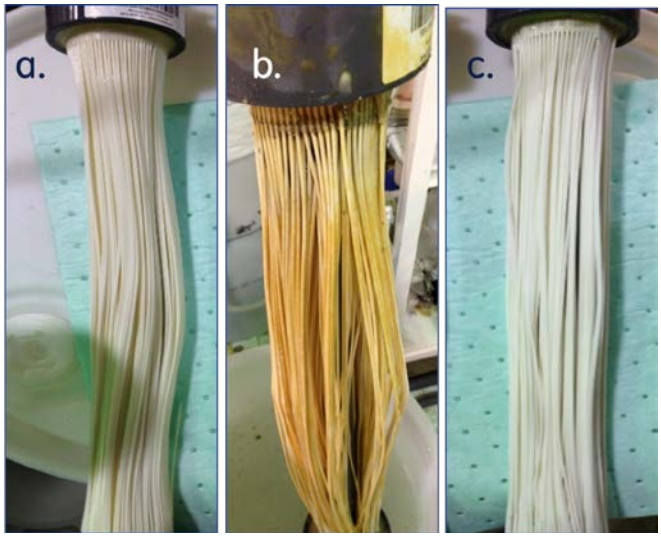

Figure 58: Images of a) new ZW-10 module; b) fouled ZW-10 module; and c) recovered module following sodium hypochlorite and citric acid cleanings.

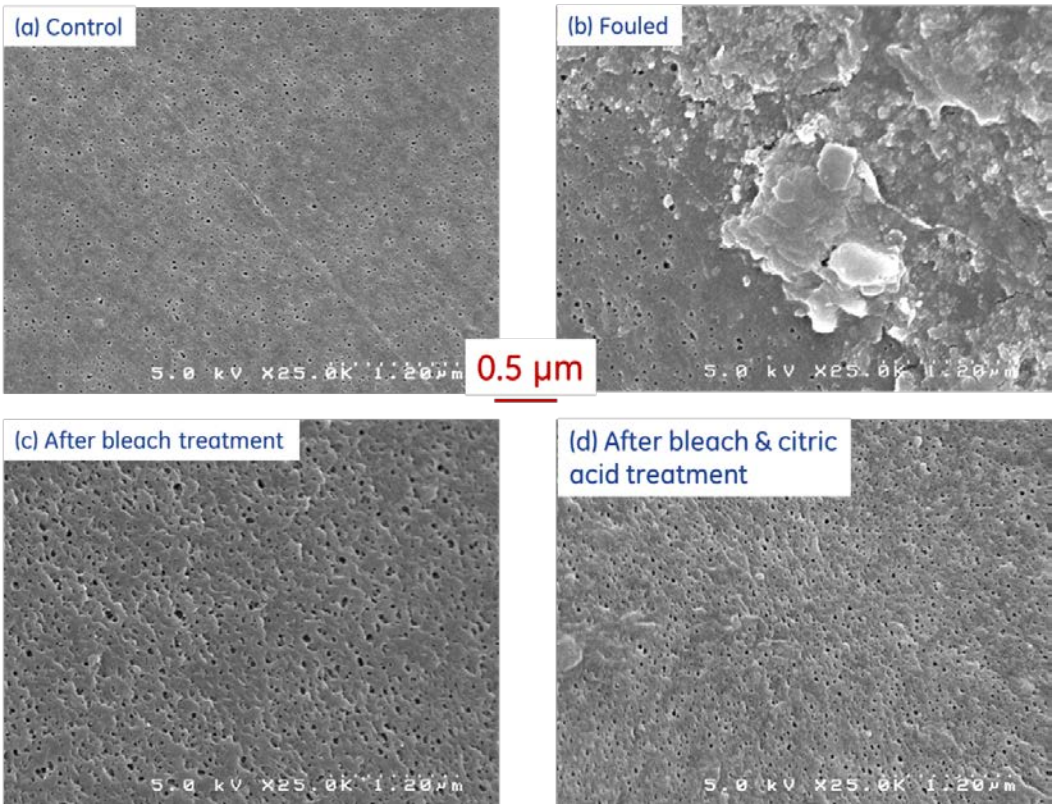

Figure 59: SEM images of a) new ZW-10 hollow fiber membranes; b) fouled ZW-10 membranes; c) recovered membranes following sodium hypochlorite; and d) recovered membranes following sodium hypochlorite and citric acid cleaning.

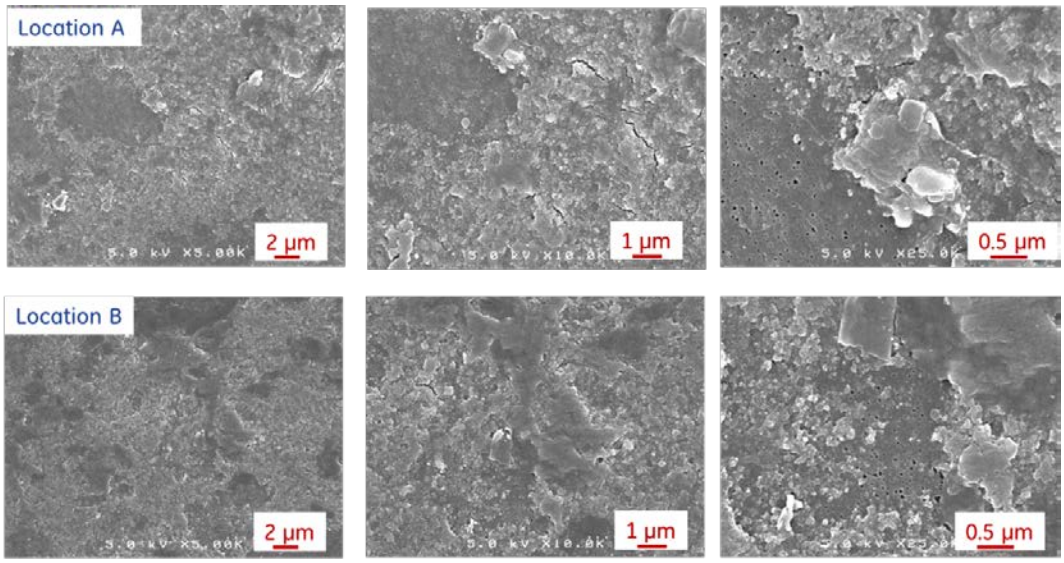

Figure 60: SEM images of fouled ZW-10 hollow fiber membranes.

4.2.5.3 Conclusions

Synthetic gray water was successfully treated with a ZW-10 MBR using a range of HRTs (from 24 hours to less than 2.5 hours) and SRTs (from 13 to 22 days). The MBR effluent was found to meet the RO feed requirements during the entire experimental period (>200 days). The demonstration of MBR to treat gray wastewater at low HRT and high SRT to produce high quality effluent that meets RO pre-treatment standards was an important milestone that enabled the design of a deployable system with a small system footprint and minimal waste discharge. The results also showed that while the MBR was operated within the recommended flux range of less than 24 GFD, membrane fouling was easily managed with membrane cleaning. When the MBR was operated above 24 GFD for an extended period of time, rapid membrane fouling occurred, as expected. The ZW-10 experiments also demonstrated successful foaming control with the addition of anti-foaming chemicals from GE Water, as well as successful membrane cleaning with sodium hypochlorite and citric acid.

4.2.6. Integration of RO system with MBR unit

Figure 61 shows the set-up of the integrated ZW-10 MBR and E-2 RO wastewater treatment system that converts gray water into high-quality water for potable and non-potable reuse. The integrated system was operated throughout the remainder of the synthetic wastewater treatment study, starting from day 177. A lab-scale AK1812 (2”x12”) low energy membrane element was used and the E-2 RO unit was operated at a constant pressure of 115 psi. RO feed and permeate conductivity were measured in order to calculate percent rejection, and permeate samples were routinely sent out for drinking water analysis (Table 15 & Table 16). The integrated system demonstrated excellent COD, BOD, TOC, TSS, and TDS removal and demonstrated the ability for both systems to operate together to achieve potable water quality standards. The RO membrane showed no signs of fouling (i.e., increased pressure or flux decline) during the experimental period.

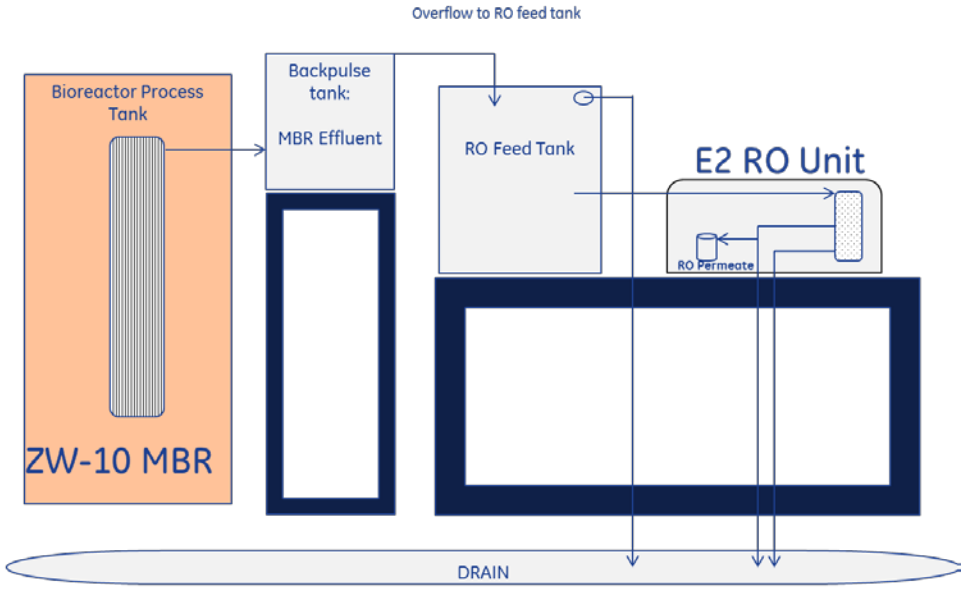

Figure 61: Schematic of the integrated ZW-10 MBR and E2 RO system.

In addition to the testing results above, the final permeate from the integrated MB/RO system was analyzed for drinking water quality by a series of tests. Excellent RO effluent that met the potable water standard was obtained (Table 17). The results of the complete drinking water analysis test revealed that the permeate met drinking water standards (Table A-3 in Appendix). It is important to note that the feed wastewater was a synthetic blend, and likely did not contain many of the constituents being tested in the drinking water analysis. Thus, treatment of laundry and kitchen wastewater was subsequently performed. The results of laundry and kitchen gray water treatment using the integrated ZW-10 MBR/E-2 RO system are summarized in the next section.

Table 15: RO feed and permeate conductivity and percent rejection data.

Day	Flux (gfd)	Feed Conductivity (μS)	Permeate Conductivity (μS)	% Rejection
177	10.5	1387	31.6	97.7
178	10.5	1348	30.7	97.7
184	8.6	1379	26.2	98.1
185	8.8	1330	25.6	98.1
188	9.3	1379	33.2	97.6
191	9.1	1220	21.1	98.3
195	10.5	1157	20	98.3
196	10.1	968	13	98.7
197	10.5	972	12.9	98.7
198	10.5	1057	18.4	98.3
199	10.5	1059	17.1	98.4
202	9.5	1429	36.8	97.4
203	10.5	1130	26.1	97.7

Table 16: Integrated system treatment of key wastewater parameters: COD, BOD, TOC, Ammonia, Total Phosphate, TDS, and Turbidity on days 154 and 198.

Day 154				
mg/L (unless noted)	Incoming Wastewater	MBR Effluent	RO effluent	% Removal
COD	339	13	NA	NA
BOD	257	<4	NA	NA
TOC	11.4	3.2	NA	NA
Ammonia	52.6	34.5	1.2	97.7
Total Phosphate	7.55	6.95	<0.02	99.7
TDS	620	510	<5	99.2
Turbidity (NTU)	41	<0.10	0.14	99.7
Day 198				

mg/L (unless noted)	Incoming Wastewater	MBR Effluent	RO Effluent	% Removal
COD	1270	9	<5	>99.6
BOD	548	17	<4	>99.3
TOC	192	5.1	<1.0	>99.5
Ammonia	55.7	2.1	0.1	99.8

Table 17: Typical sample analyses for drinking water testing[21].

Inorganics

Antimony	Lead	Fluoride	pH	Arsenic
Manganese	Chloride	Nitrate	Barium	Mercury
Sulfate	Nitrite	Beryllium	Nickel	Color
T.Dissolved Solids	Cadmium	Selenium	Odor	Turbidity
Chromium	Silver	Cyanide	Copper	Sodium
Alkalinity	Iron	Thallium	Corrosivity	Zinc
Hardness				

Volatile Organic Compounds (EPA 502.2) **(includes POCs, VOCs, THM)**

Bromochloromethane	trans-1,3 - dichloropropene	2-chlorotoluene	Bromomethane
methylene chloride	4-chlorotoluene	Carbon tetrachloride	1,1,1,2-tetrachloroethane
1,2-dichlorobenzene	Chloroethane	1,1,2,2-tetrachloroethane	1,3-dichlorobenzene
Chloromethane	Tetrachloroethene	1,4-dichlorobenzene	Dibromomethane
Dibromochloromethane	1,1,1-trichloroethane	Ethylbenzene	Dichlorodifluoromethane
1,1,2-trichloroethane	hexachlorobutadiene	1,1-dichloroethane	Trichloroethene
Isopropylbenzene	1,2-dichloroethane	trichlorofluoromethane	p-isopropyltoluene
cis-1,2-dichloroethene	1,2,3-trichloropropane	n-propylbenzene	trans-1,2-dichloroethene
benzene	Toluene	1,2-dichloropropane	bromobenzene
1,2,3-trichlorobenzene	1,3-dichloropropane	2,2-dichloropropane	sec-butylbenzene
1,2,4-trichlorobenzene	1,1-dichloropropene	tert-butylbenzene	1,2,4-trimethylbenzene
cis-1,3-dichlorpropene	chlorobenzene	m-xylene	o-xylene
p-xylene	vinyl chloride	n-butyl benzene	styrene
MTBE	1,2-Dibromo-3-Chloropropane	1,1 Dichloroethene	Ethylene Dibromide
Chloroform	Bromodichloromethane	1,2-Dibromoethane	Bromoform
135-Trimethylbenzene	Naphthalene		

Particulate Organic Compounds, Volatile organic compounds, Trihalomethanes,

4.2.7 Laundry and Kitchen Gray Water Treatment Using an Integrated ZW-10 Pilot Scale Membrane Bioreactor and E-2 RO Wastewater Treatment System

Following a long-term treatment study using synthetic wastewater, the integrated ZW-10 MBR and E-2 RO system was used to treat a mix of wastewater generated on site, comprising roughly 5% kitchen waste, 5% laundry waste, and the remainder tap water. Phosphate and ammonia, in the form of NaH_2PO_4 (23.0 mg/L) and NH_4Cl (150 mg/L), respectively, were spiked into the feed on occasion to assure adequate nutrient loading. The characteristics (e.g. BOD, COD, TOC, and TSS) of this wastewater mixture were found to be within the range of those of the gray waters from FOBs and other military facilities (Table 6 & Table 8).

The wastewater was first filtered through a 2 mm mesh bag in order to simulate typical settling/clarifying procedures performed at wastewater treatment plants. This coarse filtration step eliminated large solids from entering the process tank and damaging the membrane module. A rapid start-up protocol was designed in order to generate superior MBR effluent quality in less than 5 days using BioQuick 5130 as seed stock. The ability to rapidly start up the MBR/RO

system to generate reusable water in less than 4-5 days is very important. Deployable MBR and RO units used in forward operating bases (FOBs) and other contingency operation sites must have a small footprint and be up and running treating incoming wastewater in a matter of days.

4.2.7.1 Rapid Start-Up Protocol using Real Wastewater

The re-configured ZW-10 MBR unit, consisting of a smaller 25 gallon process tank (see Figure 43) was seeded with 6 pounds of BioQuick seed, approximately 5 pounds of BioRemove Nitrifying culture, and real wastewater feed. After initial screening of the real wastewater, the ratio was set at 5% kitchen waste, 5% laundry waste, and 90% tap water in order to achieve COD levels between 300-600 mg/L. The seeded sludge from the process tank was circulated through the externally housed membrane using a diaphragm pump. Air was supplied to the process tank and membrane holding tank at roughly 3.5 scfm for the first 24 hours without any flow. After 24 hours, flow was initiated at a hydraulic retention time (HRT) of approximately 5 hours and sludge wasting began with a solid retention time (SRT) of 25 days.

Influent and effluent samples from the ZW-10 MBR unit were collected and analyzed on days 3, 4, 5, and 6 representing 72, 96, 120, and 148 hours from the initial seeding. The typical parameters for evaluating wastewater quality were analyzed, including BOD, COD, TOC, TSS, TDS, TP, TKN, ammonia, turbidity, and pH. Potable water quality testing was also performed following RO purification on day 4 of the start-up. The rapid seeding protocol was successfully able to generate MBR effluent that met all RO feed water requirements by day 5 (Table 18), indicating that mobile deployment and start-up of an integrated MBR/RO wastewater treatment system could be completed in 5 days. The RO permeate water quality report on day 4 showed concentrations below test detection limits for over 80 of the major drinking water test parameters, including BOD, COD, and TOC (Table A-4 in Appendix).

Table 18: MBR effluent quality during rapid startup.

Parameter	RO Feed Requirements	MBR Effluent		
		Day 3	Day 4	Day 5
COD (mg/L)	<60	101	74	42
BOD (mg/L)	<20	35	<20	4
TOC (mg/L)	<20	36.7	24.7	14.6
Turbidity (NTU)	<0.4	0.13	0.1	0.1

4.2.7.2 Long term treatment study using laundry and kitchen wastewater

After a successful rapid start-up, the integrated ZW-10 MBR/E-2 RO system was used to continuously treat a mixture of laundry and kitchen wastewater for a period of 90 days. Several operational parameters were monitored on daily basis, including flux, transmembrane pressure (before, during, and after backpulse), and process tank temperature. The ZW-10 was set to permeate for 15 minute increments, followed by a 30 second back pulse to remove foulants from the membrane pores and surfaces. Air flow was maintained through the membrane module and in the reactor tank at 3.5 scfm. Mixed liquor suspended solids (MLSS) values were calculated to monitor biomass increases over the course of the study, in particular as the hydraulic retention time (HRT) was decreased. A relatively long solid retention time (SRT) of 25 days was kept over the entire study period, in an effort to increase MLSS to >8,000 mg/L and to allow nitrifying bacteria to maintain a stable population for ammonia removal. HRT was varied over the course of the study from 5 hours to less than 3 hours, and influent and effluent samples were collected weekly and analyzed for the same set of wastewater parameters. On occasion, the permeate from the E-2 RO unit was collected and analyzed for potable drinking water quality.

1. <u>MBR effluent water quality parameters</u>

<u>BOD, COD, and TOC</u> Figure 62 shows the BOD profile of the raw wastewater and MBR effluent. The average BOD values of the raw gray water and MBR effluent, after a 4 day stabilization period, were 327.3 mg/L and 4.0 mg/L, respectively. The average removal efficiency of BOD by the MBR was 98.3%. The BOD of the effluents was found to be consistently below the RO feed water quality requirement of 20 mg/L throughout the experimental period.

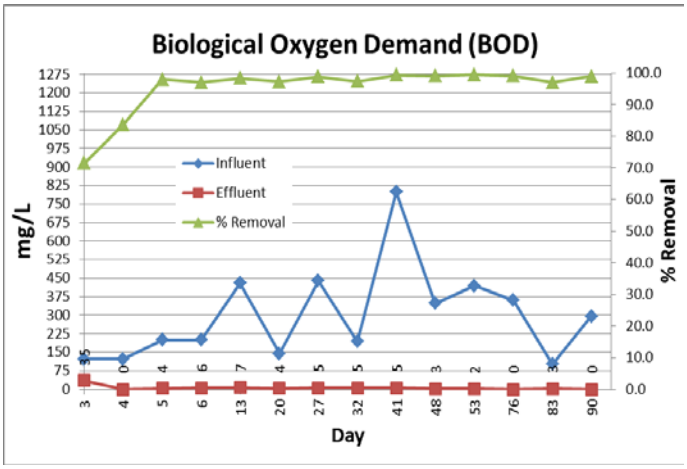

Figure 62: The BOD concentrations of influent and effluent and the BOD removal efficiency of the ZW-10 MBR system in treating real wastewater.

Figure 63 shows the COD levels of the MBR influent and effluent. The average COD values of the raw gray water and MBR effluent were 716.2 mg/L and 23.8 mg/L, respectively. The average removal efficiency of COD by the MBR was 95.6%. COD levels in the effluent dropped to below the 60 mg/L RO feed water specification following a 4 day stabilization period.

The average TOC values of the raw gray water and MBR effluent, after a 4 day stabilization period, were 88.9 mg/L and 6.9 mg/L, respectively. The average removal efficiency of COD by the MBR was 88.4%. Figure 64 shows that the TOC level mostly stabilized to 2-9 mg/L after the initial start-up period, below the 10 mg/L RO feed water specification.

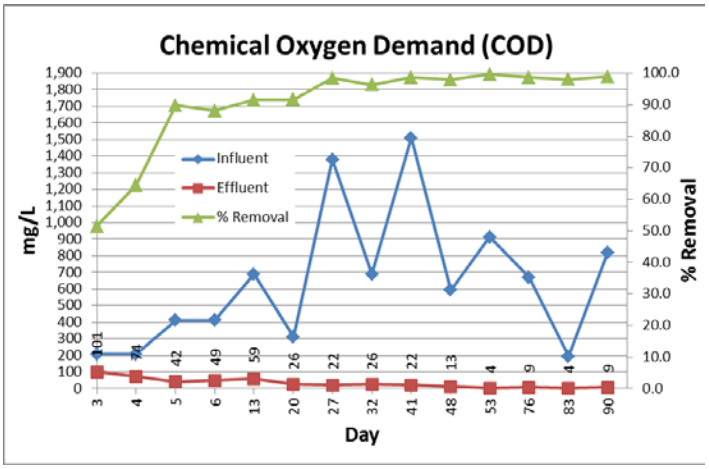

Figure 63: The COD concentrations of influent and effluent and the BOD removal efficiency of the ZW-10 MBR system in treating real wastewater.

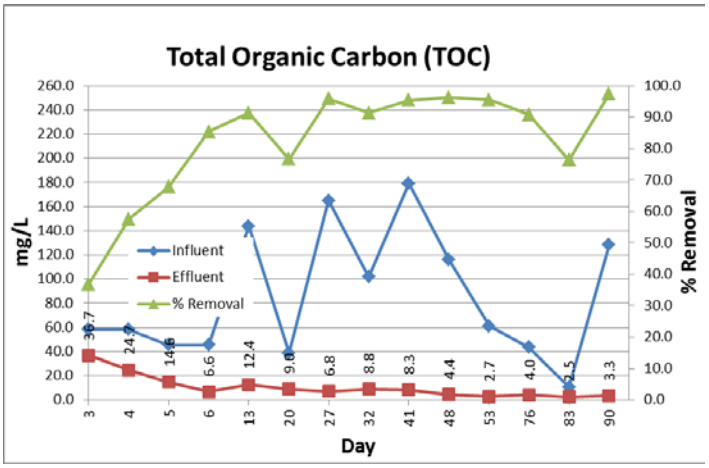

Figure 64: The TOC concentrations of influent and effluent and the BOD removal efficiency of the ZW-10 MBR system in treating real wastewater.

Nitrogen and phosphorus species In order to initiate ammonia treatment in the ZW-10 reactor, a nitrifying bacterial culture (Novozymes BioRemove™ 5805) was introduced into the process tank several times throughout the 90 day study to initiate nitrification and ammonia removal. Approximately two pounds of the stock culture were dosed in on days 7, 11, 28, and 66. After day 40, the ammonia removal increased to between 60 and 99% (Figure 65 & Figure 67) while the TKN removal efficiency increase to the range of 90 to 98% (Figure 66). SRT was maintained at 25 days throughout the experiments in order to ensure that the nitrifying population was established and population growth was adequately maintained to continue treating ammonia. Figure 68 shows that the total phosphorous concentrations of ZW-10 MBR influent were in the range of 3 to 12 mg/L, and the total phosphorous concentrations of the MBR effluent were in the range of 0.5 to 5 mg/L. The average removal efficiency of total phosphorous by the MBR was 78% after the initial start-up period.

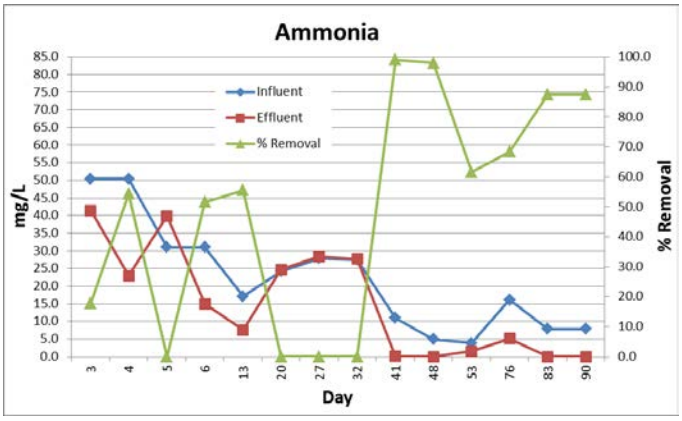

Figure 65: The ammonia concentrations of influent and effluent and the ammonia removal efficiency of the ZW-10 MBR system in treating real wastewater.

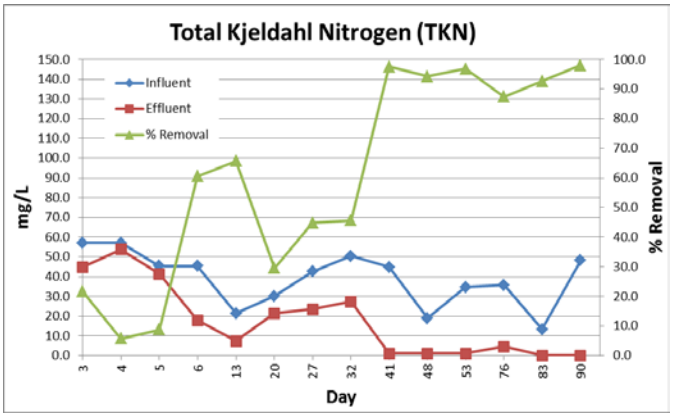

Figure 66: The TKN concentrations of influent and effluent and the TKN removal efficiency of the ZW-10 MBR system in treating real wastewater.

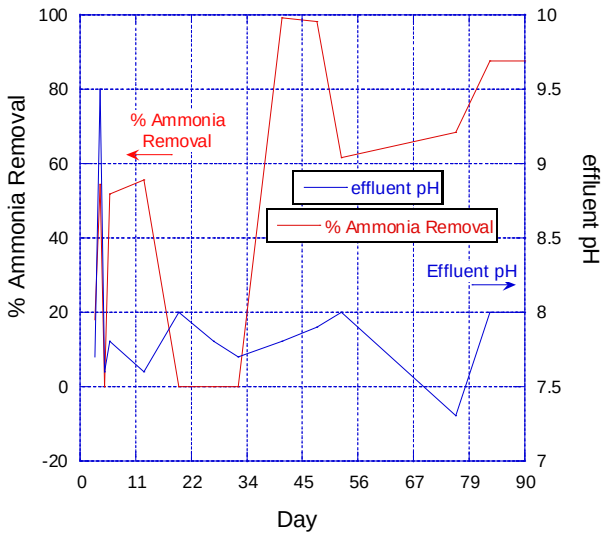

Figure 67: Percent ammonia removal and effluent pH monitored throughout the ZW-10 experimental study.

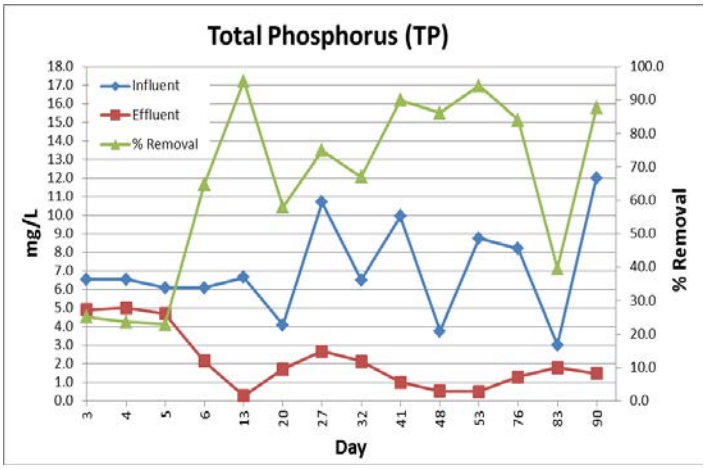

Figure 68: The TP concentrations of influent and effluent and the TP removal efficiency of the ZW-10 MBR system in treating real wastewater

<u>Turbidity and TSS</u> The feed wastewater and MBR permeate turbidity and TSS are shown in Figure 69 and Figure 70, respectively. The average BOD values of the raw gray water and MBR effluent, after a 4 day stabilization period, were 258.9 and 0.19 NTU, respectively. Permeate turbidity was consistently below the 0.4 NTU specification for RO feed water. Similarly, the TSS level for the MBR permeate was below 1 mg/L, reaching the lower detection limit.

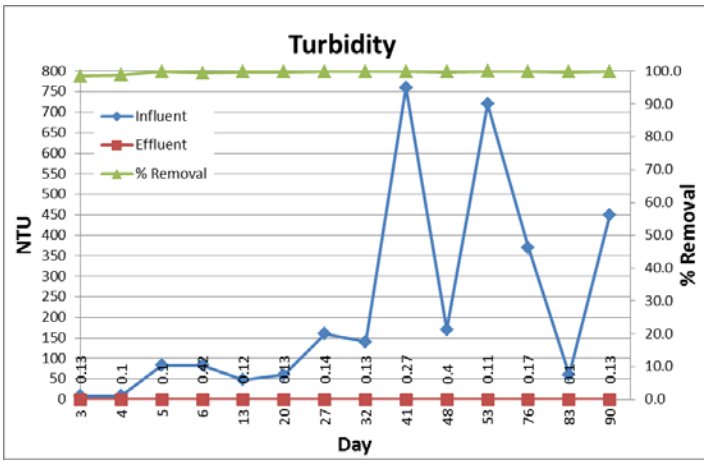

Figure 69: The turbidity level of ZW-10 MBR influent and effluent.

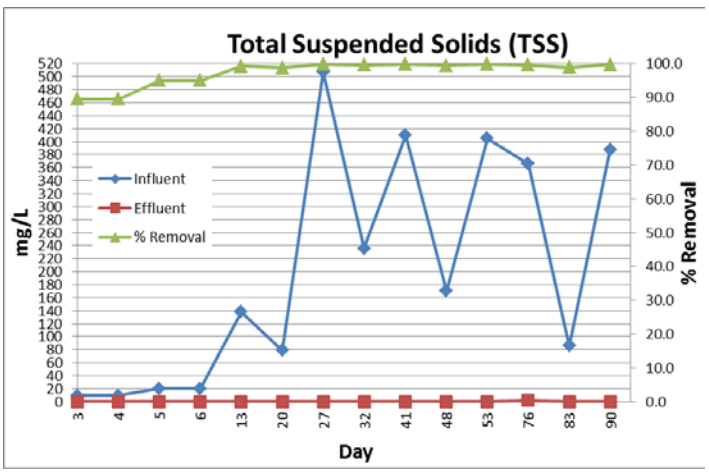

Figure 70: The TSS level of ZW-10 MBR influent and effluent.

2. MBR Operational parameters

The ZW-10 flux was increased to reach a low HRT of less than 3 hours for the experiment treating laundry and kitchen wastewater mixture (Figure 71). Despite operating with a previously used ZW-10 module, the unit achieved the desired flux to meet low HRT demands at higher transmembrane pressure without system upsets. A recovery clean was performed on day 45 of the study in an effort to decrease transmembrane pressure by removing organic and inorganic fouling species that may have been creating a biofilm or blocking membrane pores. Following a 1,000 ppm hypochlorite and 1,000 ppm citric acid soak, the transmembrane pressure decreased approximately 30% to a pressure of about10 psi. Typical operating pressures for a new membrane module are in the 2-5 psi range, however given the extremely low HRT desired, coupled with a previously used module, it is not unexpected that the baseline transmembrane pressure was higher than normal.

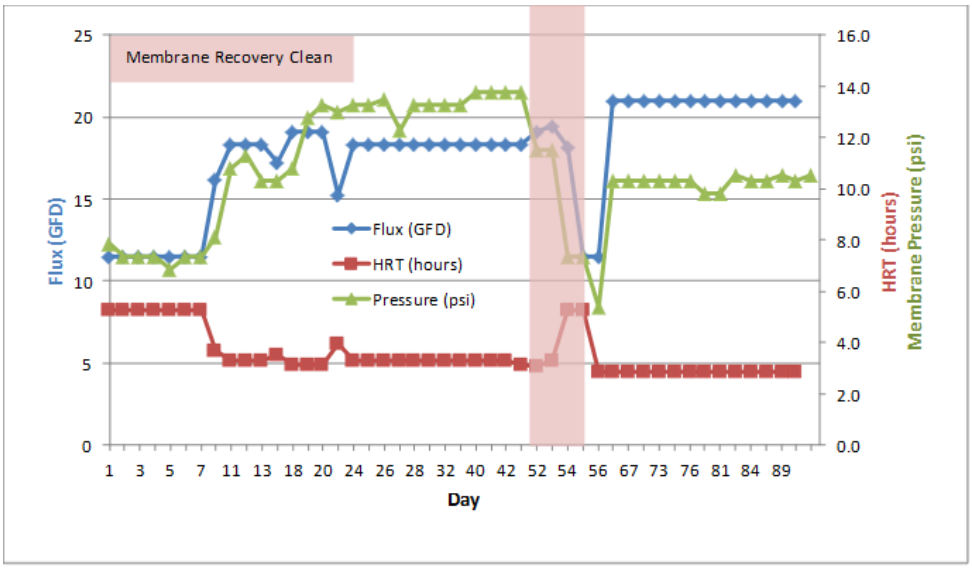

Figure 71: Variations of flux, transmembrane pressure, and HRT during the real wastewater treatment study.

Dissolved Oxygen , MLSS, and F:M Ratio. Dissolved oxygen was monitored daily over the 90 day experimental period to ensure adequate aeration was being provided to maintain a growing bacterial population to effectively treat real wastewater feed. The MBR unit was aerated with a similar flow regime as described for the synthetic wastewater experiments. Roughly 3.5 scfm air was supplied to both the externally housed membrane tank (air scouring to remove solids build-up on the membrane) and the process tank containing the mixed liquor sludge. Dissolved oxygen levels in the process tank were typically in the range of 1-9 mg/L (Figure 72).

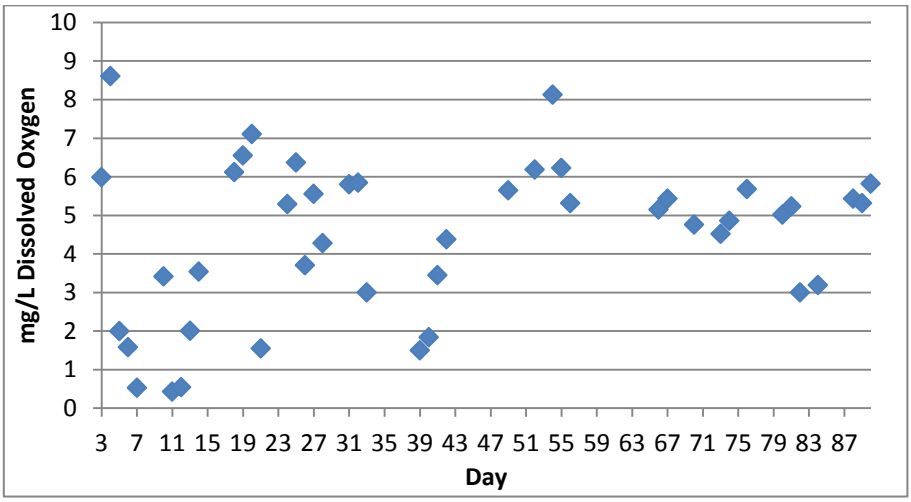

Figure 72: Dissolved oxygen levels in the ZW-10 process tank.

Mixed Liquor Suspended Solids (MLSS) was measured to monitor sludge growth over the course of the study, in particular following a decline in HRT from 5 days at start-up to less than 3 hours for the remainder of the experiment. The MLSS value climbed steadily over the 90 day experimental period, reaching a maximum of 8,114 mg/L on day 90 (Figure 73). The ZW-10 MBR can handle solid loadings of 8-10,000 mg/L, thus no system upsets were observed while maintaining a low HRT and relatively high SRT of 25 days.

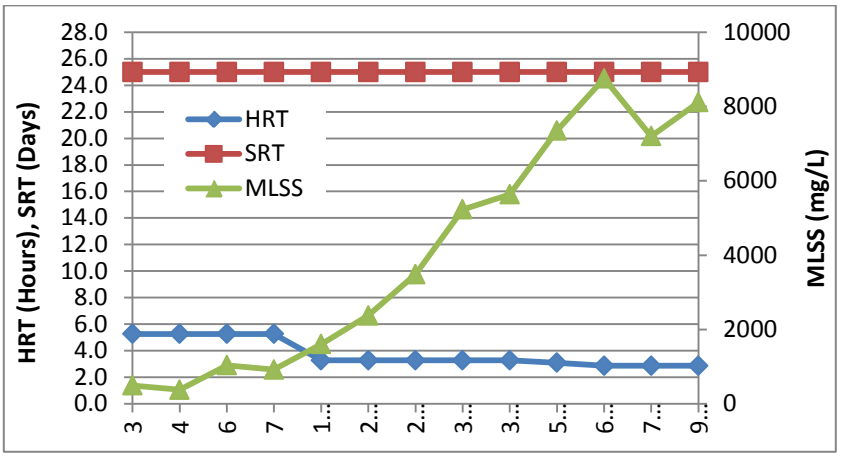

Figure 73: HRT and MLSS levels in the ZW-10 process tank.

Food to Microorganism Ratio (F:M ratio) was calculated using the influent BOD levels and measured MLSS values. The typical F:M range to avoid system upsets is between 0.3-0.4, however variability in the influent waste streams is likely to cause this ratio to vary over time, as observed in this study (Figure 74). The F:M ratio was found to stabilize to within the desired range over time.

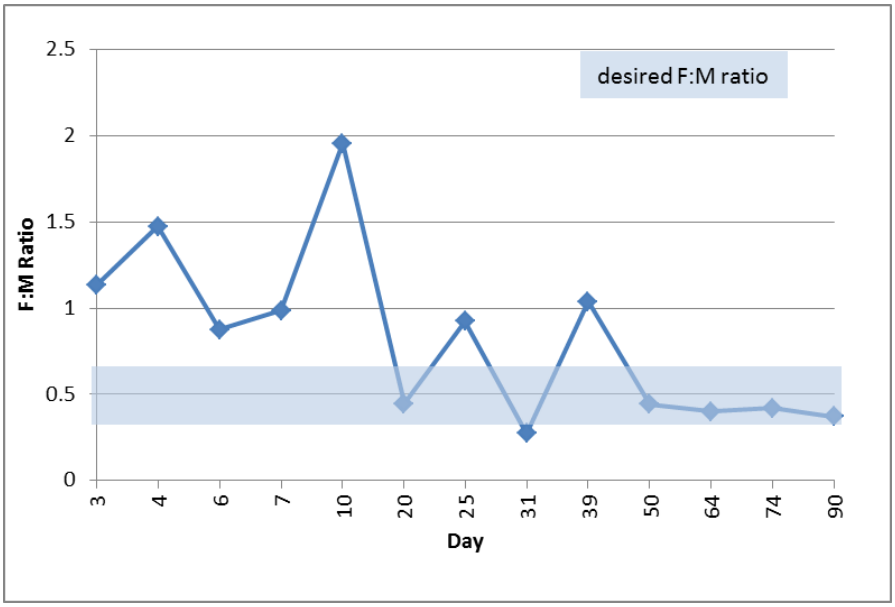

Figure 74: Food to microorganism ratio calculated from influent BOD levels, MLSS, and flux for ZW-10 MBR.

3. RO operating and effluent water quality parameters

The integrated E-2 RO unit removes dissolved solids following MBR treatment. The RO system was operated at a constant pressure of 115 psi using a low-energy AK1812 membrane at a flux of approximately 12 GFD. The membrane performed consistently well over the entire study period with minimal membrane cleaning (Figure 75). The RO concentrate was recycled back into the feed tank in order to maintain enough working volume to process. RO permeate was collected and tested for drinking water quality characterization. The results of the complete drinking water analysis test showed that the permeate met drinking water standards (Table A-7 in Appendix).

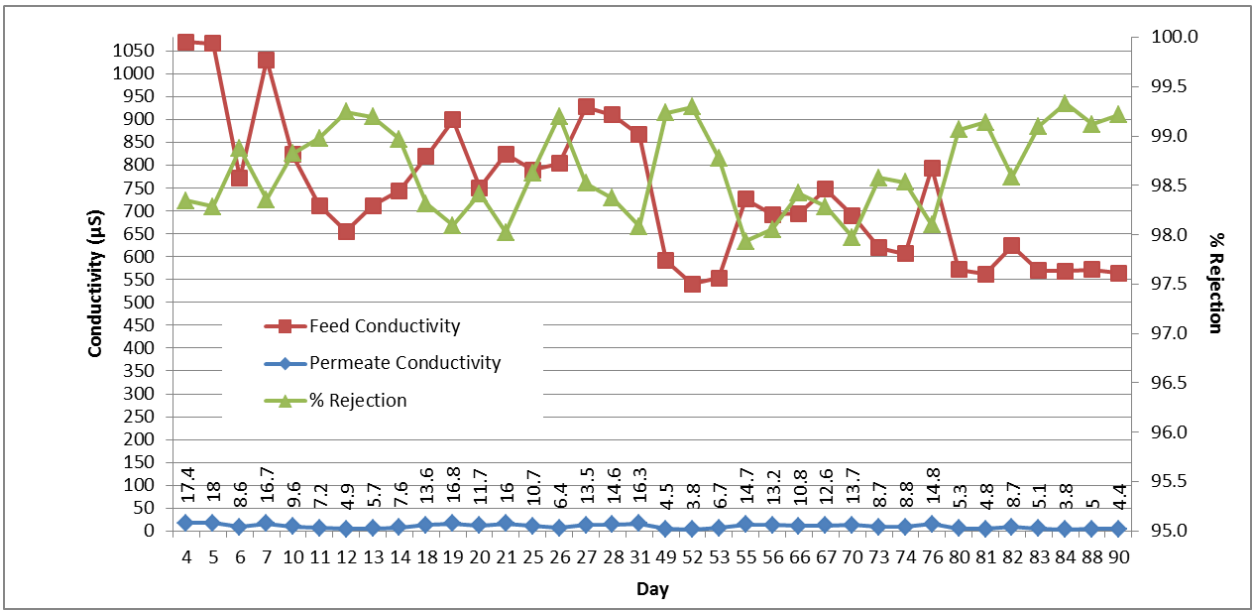

Figure 75: Feed and permeate conductivities and salt rejection of E-2 RO unit.

4.2.7.3 Conclusions

MBR/RO wastewater treatment experiments were carried out using a mixture of on-site generated kitchen and laundry wastewater and tap water to simulate a typical wastewater stream from FOBs. The combination of the decreased process tank size and real wastewater allowed for a more realistic study on the effect of feed water and operational conditions on treatment of real wastewater. The integrated MBR/RO system was found to produce high quality effluent that met potable reuse requirements when the MBR was operated at low HRT and high SRT of 2-4 hours and 20 days, respectively, using a low energy RO membrane that requires low operating pressure. In addition, a rapid seeding and start-up protocol was successfully developed to start the system and generate high quality effluent in less than 5 days. The system performance and water quality data were then used to design a low footprint, energy efficient and deployable MBR/RO system for FOBs and other contingency operation sites.

4.2.8 Development of deployable wastewater treatment system performance and cost models

4.2.8.1 Deployable Wastewater Treatment system

The deployable wastewater treatment system is designed to treat the wastewater produced by FOBs. The system must be contained in 8’ X 8’ 6” X 20’ transportable containers (Figure 76). It is comprised of the bioreactor containers and the ZW tank and process equipment containers. Some other process containers such as equalization and/or RO containers can also be added to the system if required. Several different container combinations could be utilized to meet different camp sizes and influent flow rates. Hoses and electrical cables make the connections between the containers. The power for the system is provided by the generators that are part of the FOB infrastructure.

Figure 76: GE deployable MBR/RO wastewater treatment system.

In summary, wastewater from the camp will be collected and diverted to an equalization tank and then transferred (by others) to the deployable wastewater treatment plant. This deployable wastewater treatment plant consists of one (1) bio-container; one (1) membrane container, one (1) onion break tank, and one (1) RO container.

The bio-container contains one (1) fine screen (installed on top of anoxic zone), one (1) anoxic tank, one (1) aerobic tank, and associated blowers and pumps. The raw wastewater from the equalization tank will be first injected to the fine screen with 2 mm openings installed on the top of the anoxic tank. The recirculated sludge from the membrane container will also be introduced to the anoxic tank. The overflow from the anoxic tank will be directed to the aeration tank in the same container. An aeration grid will be installed at the bottom and spray nozzles to inject defoamer (as required) will be installed just above the liquid level. An air blower will provide supplemental aeration for effective aerobic biodegradation of the wastewater pollutants.

The mixed liquor from the bio-container is transferred by re-circulation pumps to the membrane container where clean water passes through the ultrafiltration membranes and all the bacteria and inert solids overflow with excess mixed liquor back into the bio-container. Excess biosolids that

have accumulated are periodically removed (wasted) from the membrane tank for disposal either via a discharge hose by the re-circulation pump or by overflow to sludge treatment site (by others).

GE's ultrafiltration hollow fiber membrane works in an outside-in flow pattern. The membrane fibers are connected to headers at the top and bottom of a frame to form a membrane element. Several thousand fibers are contained in a single membrane module. Each membrane module has a surface area of 300 ft^2.

Suction pressure applied to the top of the membrane cassette headers by the permeate pumps causes water to be drawn perpendicularly to the membrane surface. Solid particles larger than the membrane pore size (0.04-micron) are rejected at the membrane surface while clean water is allowed to pass through the membranes.

GE membranes are self-cleaned in several ways during operation. First, they are scoured with air that is fed to the bottom header by the membrane blower and rises up along the surface of the membranes. The motion of the air acts to scour the membrane fibers slightly, allowing material that may have adhered to slough off. Secondly, the membranes are cleaned from the inside out by sending clean effluent from the backpulse tank back through the membrane under positive pressure for 30 second duration every 10-15 minutes. Lastly, GE recommends periodic maintenance/recovery cleaning with a mild hypochlorite or citric acid solution, which is backpulsed through the membranes and soaked for a pre-determined time. These patented automatic cleaning methods enable the membranes to remain in service for extended periods between more mild membrane cleanings. Treated effluent will be transferred to an onion break tank prior to further treatment by the RO container.

4.2.8.2 MBR/RO System Basis of Design

The base design case is a deployable (containerized) MBR/RO wastewater treatment system for a 600 soldier FOB. The volume of wastewater in a 600 man camp is approximately 12,000 gal for the shower, 6000 gal for the laundry, 3500 gal for the latrine, and 1400 gallons for the kitchen (Table 19).

Table 19: Representative wastewater generation for a 600 soldier FOB [1,2]

Wastewater type	Volume (gallons)
Shower	12,000
Laundry	6,000
Kitchen	1,400
Latrine	3,500
Total	22,900

1. Influent Flow Rate

Influent flow rate is detailed in Table 20.

Table 20: Wastewater influent flow rate.

Parameter	Quantity	Unit
Camp Size	600	Soldier
Design Flow Rate	25,000	gpd
Wastewater Flow Rate with One Membrane Train Off Line for less than 24 Hours	25,000	gpd

2. Influent Quality

The design solution proposed is based on the wastewater characteristics detailed in Table 21.

Table 21: Wastewater quality

Parameter	Influent	Unit
Minimum Wastewater Temperature	12	^{o}C
Maximum Wastewater Temperature in Biological and Membrane Containers	35	^{o}C
BOD	100	mg/L
TSS	190	mg/L
TKN	38	mg/L
NH3-N	24	mg/L
TP	2.4	mg/L
Alkalinity (1)	150	mg/L as $CaCO_3$

3. MBR Effluent Quality

The following performance parameters are expected upon equipment start-up based on the data listed in Section 2.1 and 2.2 and the biological and membrane designs presented in Section 3.

Table 22: MBR effluent quality data**.**

Parameter	Effluent	Unit
BOD	≤ 5	mg/L
TSS	≤ 5	mg/L
NH_3-N	≤ 1	mg/L
Turbidity	≤ 1	NTU

4. RO Effluent Quality

The RO effluent is expected to meet the EPA potable water standards (Table 23).

Table 23: RO effluent quality.

Performance Objectives	Metric	Success Criteria
RO effluent meets EPA potable water requirements	Maximum contaminant levels (MCL)	Below levels specified by EPA primary drinking water regulation[22]
	Secondary maximum contaminant levels (SMCL)	Below levels specified by EPA secondary drinking water standard[22]

4.2.8.3 MBR and RO process design and system configuration

The detailed MBR and RO process design information is listed in Table 24. It is noted that a conservative HRT of 6.4 was used in the base design case in case such system will be used to treat wastewater other than gray water. For treating gray water alone, we have demonstrated that we can operate the system at an HRT of less than 3 hours. Thus, the total MBR volume required can be reduced by 50% if only gray water will be treated by the designed MBR/RO system. The detailed MBR and RO system configuration information is provided in Table 25.

Table 24: MBR and RO process design information.

	Parameter	Quantity
MBR	No. of Biological Trains	1
	Anoxic Volume Required	1,818 US gallons
	Aerobic Volume Required (not including membrane tank)	3402 US gallons
	Membrane Tank Volume Required	1,400 US gallons
	Total MBR Volume Required	6,620 US gallons
	Design HRT	6.4 hours
	Design SRT	29.4 days
	Design MLSS	8,000-10,000 mg/L
	Total Number of Bio-containers Required	1
RO	Type of RO Membrane Modules	6 GE Low Energy AK8040 Elements
	RO Product Design Flow Rate	25 gpm

Table 25: Details of MBR and RO system configuration.

	Parameter	Quantity/Explanation
MBR	Type of Membrane Modules	ZeeWeed® 500Ds
	Number of Membrane Trains	2
	Total Membrane Cassettes Installed in Each Membrane Train	1 of 8-module cassette
	Total Number of Membrane Cassettes Required	2 of 8-module cassettes
	Total Number of Membrane Modules Required	16
	Total Number of Membrane Containers Required	1
RO	Total Number of Membrane Modules Required	6
	Number of Membrane Housing Required	1

4.2.8.4 Power & Membrane Cleaning Chemical Consumption Estimates

1. MBR and RO Power Consumption Estimate

The power consumption, based on annual average daily flow, is shown in Table 26.

Table 26: MBR and RO system power consumption estimate.

	Equipment	kWh/day
MBR	Permeate/Backpulse Pumps	2
	Membrane Blowers	32
	Recirculation/Transfer Pumps	6
	Submersible Mixer	2
	Process Blower	19
	Compressors	8
RO	Feed Pump	27
	Total for the above Equipment	**96**

2. Annual MBR and RO Chemical Consumption Estimate

Table 27 lists the details of the annual chemical consumption estimate for the MBR/RO system.

Table 27: Annual MBR and RO system chemical consumption estimate

Chemical	USgal/year
Sodium Hypochlorite (10.3% w/w, SG:1.168)	70
Citric Acid (50.0% w/w, SG: 1.24)	54
Kleen™ MCT103 (low pH cleaning chemical, SG: 1.35)	16
Kleen™ MCT511 (high pH cleaning chemical, SG: 1.197)	18
Sodium Bisulfite (S.G:1.48)	2
BioPlus 2900 seeding cultures for MBR start-up	100
Total	160 USgal (chemicals) + 100 lb (seeding cultures)

Note: Cleaning chemical consumption estimates based on the frequencies and concentrations summarized in the table below. Frequencies are assumed, actual frequency of maintenance and recovery cleans may change with final design, or may change once system is in operation.

4.2.8.5 System Price and Return of Investment

Pricing for the proposed equipment is summarized in Table 28. All pricing is based on the operating conditions and influent analysis that are detailed in the Basis of Design in Section 4.2.8.2.

Table 28: Pricing for the integrated MBR/RO system.

Item	Price	Unit
Budgetary System Price for the deployable MBR/RO system: Part I-MBR subsystem	**$1,800,000**	**USD**
Budgetary System Price for the deployable MBR/RO system: Part II-RO subsystem	**$394,000**	**USD**
Total budgetary price for integrated MBR/RO system	**$2,194,000**	**USD**

The cost of fresh water at FOBs ranges from $4.78 to over $50 per gallon[3]. The designed MBR/RO system could save $30 to $300 million per year for each FOB with 600 soldiers, compared to the current practice of using bottled water. Assuming the same range of cost for membrane cleaning chemicals, Table 29 shows that the payback period of the MBR/RO system is as low as 3 to 27 days. Thus, the deployable MBR/RO wastewater treatment and reuse system offers great cost savings to the US military.

Table 29: Payback calculation of the designed MBR/RO system.

Item	Scenario 1[a]	Scenario 2[b]
System cost	$2,194,000	$2,194,000
Annual water production by MBR/RO system	6,394,253 gallons	6,394,253 gallons
Value of annual water production by MBR/RO system	$30,564,527	$319,712,625
Annual operating chemical quantity	160 USgal+100 lb	160 USgal+100 lb
Annual operating chemical cost	$2265	$10,000
Annual electricity consumption	31536 kWh	31536 kWh
Annual diesel usage for generating electricity by diesel generator [c]	2426 gallons	2426 gallons
Annual diesel cost	$11,596	$121,292
Operator and maintenance cost [d]	$150,000	$300,000
Net annual cost savings	$30,400,666	319,281,333.00
Simple payback period	27 days	<3 days

a: assumption: water, chemical, and diesel costs are all $4.78/US gallon at FOBs, $15/lb seeding culture cost, 85% water recovery for MBR/RO system, 90% MBR/RO system up time.

b: assumption: water and chemical cost are all $50/US gallon at FOBs; $20/lb seeding culture cost, 85% water recovery for MBR/RO system, 90% MBR/RO system up time.

c: assumption: each gallon of diesel generates 13 kWh of electricity (http://www.eia.gov/tools/faqs/faq.cfm?id=667&t=6)

d: assumption: 1 operator, 2 hours a day, 5 days per week.

4.2.8.6 Conclusions

A containerized, military deployable MBR/LE RO wastewater treatment system capable of treating 25,000 GPD of gray water was designed for a 600 soldier FOB. Based on the operational parameters and performance of the lab-scale MBR/LE RO membrane system, performance models were developed for the deployable FOB wastewater treatment system. Using the energy and mass balances from these models along with capital investment estimates, preliminary CAPEX and OPEX for the designed MBR/ULE RO process were determined. The results indicate that the investment of the designed deployable MBR/RO wastewater treatment system will be paid back in less than 1 month after deployment in an FOB, offering tremendous cost savings for the US military and improved base environment and security.

4.2.9 Conclusions from Task 2

A lab-scale, integrated MBR/LE RO system was designed and validated with representative gray waters. System design and operational parameters were optimized to reduce energy demand and footprint while efficiently removing contaminants. The purified water from the MBR/LE RO system met the water quality specifications for potable and non-potable applications. Using the information from the lab piloting experiments and GE's vast commercial MBR and RO product design experience, a containerized, military deployable MBR/ULE RO wastewater treatment system capable of treating 25,000 GPD of gray water was designed for a 600 soldier FOB. Performance models were also developed for the deployable FOB wastewater treatment system. The results indicate that the investment of the GE deployable, low energy MBR/RO wastewater treatment system will be paid back in less than 1 month after deployment in FOBs, offering tremendous cost savings for the US military and an improved base environment and security.

V. Conclusions and Implications for Future Research

5.1 Overview and Summary of Project Results

This is the final report for this project supported by SERDP (contract # W912HQ-12-C-0046). The principal goal of this project is to develop a deployable and energy efficient membrane bioreactor (MBR) and reverse osmosis (RO) system for on-site wastewater treatment for forward operating bases (FOBs) to produce high-quality water for potable and non-potable reuse, minimizing water demand from off-base sources. The approaches in this project are to i) develop ultra-low-energy (ULE), high permeance membrane technology by incorporating highly engineered nanomaterials; ii) build a lab-scale MBR/RO wastewater treatment system to demonstrate its ability to produce high-quality water for reuse; and iii) perform a techno-economic feasibility assessment of a deployable MBR/RO system configuration based on lab-scale experimental data with representative wastewater samples and suitable performance modeling.

Mesoporous silica nanoparticles with controlled, uniform particle size of 30-50 nm and large surface area (>700 m^2/g) have been successfully synthesized following a condensation reaction in an aqueous solution with the use of a cationic surfactant as a templating agent. Performing the synthesis at room temperature helped to controlled particle growth and a final dilution in water left highly stable particle suspensions. The use of an intermediate freeze-drying step prior to template extraction (via calcination) appears to be a crucial step in preventing increased agglomeration of the highly concentrated particle solution upon drying. Heating the dried particles to 400 °C and 600 °C removed the templating agent and all organic material, leaving behind silica nanoparticles in a solid powder form that could be re-suspended in ethanol and organic solutions, including Isopar G. The synthesized silica nanoparticles were successfully incorporated into the thin films of GEGR-produced RO membranes. It appears that the small particle sizes (<50nm) observed in the GEGR-made particles may be more effective than previously used commercial products that often display wide particle size distributions. Improvements were observed in membrane performance, in particular, increased salt rejection was observed with higher permeance compared to control membranes (without particles).

Nanocomposite RO membrane pilot coating trials have been conducted to understand the effects of formulation and process variables on membrane separation performance. The effects of material (e.g. particle size, particle loading) and operating parameters (line speed, organic delivery method) have been systematically studied. Results demonstrated the entitlement of the targets of water permeance (A) =16 and sodium chloride rejection = 99.5% by using silica nanoparticles and organic additives. The project team also established and validated the prototype 1.8” (diameter) x12” (length) spiral-wound RO membrane element fabrication capability at GEGR.

The chemical and morphological characteristics of the nanocomposite RO membranes have been assessed using a variety of characterization techniques, including high resolution SEM, TEM, and EDS. High resolution SEM shows that GEGR synthesized mesoporous silica nanoparticles have superior dispersibility and dispersion stability as compared to commercially obtained

nanoparticles. TEM of microtomed membrane cross-sections showed that small agglomerates of silica nanoparticles may be fully incorporated into the polyamide layer, although the volume fraction of such nanoparticle incorporation remains difficult to quantify. The results of the nanocomposite RO membrane fabrication, characterization and testing demonstrated the success of nanocomposite RO membranes in meeting the performance targets.

To achieve the objective of an easily deployable system for on-site wastewater treatment at FOBs, it is critical to optimize MBR operating conditions and system performance by minimizing the hydraulic retention time (HRT) of the MBR system while maximizing the sludge retention time (SRT). Low HRT allows the use of small MBR process tanks, enabling a small system footprint. High SRT minimizes the solid waste handling requirements. The ZW-10 MBR experiments were first conducted over the course of 200 days using synthetic gray water. During that time period, water quality data was collected on the synthetic gray water influent as well as the MBR treated effluent. The data showed that high quality MBR effluents were produced even with an HRT as low as 4.5 hours. The MBR treated water had very low levels of contaminants, well within the RO feed water specifications. In addition, MBR effluent was used as RO feed water in GE Global Research's flat sheet cross-flow test bench to determine the ULE RO membrane performance and the quality of the RO-purified water (including conductivity, turbidity, organic, ammonia and nitrate content, hardness, E. coli and virus content, and trace organic contaminant levels). The RO permeate was found to meet the potable water quality requirement.

Subsequently, MBR/RO wastewater treatment experiments were carried out using a mixture of on-site generated kitchen and laundry wastewater and tap water to simulate a typical wastewater stream from FOBs. The combination of the decreased process tank size and real wastewater allows for a more realistic study on the effect of feed water and operational conditions on treatment of real wastewater. The integrated MBR/RO system was found to produce high quality effluents that met potable reuse requirements when the MBR was operated at low HRT (2-4 hours) and high SRT (20-25 days) while using a low energy RO membrane that requires low operating pressure. In addition, a rapid seeding start-up procedure was successfully developed to start the system and generate high quality effluent in less than 5 days. The system performance and water quality data were used next to design a low footprint, energy efficient, and deployable MBR/RO system for FOBs and other contingency operation sites.

Using the information from the laboratory-scale piloting experiments and GE’s vast commercial MBR and RO product and process design experience, a containerized, military deployable MBR/ULE RO wastewater treatment system capable of treating 25,000 GPD of gray water was designed for a 600 soldier FOB. Performance models were developed for the deployable FOB wastewater treatment system. Using the energy and mass balances from these models along with capital investment estimates, preliminary CAPEX and OPEX for the designed MBR/ULE RO process were determined. The results indicate that the investment of the GE deployable, low energy MBR/RO wastewater treatment system will be paid back in less than 1 month after deployment in FOBs, offering tremendous cost savings for the US military and an improved base environment and security.

5.2 Conclusions

The following conclusions can be drawn from this study:

1. An optimized method of synthesizing mesoporous silica nanoparticles with controlled, uniform particle size of 30-50 nm and high surface area (>700 m^2/g) was developed. The use of an intermediate freeze-drying step prior to template extraction (via calcination) is a novel and crucial step in preventing increased agglomeration of the highly concentrated particle solution upon drying. The synthesized silica nanoparticles were successfully used in the fabrication of the thin film composite RO membrane.

2. Low energy nanocomposite membranes and roll-to-roll fabrication processes have been optimized on a pilot scale. These low energy membranes have over two-fold permeance enhancement compared to conventional RO membranes, while maintaining their characteristic 99.5% salt rejection. Lab-scale (2”x12”) ULE RO membrane elements were fabricated and tested.

3. A combined MBR/low energy RO gray water treatment system has been demonstrated on a lab-scale using a mixture of on-site generated kitchen and laundry wastewater and tap water to simulate a typical wastewater stream from FOBs. Results showed that the MBR is an effective RO pretreatment method for removal of organics and nutrients from wastewater for stable and robust low energy RO operation. Prior to the efforts summarized in this report, these high permeance membranes have not been used with an MBR to treat complex wastewaters.

4. The integrated MBR/RO system was found to produce high quality effluent that met potable reuse requirements when the MBR was operated at low HRT and high SRT of 2-4 hours and 20 days, respectively, using a low energy RO membrane that requires low operating pressure. The extensive lab testing results have retired major technical risks, ensuring a smooth transition to field pilot demonstration and field deployment.

5. Rapid biological seeding and start-up procedures were successfully developed to start the system and generate high quality effluent in less than 5 days.

6. The system performance and water quality data from this study were used to design a low footprint, energy efficient, and deployable MBR/RO system for FOBs and other contingency operation sites. A containerized, military deployable MBR/LE RO wastewater treatment system capable of treating 25,000 GPD of gray water was designed for a 600 soldier FOB.

7. Performance models were developed for the deployable FOB wastewater treatment system. Preliminary CAPEX and OPEX for the designed MBR/ULE RO process were determined.

8. Techno-economic analysis indicates that the investment of the designed deployable MBR/RO wastewater treatment system will be paid back in less than 1 month after deployment in an FOB, offering tremendous cost savings for the US military and improved base environment and security. The cost saving for a 600 soldier FOB range from $30 MM to $300MM, assuming the cost of fresh water at FOBs in the range of $4.78 to over $50 per gallon[3].

9. In summary, the results summarized in this report demonstrated for the first time the technical and economic feasibility of a containerized, military deployable MBR/low energy RO system for wastewater reuse for FOBs.

5.3. Implications for Future Research

One area of future research is the full scale manufacturing of high permeance nanocomposite RO membranes, including scale-up of nanoparticle dispersion, fluid delivery, and mitigating environment, health and safety concerns related to nanomaterials.

Another area of future research is advanced RO membrane system design. When the conventional RO system configuration is used with high permeance membranes, an unbalanced flux distribution with excessive lead element flux and poor tail element utilization will occur, resulting in poor membrane durability and reliability. Future research is needed to optimize advanced system design and explore novel designs to maximize energy savings of high permeance membranes while ensuring stable system performance.

A third area of research includes field testing of an integrated, deployable MBR/ULE RO demonstration/validation system at a scale of 10-20 gallons per minute (gpm). Such field testing should be operated at DoD facilities using commercial-scale MBR and RO membrane modules. The 10-20 gpm (14,400 to 28,800 gpd) capacity of the proposed demonstration unit fits exactly in the range of wastewater generated by FOBs with 300-600 soldiers.

The results summarized in this report is focused on low footprint, energy efficient, and easily deployable MBR and ULE RO system for on-site wastewater treatment at FOBs. A natural extension of the current research is for waste water treatment at fixed military bases. DoD installations produce several types of wastewater, ranging from conventional wastewater—similar to domestic, or municipal wastewater—to more complex industrial wastewater. Wastewater reuse is a key approach for improving water sustainability at DoD installations. Many installations are reusing tertiary-treated wastewater for irrigation. Recycling water at wash racks is also becoming a common practice. These are generally considered low-tier reuse applications, in that they do not involve substantial risk associated with human contact with the water. As water stress continues to grow, the DoD will need better wastewater treatment technologies that can produce pure water suitable for high-tier reuse applications (e.g., shower, laundry, and aquifer recharge) that involve more direct human exposure. A major barrier to this

desired capability is the energy cost of purifying water to these levels. Wastewater treatment currently represents 3% of the US electricity demand [38], and adding an energy-intensive purification process for tertiary treatment and high-tier reuse is not economically feasible in most cases. The integrated MBR/ULE RO system developed in this work, with its reduced the energy requirements and ultra-efficient tertiary treatment, is a promise technologies for wastewater treatment system to convert wastewater to high-quality water for a wide-range of reuse applications at fixed military bases.

In addition to removing conventional contaminants such as BOD, COD, TSS, and TDS, it is important to remove other contaminants that may be present in wastewater, including heavy metals, endocrine disrupting compounds, and pharmaceuticals that are often present in DoD municipal and industrial wastewaters at DOD installations. These pollutants are very toxic to human health, the environment, and aquatic life, and will need to be removed to meet environmental regulations. DOE wastewaters may also contain specific compounds under the category of tentatively identified compounds (TICs) that need to be characterized and removed [40]. A recent study comparing the performance of conventional activated sludge (CAS) and MBR processes showed that the use of ultrafiltration (UF) MBR technology offered superior heavy metals removal over the CAS process [39]. Future work should be performed to evaluate and optimize the MBR/ULE RO system to remove these types of contaminants to meet EPA potable water reuse regulations.

VI. Bibliography

1. US Army Field Manual 3-34.400 (FM 5-104) “General Engineering”.
2. The USAREUR Blue Book “Base Camp Baseline Standards”.
3. SERDP ‘Sustainable Forward Operating Bases’. http://www.serdp-estcp.org/content/download/8524/104509/file/FOB_Report_Public.pdf
4. D. Pickard, "Small Scale Waste to Energy Conversion for Military Field Waste", US Army Natick Soldier RD&E Center, May 20-21, 2008.
5. USAREUR, “Base Camp Facilities Standards for Contingency Operations (Red Book)”. W. H. Ruppert et al, "Force Provider Solid Waste Characterization Study", Technical Report Natick/TR-04/017, August 2004.
6. Lee E. K., Koros W. J., "Membranes, Synthetic, Applications", Encyclopedia of Physical Science and Technology, 3rd Edition, Ed. R. A. Meyers, Academic Press, New York pp. 279-345, 2002.
7. National Research Council "Review of the Desalination and Water Purification Technology Roadmap", The National Academies Press, Washington, D.C. 2004.
8. National Research Council "Desalination: A National Perspective". The National Academies Press, Washington, D.C. 2008.
9. Helmut Kaiser Consultancy "Water Markets Worldwide 2008-2015", 2008. http://www.hkc22.com/watermarketsworldwide.html
10. Freeman B. D. "Basic of permeability/selectivity trade-off relationships in gas separation membranes", Macromolecules, 32, 375, 1999
11. G. M. Geise, H. B. Park, A. C. Sagle, B D. Freeman, J. E. McGrath, "Water Permeability and Water/salt Selectivity Tradeoff in Polymers For Desalination", J Membr. Sci. 369 (2011) 130-138.
12. K. Möller, J. Kobler, and T. Bein. 2007. Colloidal Suspensions of Nanometer-sized Mesoporous Silica. Adv. Funct. Mater. 17: 605-612.
13. J. Kobler, K. Möller, and T. Bein. 2008. Colloidal Suspensions of Functionalized Mesoporous Silica Nanoparticles. Amer. Chem. Soc. 2(4): 791-799
14. GE Water and Process Technologies, Operating Guidelines: Temperature Correction Factors. https://knowledgecentral.gewater.com/kcpguest/salesedge/documents/Manuals_Cust/Americas/English/Temperature_Correction_Factor_Guidelines.pdf
15. R.F. Probstein, Physicochemical Hydrodynamics: An Introduction, 2nd ed., John Wiley & Sons, Inc., New York, 1994.
16. U. Merten, H.K. Lonsdale, R.L. Riley, “Boundary-layer effects in reverse osmosis”, Ind. Eng. Chem. Fundam. 3 210–213, 1964
17. T.K. Sherwood, P.L.T. Brian, R.E. Fisher, L. Dresner, “Salt concentration at phase boundaries in desalination by reverse osmosis”, Ind. Eng. Chem. Fundam. 4, 113–118, 1965
18. E. Van Wagner, A. C. Sagle, M. M. Sharma, B. D. Freeman, “Effect of crossflow testing conditions, including feed pH and continuous feed filtration, on commercial reverse osmosis membrane performance”, 345 , 97–109, 2009.
19. P K. Eriksson “Osmotic Pressures and Conductivities of Sodium Chloride Solutions”, Nov. 4 1999.
20. US EPA/625/R-04/108. September 2004. Guidelines for Water Reuse. http://www.wef.org/WorkArea/DownloadAsset.aspx?id=3884
21. US EPA, Current Drinking Water Regulations. http://water.epa.gov/lawsregs/rulesregs/sdwa/currentregulations.cfm http://www.epa.gov/ogwdw/consumer/pdf/mcl.pdf, http://www.epa.gov/ogwdw/consumer/pdf/mcl.pdf
22. Ryan Eckert “Force Provider Wastewater Treatment”, 2001.
23. EPA-842-R-99-001 (1999)

http://water.epa.gov/lawsregs/lawsguidance/cwa/vessel/unds/upload/2007_07_10_oceans_regulatory_unds_TDDdocuments_appAgraywater.pdf
24. Whelan, Mary. Graywater Characterization, TM-28-89-01. March 1989.
25. Talts, A. and D. R. Decker. Naval Ship Research and Development Center. Nonoily Aqueous Waste Streams on the USS Sierra (AD18), Volume 1. Bethesda, Maryland. Report 4182, April 1974
26. Naval Ship Research and Development Center. Nonoily Aqueous Waste Streams on USS Seattle (AOE 3), Volume I, Bethesda, Maryland. Report 4192, June 1974.
27. Van Hees, W., D. Decker, A. Talts. Naval Ship Research and Development Center. Nonoily Aqueous Waste Streams on USS O'Hare (DD 889), Volume I, Bethesda, Maryland. Rpt 4193, June 1974
28. Friedler E. (2004) "Quality of Individual Domestic Graywater Streams and Its Implication for On-Site Treatment and Reuse Possibilities ", Environmental Technology, Vol. 25. pp 997-1008
29. Li, F., K. Wichmann, and R. Otterpohl. 2009. Review of the technological approaches for gray water treatment and reuses. Science of the Total Environment. 407: 3439-3449
30. Scheumann, R. and M. Kraume. 2009. Influence of hydraulic retention time on the operation of a submerged membrane sequencing batch reactor (SM-SBR) for the treatment of graywater. Desalination. 246: 444-451
31. Fenner, R.A. and K. Komvuschara. 2005. A New Kinetic Model for Ultraviolet Disinfection of Graywater. Journal of Environmental Engineering. 131(6): 850-864.
32. Fenner, R.A. and K. Komvuschara. 2005. A New Kinetic Model for Ultraviolet Disinfection of Graywater. Journal of Environmental Engineering. 131(6): 850-864.
33. Nghiem, D.L., N. Oschmann, and A.I. Schäfer. 2006. Fouling in graywater recycling by direct ultrafiltration. Desalination. 187: 283-290.
34. X. Li., F. Gao, Z. Hua, G. Du, J. Chen. 2005. Treatment of synthetic wastewater by a novel MBR with granular sludge developed for controlling membrane fouling. Separation and Purification Technology 46: 19–25.
35. Tchobanoglous G., Burton F. L., and Stense H. D (2002) "Wastewater Engineering: Treatment and Reuse" 4th edition.. McGraw-Hill.
36. Judd S. (2011) "The MBR Book, Principles and Applications of Membrane Bioreactors for Water and Wastewater Treatment", 2nd edition. Butterworth-Heinemann.
37. P. Cote , Z. Alam, and J Penny (2012) "Hollow fiber membrane life in membrane bioreactors (MBR)" Desalination 288, 145–151
38. EPA Office of Water. Wastewater Management Fact Sheet, Energy Conservation, EPA 832-F-06-024; U.S. Environmental Protection Agency: Washington DC, 2006; p 1. http://water.epa.gov/scitech/wastetech/upload/2008_01_16_mtb_energycon_fasht_final.pdf
39. G Carletti, P Pavan, D Bolzonella (2007) "Occurrence and removal of heavy metals from industrial and municipal wastewater: a comparison between MBR and conventional activated sludge processes", Chem Engr. Trans. 11, 875-880.
40. USEPA (2006) "Tentatively Identified Compounds-What are they and why are they important?" http://www.epa.gov/region3/esc/qa/pdf/tics.pdf.

Appendix: Additional Tables

Table A-1: Water characteristics of the ZW-10 MBR influent synthetic gray water and effluent, including turbidity, COD, BOD, TOC, and pH.

Day	Turbidity			Chemical Oxygen Demand (COD)			Biological Oxygen Demand (BOD)			Total Organic Carbon (TOC)			pH	
	NTU			mg/L			mg/L			mg/L			pH units	
	Influent	Effluent	% Removal	Influent	Effluent	% Removal	Influent	Effluent	% Removal	Influent	Effluent	% Removal	Infuent	Effluent
8	230	0.29	99.9	1,020	45	95.6	419	<4	99.3	80.1	16.2	79.8	7.1	8.0
15	190	0.3	99.8	1,080	233	78.4	527	10	98.1	105.0	67.9	35.3	6.9	8.4
22	54	0.19	99.6	382	71	81.4	215	<4	98.6	104.0	23.0	77.9	6.7	8.2
29	75	<0.1	99.9	368	34	90.8	295	<4	99.0	51.7	9.0	82.6	6.8	8.4
36	28	0.13	99.5	524	18	96.6	322	<4	99.1	135.0	5.5	95.9	6.4	8.0
43	150	0.18	99.9	1,220	65	94.7	409	<5	99.3	37.5	5.3	85.9	7.0	8.1
50	71	<0.1	99.9	817	5	99.4	293	<4	99.0	87.3	2.2	97.5	5.9	7.7
56	120	<0.1	99.9	650	9	98.6	334	<4	99.1	66.9	4.3	93.6	6.9	8.1
58	120	<0.1	99.9	670	9	98.7	302	<4	99.0	110.0	3.0	97.3	6.4	8.0
63	300	<0.1	100.0	613	13	97.9	750	<4	99.6	91.7	3.9	95.7	6.6	8.0
65	220	0.18	99.9	1,420	9	99.4	805	<4	99.6	96.8	6.1	93.7	6.6	7.9
70	240	0.12	100.0	1,040	9	99.1	514	<4	99.4	95.2	3.8	96.0	6.8	8.0
72	13	0.16	98.8	233	13	94.4	103	<4	97.1	67.3	5.7	91.5	8.0	8.2
77	170	0.11	99.9	455	18	96.0	443	25	94.4	134.0	6.3	95.3	6.5	8.0
79	160	<0.1	99.9	975	9	99.1	430	31	92.8	92.1	3.4	96.3	6.9	8.0
84	90	0.18	99.8	680	9	98.7	312	120	61.5	65.2	3.9	94.0	7.8	7.1
86	170	<0.1	99.9	915	13	98.6	536	98	81.7	46.9	2.6	94.5	6.9	6.9
91	240	0.2	99.9	938	5	99.5	597	8	98.7	12.6	4.1	67.5	6.7	6.1
93	240	<0.1	100.0	1,420	9	99.4	709	<6	99.6	143.0	3.1	97.8	6.4	5.9
98	330	0.22	99.9	1,590	45	97.2	610	<6	99.5	113.0	17.6	84.4	6.6	5.2
100	170	0.14	99.9	1,100	77	93.0	568	<6	99.5	100.0	20.9	79.1	6.9	5.4
105	82	0.7	99.1	710	26	96.3	373	<6	99.2	129.0	7.5	94.2	6.5	5.7
107	200	0.14	99.9	1,420	13	99.1	680	<6	99.6	183.0	6.9	96.2	6.3	5.3
112	300	<0.1	100.0	1,830	5	99.7	1220	<6	99.8	186.0	5.0	97.3	6.4	5.3
114	31	0.46	98.5	400	13	96.8	288	<4	99.0	15.7	5.6	64.3	6.3	5.4
119	47	0.38	99.2	412	5	98.8	193	<4	98.4	78.4	4.5	94.3	7.1	5.8
121	28	<0.1	99.6	368	13	96.5	203	<4	98.5	106.0	4.9	95.4	6.8	7.6
126	32	0.12	99.6	459	9	98.0	206	<4	98.5	15.4	3.5	77.3	6.9	7.2
128	28	0.15	99.5	339	9	97.3	209	<4	98.6	109.0	3.8	96.5	6.9	7.4
133	63	<0.1	99.8	368	18	95.1	202	<4	98.5	83.2	4.4	94.7	7.0	7.3
135	50	0.18	99.6	427	18	95.8	238	2	99.2	123.0	7.3	94.1	6.9	7.4
140	63	0.12	99.8	325	5	98.5	132	<1	97.7	62.3	3.2	94.9	7.0	7.6
142	38	0.9	97.6	284	5	98.2	166	<4	98.2	78.1	3.5	95.5	6.4	7.5
147	30	0.18	99.4	427	13	97.0	249	<4	98.8	112.0	3.3	97.1	6.7	7.4
149	30	<0.1	99.7	298	9	97.0	178	<4	98.3	83.8	3.8	95.5	6.9	7.4
154	41	<0.1	99.8	339	13	96.2	257	<4	98.8	11.4	3.2	71.9	6.6	7.4
156	27	<0.1	99.6	220	9	95.9	137	<4	97.8	60.3	3.3	94.5	7.0	6.6
168	83	0.11	99.9	576	<5	99.1	296	<4	99.0	135	4.7	96.5	6.6	7.5
170	470	0.12	100.0	710	<5	99.3	783	<4	99.6	169	5.4	96.8	6.5	6.5
175	570	0.1	100.0	888	30	96.6	654	<4	99.5	202	5.4	97.3	6.7	7.1
177	170	0.11	99.9	1,050	34	96.8	511	3	99.4	199	7.3	96.3	7.5	6.7
184	130	0.25	99.8	840	55	93.5	493	<4	99.4	216	6.5	97.0	6.6	8.0
189	250	0.17	99.9	817	13	98.4	437	5	99.3	175	6.1	96.5	6.5	7.9
191	320	0.15	100.0	795	18	97.7	488	11	99.4	182	5.9	96.8	7.8	6.6
196	210	0.5	99.8	730	9.0	98.8	456	27.0	99.3	143	2.5	98.3	6.5	7.6
198	230	0.5	99.8	1,270	9.0	99.3	548	17.0	99.5	192	5.1	97.3	6.5	7.4
203	180	0.1	99.9	1340	13.0	99.0	638	9.0	99.5	242	4.4	98.2	6.5	7.9

Table A-2: Water characteristics of the ZW-10 MBR influent synthetic gray water and effluent, including TDS, TSS, ammonia, total nitrogen, and total phosphorous.

Day	Total Dissolved Solids (TDS)			Total Suspended Solids (TSS)			Ammonia			Total Kjeldahl Nitrogen (TKN)			Total Phosphorus (TP)		
	mg/L			mg/L			mg/L			mg/L			mg/L		
	Influent	Effluent	% Removal	Influent	Effluent	% Removal	Influent	Effluent	% Removal	Influent	Effluent	% Removal	Influent	Effluent	% Removal
8	600	560	6.7	379	1.5	99.6	53.8	71.1	*	67.2	71.7	*	9.1	10.7	*
15	600	590	1.7	418	0.1	100.0	45.9	47.6	*	59.4	50.4	15.2	14.2	10.0	29.6
22	625	565	9.6	48.5	<0.1	97.9	45.3	70.8	*	56.0	68.3	*	13.9	13.8	0.7
29	520	490	5.8	379	0.1	100.0	42.0	55.2	*	58.2	45.9	21.1	10.2	8.9	12.7
36	430	380	11.6	29	0.1	99.7	40.0	40.8	*	50.4	39.2	22.2	9.9	6.7	32.0
43	605	580	4.1	724	2	99.7	40.8	45.7	*	53.8	41.4	23.0	12.5	7.2	42.8
50	315	295	6.3	678	<0.1	99.9	49.0	47.7	2.7	68.3	47.0	31.2	10.4	7.4	28.8
56	415	285	31.3	61	<0.1	98.4	42.4	48.1	*	65.0	52.6	19.1	10.2	7.4	27.5
58	500	420	16.0	281	<0.1	99.6	65.9	59.7	9.4	63.8	50.4	21.0	12.2	8.8	28.3
63	640	445	30.5	502	<0.1	99.8	46.4	57.1	*	61.6	51.5	16.4	12.2	9.1	25.4
65	530	400	24.5	712	<0.1	99.9	49.4	55.0	*	72.8	54.9	24.6	14.5	9.1	37.2
70	745	415	44.3	573	<0.1	99.8	48.7	44.2	9.2	75.0	47.0	37.3	15.8	5.6	64.6
72	565	430	23.9	42.5	<0.1	97.6	47.1	64.8	*	59.4	62.7	*	7.8	8.5	-9.0
77	615	435	29.3	46	<0.1	97.8	49.6	48.1	3.0	66.1	44.8	32.2	10.9	5.5	50.0
79	540	455	15.7	470	<0.1	99.8	44.7	39.4	11.9	50.4	40.3	20.0	9.4	4.9	48.4
84	595	555	6.7	385	2	99.5	42.9	17.4	59.4	44.8	16.8	62.5	9.3	6.7	27.6
86	655	535	18.3	445	1.5	99.7	43.1	13.6	68.4	78.4	17.9	77.2	12.4	7.0	44.0
91	535	525	1.9	581	<0.1	99.8	43.7	7.4	83.1	62.7	9.0	85.6	7.4	4.9	34.5
93	615	610	0.8	1100	<0.1	99.9	54.7	3.3	94.0	73.9	13.4	81.9	8.6	4.2	51.2
98	665	725	*	802	<0.1	99.9	51.9	18.2	64.9	105.0	37.0	64.8	11.0	9.8	10.9
100	570	635	*	580	<0.1	99.8	20.8	7.7	63.0	87.4	38.1	56.4	7.8	6.7	13.5
105	610	595	2.5	242	2.5	99.0	49.2	13.1	73.4	54.9	14.6	73.4	6.7	6.7	0.7
107	675	615	8.9	770	<0.1	99.9	44.8	4.7	89.5	69.4	20.2	70.9	7.9	6.3	20.3
112	645	565	12.4	1630	<0.1	99.9	48.8	18.5	62.1	87.4	30.2	65.4	9.1	6.2	31.9
114	460	485	*	56	<0.1	98.2	57.0	19.1	66.5	71.7	28.0	60.9	6.7	6.5	3.0
119	575	595	*	133	<0.1	99.2	50.1	14.0	72.1	91.8	26.9	70.7	6.0	5.9	0.8
121	530	494	6.8	20.7	<0.1	95.2	50.2	29.7	40.8	58.2	38.1	34.5	5.1	4.3	15.8
126	685	705	*	60.5	<0.1	98.3	53.8	23.0	57.2	76.2	25.8	66.1	7.9	6.3	20.4
128	530	515	2.8	34.5	<0.1	97.1	58.9	28.8	51.1	63.8	39.2	38.6	7.3	4.4	40.4
133	580	630	*	48	<0.1	97.9	51.6	25.3	51.0	70.6	38.1	46.0	7.4	4.8	35.8
135	655	565	13.7	72	<0.1	98.6	59.6	46.9	21.3	79.5	60.5	23.9	8.5	5.2	38.8
140	460	575	*	69.5	<0.1	98.6	33.8	8.3	75.4	60.5	24.6	59.3	6.8	4.6	33.1
142	445	395	11.2	36.5	<0.1	97.3	50.6	38.7	23.5	61.6	52.6	14.6	6.4	5.7	11.0
147	575	510	11.3	63.5	<0.1	98.4	63.2	37.8	40.2	85.1	57.1	32.9	8.5	6.5	23.1
149	480	620	*	32	<0.1	96.9	38.8	23.7	38.9	56.0	38.1	32.0	9.9	6.2	37.4
154	620	510	17.7	34.5	<0.1	97.1	52.6	34.5	34.4	73.9	47.0	36.4	7.6	7.0	7.9
156	400	455	*	21	<0.1	95.2	49.3	10.5	78.7	68.3	24.6	64.0	6.0	4.8	20.2
168	555	570	*	292	<1	99.7	55.0	32.0	41.8	84.0	52.6	37.4	8.1	5.7	29.8
170	625	625	*	230	<1	99.6	69.5	29.1	58.1	94.1	30.2	67.9	12.4	8.4	32.7
175	675	635	5.9	446	<1	99.8	61.7	29.9	51.5	110.0	35.8	67.5	14.8	7.1	52.0
177	680	610	10.3	264	<1	99.6	72.9	47.9	34.3	142.0	61.6	56.6	15.8	8.3	47.5
184	735	580	21.1	165	<1	99.4	73.1	46.6	36.3	121.0	48.2	60.2	11.9	5.3	55.5
189	655	515	21.4	240	<1	99.6	56.3	50.2	10.8	102.0	58.2	42.9	14.2	9.4	34.2
191	670	605	9.7	134	<1	99.3	57.3	38.6	32.6	98.6	42.6	56.8	16.2	11.3	30.2
196	670	575	14.2	148	<1	99.3	50.6	1.6	96.8	70.6	14.6	79.3	12.4	8.5	31.9
198	675	615	8.9	818	<1	99.9	55.7	2.1	96.2	58.2	9.0	84.5	15.6	8.8	43.9
203	735	550	25.2	920	1	99.9	58.8	30.8	47.6	93.0	35.8	61.5	17.4	9.7	44.5

Table A-3: MLSS and F:M ratio data for ZW-10 MBR treatment of synthetic gray water.

Day	HRT (Hours)	SRT (days)	MLSS (mg/L)	Influent BOD (mg/L)	Food (F, lb)	Microorganism (M, lb)	F:M Ratio
20	15.3	13	2,152	215	0.11	0.72	0.16
28	18.0	13	1,581	295	0.13	0.53	0.25
34	14.8	13	1,424	322	0.17	0.48	0.37
42	5.7	13	1,636	409	0.57	0.55	1.05
55	5.3	13	2,942	334	0.51	0.98	0.52
58	6.2	16	3,210	302	0.39	1.07	0.37
63	5.6	16	3,593	750	1.07	1.20	0.89
65	4.2	16	3,229	805	1.53	1.08	1.42

70	4.8	16	7,672	514	0.86	2.56	0.33
73	4.9	16	5,047	103	0.17	1.68	0.10
77	5.0	16	4,460	227	0.36	1.49	0.24
79	4.6	16	3,320	227	0.40	1.11	0.36
84	4.4	16	2,834	312	0.56	0.95	0.60
96	4.9	16	3,394	536	0.88	1.13	0.78
91	4.6	16	3,307	597	1.04	1.10	0.94
93	5.3	16	6,133	610	0.93	2.05	0.45
105	6.8	16	2,511	373	0.44	0.84	0.52
121	4.0	16	2,819	203	0.40	0.94	0.43
128	3.9	20	4,007	209	0.43	1.34	0.32
133	3.0	20	4,244	202	0.54	1.42	0.38
135	3.0	20	4,311	238	0.63	1.44	0.44
140	3.1	20	4,180	132	0.34	1.39	0.25
142	3.2	20	4,743	166	0.41	1.58	0.26
147	2.5	20	4,829	249	0.79	1.61	0.49
149	2.7	20	4,894	178	0.54	1.63	0.33
156	3.0	20	4,911	137	0.37	1.64	0.23
168	4.2	20	5,240	296	0.56	0.96	0.59
177	5.0	20	5,453	511	0.81	1.00	0.81
189	3.5	22	4,494	437	0.55	0.82	0.67
191	3.5	22	6,776	488	0.62	1.24	0.50
196	5.5	22	6,960	456	0.37	1.28	0.29
198	6.9	22	7,327	548	0.35	1.34	0.26
203	6.9	22	8,729	638	0.40	1.60	0.25

Table A-4: Characteristics of the RO permeate from MBR/RO treatment of synthetic gray water.

Analysis	Result	Practical Quantification Limit	Unis
Antimony	<0.008	0.0008	mg/L
Arsenic	<0.005	0.0005	mg/L
Total Hardness	<5	5	mg/L $CaCO_3$
ICP Metals			
Barium	<0.002	0.002	mg/L
Beryllum	0.0005	0.0003	mg/L
Cadmium	0.0032	0.001	mg/L
Chromium	<0.005	0.005	mg/L
Copper	0.0051	0.005	mg/L
Iron	<0.050	0.05	mg/L
Manganese	0.0618	0.01	mg/L
Nickel	<0.005	0.005	mg/L

Silver	<0.010	0.01	mg/L
Sodium	1.68	0.05	mg/L
Zinc	0.0348	0.01	mg/L
Lead	<0.001	0.001	mg/L
Mercury	<0.0002	0.0002	mg/L
Selenium	<0.002	0.002	mg/L
Thallium	<0.0007	0.0007	mg/L
Anions by Ion Chromatography			
Fluoride	<0.100	0.1	mg/L
Chloride	1.24	1	mg/L
Nitrate, Nitrogen (as N)	<0.010	0.01	mg/L
Sulfate	<2.00	2	mg/L
Purgeable Organic Compounds			
1,1,1,2-Tetrachloroethane	<0.5	0.5	µg/L
1,1,1-Trichloroethane	<0.5	0.5	µg/L
1,1,2,2-Tetrachloroethane	<0.5	0.5	µg/L
1,1,2-Trichloroethane	<0.5	0.5	µg/L
1,1- Dichloroethane	<0.5	0.5	µg/L
1,1-Dichloroethene	<0.5	0.5	µg/L
1,1-Dichloropropene	<0.5	0.5	µg/L
1,2,3-Trichlorobenzene	<0.5	0.5	µg/L
1,2,3-Trichloropropane	<0.5	0.5	µg/L
1,2,4- Trichlorobenzene	<0.5	0.5	µg/L
1,2,4- Trimethylbenzene	<0.5	0.5	µg/L
1,3,5-Trimethylbenzene	<0.5	0.5	µg/L
1,3-Dichlorobenzene	<0.5	0.5	µg/L
1,3-Dichloropropane	<0.5	0.5	µg/L
1,4-Dichlorobenzene	<0.5	0.5	µg/L
2,2-Dichloropropane	<0.5	0.5	µg/L
2-Chlorotoluene	<0.5	0.5	µg/L
4-Chlorotoluene	<0.5	0.5	µg/L
4-Isopropyltoluene	<0.5	0.5	µg/L
Benzene	<0.5	0.5	µg/L
Bromobenzene	<0.5	0.5	µg/L
Bromochloromethane	<0.5	0.5	µg/L
Bromodichloromethane	<0.5	0.5	µg/L
Bromoform	<0.5	0.5	µg/L
Bromomethane	<0.5	0.5	µg/L
Carbon tetrachloride	<0.5	0.5	µg/L
Chlorobenzene	<0.5	0.5	µg/L

Chloroethane	<1.0	1	µg/L
Chloroform	<0.5	0.5	µg/L
Chloromethane	<0.5	0.5	µg/L
cis-1,2-Dichloroethene	<0.5	0.5	µg/L
cis-1,3-Dichloropropene	<0.5	0.5	µg/L
Dibromochloromethane	<0.5	0.5	µg/L
Dibromomethane	<0.5	0.5	µg/L
Dichlorodifluoromethane	<0.5	0.5	µg/L
Ethylbenzene	<0.5	0.5	µg/L
Hexachlorobutadiene	<0.5	0.5	µg/L
Isopropylbenzene	<0.5	0.5	µg/L
m,p-Xylene	<0.5	0.5	µg/L
Methyl tert-butyl ether	<2.0	2	µg/L
Methylene chloride	<0.5	0.5	µg/L
Naphthalene	<0.5	0.5	µg/L
n-Butylbenzene	<0.5	0.5	µg/L
n-Propylbenzene	<0.5	0.5	µg/L
o-Xylene	<0.5	0.5	µg/L
sec-Butylbenzene	<0.5	0.5	µg/L
Styrene	<0.5	0.5	µg/L
tert-Butylbenzene	<0.5	0.5	µg/L
Tetrachloroethene	<0.5	0.5	µg/L
Toluene	<0.5	0.5	µg/L
trans-1,2-Dichloroethene	<0.5	0.5	µg/L
trans-1,3-Dichloropropene	<0.5	0.5	µg/L
Trichloroethene	<0.5	0.5	µg/L
Trichlorofluoromethane	<0.5	0.5	µg/L
Vinyl chloride	<0.5	0.5	µg/L
Alkalinity	28	1	mg/L CaCO3
Ammonia	7.2	1	mg/L
Corrosivity, Langelier Value	-1.26	0	SI
Cyanide	<0.01	0.01	mg/L
Total Phosphate	<0.02	0.02	mg/L
TDS	40	10	mg/L
Color	5	5	CPU
Nitrite	<0.01	0.01	mg/L
pH	10	1	pH unit
Turbidity	0.29	0.1	NTU

Table A-5: ZW-10 MBR influent (laundry and kitchen mixture) and effluent water quality data for turbidity, COD, BOD, TOC, and pH.

Day	Turbidity			Chemical Oxygen Demand (COD)			Biological Oxygen Demand (BOD)			Total Organic Carbon (TOC)			pH	
	NTU			mg/L			mg/L			mg/L			pH units	
	Influent	Effluent	% Removal	Influent	Effluent	% Removal	Influent	Effluent	% Removal	Influent	Effluent	% Removal	Infuent	Effluent
2														
3	8.6	0.13	98.5	208	101	51.4	123	35	71.5	58.1	36.7	36.8	6.6	7.7
4	8.6	0.1	98.8	208	74	64.4	123	<20	83.7	58.1	24.7	57.5	6.6	9.5
5	83	0.1	99.9	412	42	89.8	199	4	98.0	45.4	14.6	67.8	6.6	7.6
6	83	0.42	99.5	412	49	88.1	199	6	97.0	45.4	6.6	85.5	6.6	7.8
13	48	0.12	99.8	690	59	91.4	429	7	98.4	144.0	12.4	91.4	6.2	7.6
20	60	0.13	99.8	311	26	91.6	145	4	97.2	38.6	9.0	76.7	6.8	8.0
27	160	0.14	99.9	1,380	22	98.4	440	5	98.9	165.0	6.8	95.9	6.4	7.8
32	140	0.13	99.9	690	26	96.2	194	5	97.4	102.0	8.8	91.4	6.4	7.7
41	760	0.27	100.0	1,510	22	98.5	799	5	99.4	179.0	8.3	95.4	6.4	7.8
48	170	0.4	99.8	594	13	97.8	348	3	99.1	116.0	4.4	96.2	6.5	7.9
53	720	0.11	100.0	913	4	99.6	418	2	99.5	61.2	2.7	95.6	6.8	8.0
76	370	0.17	100.0	670	9	98.7	361	<4	99.2	43.4	4.0	90.8	6.9	7.3
83	60	0.1	99.8	195	4	97.9	101	3	97.0	10.6	2.5	76.4	7.2	8.0
90	450	0.13	100.0	817	9	98.9	295	<4	99.0	128.0	3.3	97.4	7.0	8.0

Table A-6: ZW-10 MBR influent (laundry and kitchen mixture) and effluent water quality data for TDS, TSS, Ammonia, TKN, and TP.

Day	Total Dissolved Solids (TDS)			Total Suspended Solids (TSS)			Ammonia			Total Kjeldahl Nitrogen (TKN)			Total Phosphorus (TP)		
	mg/L			mg/L			mg/L			mg/L			mg/L		
	Influent	Effluent	% Removal	Influent	Effluent	% Removal	Influent	Effluent	% Removal	Influent	Effluent	% Removal	Influent	Effluent	% Removal
3	430	515	0.0	9.5	<1	89.6	50.4	41.4	17.9	57.1	44.8	21.5	6.6	4.9	25.2
4	430	435	0.0	9.5	<1	89.6	50.4	23.0	54.4	57.1	53.8	5.8	6.6	5.0	23.7
5	515	440	14.6	20	<1	95.1	31.0	39.9	0.0	45.4	41.4	8.8	6.1	4.7	23.0
6	515	380	26.2	20	<1	95.1	31.0	15.0	51.6	45.4	17.9	60.6	6.1	2.2	64.8
13	505	395	21.8	138	<1	99.3	17.1	7.6	55.6	21.3	7.3	65.7	6.7	0.3	95.6
20	380	335	11.8	79	<1	98.7	24.2	24.7	0.0	30.2	21.3	29.5	4.1	1.7	58.0
27	525	400	23.8	507	<1	99.80	27.9	28.4	0.0	42.6	23.5	44.8	10.7	2.7	75.0
32	420	345	17.9	236	<1	99.58	27.5	27.7	0.0	50.4	27.4	45.6	6.5	2.1	67.1
41	470	320	31.9	410	<1	99.76	11.0	0.1	99.1	44.8	1.1	97.5	10.0	1.0	89.9
48	365	305	16.4	170	<1	99.42	4.9	<0.1	98.0	19.0	1.1	94.2	3.8	0.5	86.1
53	280	275	1.8	405	<1	99.76	3.9	1.5	61.5	34.7	1.1	96.8	8.8	0.5	94.2
76	360	495	0.0	366	1.5	99.6	16.1	5.1	68.3	35.8	4.5	87.4	8.2	1.3	84.0
83	305	350	0.0	86	<1	98.8	7.9	<0.1	87.5	13.4	<1	92.6	3.0	1.8	39.7
90	320	285	10.9	388	<1	99.7	7.9	<0.1	87.5	48.2	<1	97.9	12.0	1.5	87.7

Table A-7: E2 RO permeate drinking water quality characterization results for laundry and kitchen wastewater treatment study.

Parameter	Day 4	Day 20	Day 53	Day 90	Practical Quantification Limit	Units
Alkalinity	8	4	2	4	1	mg/L CaCO3
BOD	<4	<4	<4	<4	4	mg/L
COD	<5	<5	<5	<5	5	mg/L
TOC	<1	<1	<1	<1.0	1	mg/L
Ammonia	1.5	1.3	0.1	<0.1	1	mg/L
Corrosivity, Langelier Value	-4.85	-4.2	-6.37	-5.26	0	SI
Cyanide	<0.01	<0.01	<0.01	<0.01	0.01	mg/L
Total Phosphate	0.05	<0.02	<0.02	<0.02	0.02	mg/L
TDS	<5	<5	5	<5	5	mg/L
Color	5	5	<5	5	5	cpu

Nitrite	<0.01	<0.01	0.01	<0.01	0.01	mg/L
pH	7.1	7.6	5.9	7	1	pH units
Turbidity	<0.10	0.12	0.1	<0.10	0.1	NTU
Antimony	<0.0008	<0.0008	<0.0008	<0.0008	0.0008	mg/L
Arsenic	<0.0005	<0.0005	<0.0005	<0.0005	0.0005	mg/L
Total Hardness	<5	<5	<5	<5	5	mg/L CaCO3
ICP Metals						
Barium	<0.0020	<0.0020	<0.0020	<0.0020	0.002	mg/L
Beryllum	<0.0003	<0.0003	<0.0003	<0.0003	0.0003	mg/L
Cadmium	<0.0010	<0.0010	<0.0010	<0.0010	0.001	mg/L
Chromium	<0.0050	<0.0050	<0.0050	<0.0050	0.005	mg/L
Copper	<0.0050	<0.0050	<0.0050	0.0078	0.005	mg/L
Iron	<0.0500	<0.0500	<0.0500	<0.0500	0.05	mg/L
Manganese	<0.0100	<0.0100	<0.0100	<0.0100	0.01	mg/L
Nickel	<0.0050	<0.0050	<0.0050	<0.0050	0.005	mg/L
Silver	<0.0100	<0.0100	<0.0100	<0.0100	0.01	mg/L
Sodium	0.629	0.772	0.603	1.14	0.05	mg/L
Zinc	<0.0100	0.0136	<0.0100	<0.0100	0.01	mg/L
Lead	<0.001	<0.001	<0.001	<0.001	0.001	mg/L
Mercury	<0.0002	<0.0002	<0.0002	<0.0002	0.0002	mg/L
Selenium	<0.002	<0.002	<0.002	<0.002	0.002	mg/L
Thallium	<0.0007	<0.0007	<0.0007	<0.0007	0.0007	mg/L
Anions by Ion Chromatography						
Fluoride	<0.100	<0.100	<0.100	<0.100	0.1	mg/L
Chloride	<1	1.08	<1	<1	1	mg/L
Nitrate, Nitrogen (as N)	<0.010	0.83	<0.010	0.136	0.01	mg/L
Sulfate	<2.00	<2.00	<2.00	<2.00	2	mg/L
Purgeable Organic Compounds						
1,1,1,2-Tetrachloroethane	<0.5	<0.5	<0.5	<0.5	0.5	µg/L
1,1,1-Trichloroethane	<0.5	<0.5	<0.5	<0.5	0.5	µg/L
1,1,2,2-Tetrachloroethane	<0.5	<0.5	<0.5	<0.5	0.5	µg/L
1,1,2-Trichloroethane	<0.5	<0.5	<0.5	<0.5	0.5	µg/L
1,1- Dichloroethane	<0.5	<0.5	<0.5	<0.5	0.5	µg/L
1,1-Dichloroethene	<0.5	<0.5	<0.5	<0.5	0.5	µg/L
1,1-Dichloropropene	<0.5	<0.5	<0.5	<0.5	0.5	µg/L
1,2,3-Trichlorobenzene	<0.5	<0.5	<0.5	<0.5	0.5	µg/L
1,2,3-Trichloropropane	<0.5	<0.5	<0.5	<0.5	0.5	µg/L
1,2,4- Trichlorobenzene	<0.5	<0.5	<0.5	<0.5	0.5	µg/L
1,2,4- Trimethylbenzene	<0.5	<0.5	<0.5	<0.5	0.5	µg/L

1,3,5-Trimethylbenzene	<0.5	<0.5	<0.5	<0.5	0.5	µg/L
1,3-Dichlorobenzene	<0.5	<0.5	<0.5	<0.5	0.5	µg/L
1,3-Dichloropropane	<0.5	<0.5	<0.5	<0.5	0.5	µg/L
1,4-Dichlorobenzene	<0.5	<0.5	<0.5	<0.5	0.5	µg/L
2,2-Dichloropropane	<0.5	<0.5	<0.5	<0.5	0.5	µg/L
2-Chlorotoluene	<0.5	<0.5	<0.5	<0.5	0.5	µg/L
4-Chlorotoluene	<0.5	<0.5	<0.5	<0.5	0.5	µg/L
4-Isopropyltoluene	<0.5	<0.5	<0.5	<0.5	0.5	µg/L
Benzene	<0.5	<0.5	<0.5	<0.5	0.5	µg/L
Bromobenzene	<0.5	<0.5	<0.5	<0.5	0.5	µg/L
Bromochloromethane	<0.5	<0.5	<0.5	<0.5	0.5	µg/L
Bromodichloromethane	<0.5	<0.5	<0.5	<0.5	0.5	µg/L
Bromoform	<0.5	<0.5	<0.5	<0.5	0.5	µg/L
Bromomethane	<0.5	<0.5	<0.5	<0.5	0.5	µg/L
Carbon tetrachloride	<0.5	<0.5	<0.5	<0.5	0.5	µg/L
Chlorobenzene	<0.5	<0.5	<0.5	<0.5	0.5	µg/L
Chloroethane	<1.0	<1.0	<1.0	<1.0	1	µg/L
Chloroform	<0.5	<0.5	<0.5	<0.5	0.5	µg/L
Chloromethane	<0.5	<0.5	<0.5	<0.5	0.5	µg/L
cis-1,2-Dichloroethene	<0.5	<0.5	<0.5	<0.5	0.5	µg/L
cis-1,3-Dichloropropene	<0.5	<0.5	<0.5	<0.5	0.5	µg/L
Dibromochloromethane	<0.5	<0.5	<0.5	<0.5	0.5	µg/L
Dibromomethane	<0.5	<0.5	<0.5	<0.5	0.5	µg/L
Dichlorodifluoromethane	<0.5	<0.5	<0.5	<0.5	0.5	µg/L
Ethylbenzene	<0.5	<0.5	<0.5	<0.5	0.5	µg/L
Hexachlorobutadiene	<0.5	<0.5	<0.5	<0.5	0.5	µg/L
Isopropylbenzene	<0.5	<0.5	<0.5	<0.5	0.5	µg/L
m,p-Xylene	<0.5	<0.5	<0.5	<0.5	0.5	µg/L
Methyl tert-butyl ether	<2.0	<2.0	<2.0	<2.0	2	µg/L
Methylene chloride	<0.5	<0.5	<0.5	<0.5	0.5	µg/L
Naphthalene	<0.5	<0.5	<0.5	<0.5	0.5	µg/L
n-Butylbenzene	<0.5	<0.5	<0.5	<0.5	0.5	µg/L
n-Propylbenzene	<0.5	<0.5	<0.5	<0.5	0.5	µg/L
o-Xylene	<0.5	<0.5	<0.5	<0.5	0.5	µg/L
sec-Butylbenzene	<0.5	<0.5	<0.5	<0.5	0.5	µg/L
Styrene	<0.5	<0.5	<0.5	<0.5	0.5	µg/L
tert-Butylbenzene	<0.5	<0.5	<0.5	<0.5	0.5	µg/L
Tetrachloroethene	<0.5	<0.5	<0.5	<0.5	0.5	µg/L
Toluene	<0.5	<0.5	<0.5	<0.5	0.5	µg/L
trans-1,2-Dichloroethene	<0.5	<0.5	<0.5	<0.5	0.5	µg/L
trans-1,3-Dichloropropene	<0.5	<0.5	<0.5	<0.5	0.5	µg/L

Trichloroethene	<0.5	<0.5	<0.5	<0.5	0.5	µg/L
Trichlorofluoromethane	<0.5	<0.5	<0.5	<0.5	0.5	µg/L
Vinyl chloride	<0.5	<0.5	<0.5	<0.5	0.5	µg/L